GENETIC STUDY OF ENDOPLASMIC RETICULUM-MEDIATED PROTEIN QUALITY CONTROL IN *ARABIDOPSIS*

by

Yidan Liu

A dissertation submitted in partial fulfillment
of the requirement for the degree of
Doctor of Philosophy
(Molecular, Cellular and Developmental Biology)
in The University of Michigan
2015

Doctoral Committee:
Professor Jianming Li, Chair
Associate Professor Amy Chang
Associate Professor Erik E. Nielsen
Professor Billy Tsai
Associate Professor Yanzhuang Wang

To My Family

ACKNOWLEDGEMENTS

This thesis covers my work that has been done since I joined Li Lab in the spring of 2010. I would not be able to finish this dissertation without the help of many people who have assisted me in the past five years. First of all, I would like to express my deepest gratitude to my advisor Dr. Jianming Li for his constant guidance, encouragement, patience and support throughout my study. His acute intuition on the "big picture" and keen insights on the details have guided my research while his passion and attitude towards science have always inspired me. I have learnt a lot from him both inside and outside scientific research.

I also owe sincere thanks to the members of my thesis committee, Dr. Amy Chang, Dr. Erik Nielsen, Dr. Billy Tsai and Dr. Yanzhuang Wang for their valuable advice and continuous support through the years. Dr. Chang and Dr. Tsai have shared experiment materials to let me test my hypothesis in other model organisms. The study of EBS7 would not be thorough enough without their kindly gifts. Dr. Nielsen has always been very familiar with my work, especially the *Arabidopsis* physiological part and has given a lot of insightful suggestions. Dr. Wang is an expert in the protein trafficking field and he has provided great advice and technical support in many biochemical experiments.

I also owe my thanks to former and current members of Li Lab. Dr. Zhi Hong, Dr. Wei Su and Dr. Yongyou Zhu taught me many techniques in my early years here. I want to thank Yang Xia, Zhuobin Liang, Dr. Kamy Sanger, Dr. Jianjun Zhang and Dr. Zhaohai

Zhu for the helpful discussions. I would also like to provide my gratitude to our plant research group for the plant journal club meeting discussion and collaboration.

Finally, I want to give my thanks to my parents, other family members and especially my husband. This thesis would not have been what it is without his love, encouragement and support.

PREFACE

Most parts of Chapter 1 were modified from a review published in *Front Plant Sci*. 2014 Apr; 5:162. All the figures Chapter 2 were published in *Plant Signal Behav*. 2013 Apr; 8(4): e23864 and *Mol Plant*. 2013 May; 6(3): 985-7.

TABLE OF CONTENTS

LIST OF FIGURES

LIST OF TABLES

ABSTRACT

Endoplasmic reticulum (ER) quality control (ERQC) is an essential cellular process that permits trafficking of only correctly folded proteins to their final destinations, allows additional folding cycles of incompletely-folded proteins, repairs misfolded ones, and removes terminally-misfolded ones via ER-associate degradation (ERAD). Most of our current knowledge on ERQC and ERAD came from genetic and biochemical investigations in yeast and mammalian cells. Recent studies in the reference plant *Arabidopsis thaliana* uncovered homologous components and similar mechanisms in plants for monitoring protein folding and for retaining, repairing, and removing misfolded proteins. Among these components, one important chaperone-like lectin Calreticulin (CRT), who participates in the glycoprotein folding cycle regulation, has three homologs in *Arabidopsis* named AtCRT1, AtCRT2 and AtCRT3. Recent studies revealed a crucial role for CRT3 but not the other CRTs in ER retention of a mutant brassinosteroid receptor, brassinosteroid-insensitive 1-9 (bri1-9) and in complete folding of a plant immunity receptor EF-Tu Receptor (EFR). In this study, the specificity of CRT3 over CRT1/2 in retaining misfolded proteins inside ER was investigated and discussed. I identified a CRT3-specific C-terminal positively charged tetrapeptide that is indispensable for its chaperone function. In addition to the study on this conserved ERQC member, this thesis also reported a novel and plant-specific ERAD component that involves in the degradation of bri1-9 and bri1-5, two ER-retained mutant variants of the cell surface receptor for brassinosteroids (BRs). Loss-of-function *ebs7* mutations prevent

ERAD of bri1-9 and bri1-5, causing their accumulation in the ER and consequential leakage to the plasma membrane, which is responsible for restoration of BR sensitivity and phenotypic suppression of the *bri1-9* and *bri1-5* mutants, respectively. EBS7 localizes on ER membrane and it accumulates under ER stress. Mechanistically, EBS7 interacts with the ER membrane-anchored ubiquitin ligase AtHrd1, one of the central components of the *Arabidopsis* ERAD machinery, and an *ebs7* mutation destabilizes AtHrd1 to reduce polyubiquitination of bri1-9. Taken together, this thesis project not only investigated the function of conserved ERQC members through the study in *Arabidopsis*, but also shed light on mechanisms of plant-specific regulation of ERAD.

CHAPTER 1
MOLECULAR MECHANISM OF ENDOPLASMIC RETICULUM QUALITY CONTROL AND ENDOPLASMIC RETICULUM-ASSOCIATED DEGRADATION

Abstract

It is well known that the proper function of a protein strictly depends on its native conformation, but protein folding is a fundamentally error-prone process. The endoplasmic reticulum (ER) is the cellular port of entry for secretory and membrane proteins to enter the secretory pathway and is a folding compartment for proteins to attain their native conformations through interactions with molecular chaperones, sugar-binding lectins, and folding enzymes. Misfolded proteins not only lead to functional deficiency but also induce dominant-negative effects and cellular toxicity. It is thus essential that the ER should possess several highly stringent protein quality control mechanisms to closely monitor the folding process, allowing export of only correctly folded proteins to their final destinations and retaining incompletely/mis-folded proteins for additional rounds of chaperone-assisted folding. A highly-efficient ER-mediated protein quality control (ERQC) system can also differentiate terminally misfolded proteins from folding intermediates and/or reparable misfolded proteins, stopping the futile folding cycles of the former proteins and eliminating them via a multistep degradation process widely known as ER-associated degradation (ERAD) that involves ubiquitination,

retrotranslocation, and cytosolic proteasome-mediated degradation. Our current understanding of the eukaryotic ERQC/ERAD system is derived largely from studies in yeast and mammalian cells. Recent genetic, biochemical, and cell biological studies in the reference plant *Arabidopsis thaliana* and other model plant species however, not only identified homologous ERQC/ERAD components but also revealed evolutionarily conserved features as well as unique aspects of the plant ERQC/ERAD mechanisms, especially in relation to stress tolerance and plant defense pathways.

The Quality Control System Monitors Protein Folding Process in the ER

N-Glycan-Based ER Retention Mechanism in Eukaryotes

Many secretory and membrane proteins are co-translationally glycosylated when entering the ER (1). The so-called N-linked glycosylation occurs on the asparagine (Asn or N) residues within the Asn-X-Ser/Thr sequons (X indicating any amino acid except proline while Ser/Thr denoting serine/threonine residue) of a nascent polypeptide. This reaction is catalyzed by the enzyme oligosaccharyltransferase (OST), an integral membrane protein complex that transfers a preassembled oligosaccharide precursor $Glc_3Man_9GlcNac_2$ (Glc, Man and GlcNac denoting glucose, mannose and *N*-acetylglucosamine, respectively) from a membrane-anchored dolichylpyrophosphate (DolPP) carrier to the Asn residue (Fig. 1.1A) (2). The assembly of $Glc_3Man_9GlcNac_2$ involves a series of highly specific asparagine-linked glycosylation (ALG) proteins that sequentially add a monosaccharide onto the DolPP linker or a DolPP-linked oligosaccharide precursor (Fig. 1.1A) (1). The structure of an N-linked glycan plays an

important role in the protein folding and quality control (3). Immediately after transferring of $Glc_3Man_9GlcNac_2$ to an Asn residue, the terminal and middle Glc residues are removed sequentially by glucosidase I (GI) and glucosidase II (GII), producing a monoglucosylated *N*-glycan, $GlcMan_9GlcNac_2$, which is recognized by the ER chaperone-like lectins, a membrane-anchored calnexin (CNX) and its ER luminal homolog calreticulin (CRT; Fig. 1.2) (4). The high-specificity high-affinity binding between $GlcMan_9GlcNac_2$ and CNX/CRT is crucial for folding a nascent polypeptide as CNX/CRT can recruit other ER-chaperones and folding enzymes, including protein disulfide isomerases (PDIs) essential for generating inter/intra-molecular disulfide bonds. The removal of the remaining Glc residue by GII releases the nascent glycoprotein from CNX/CRT, thus terminating its folding process (4). If the protein folds correctly, it will be transported out of the ER to reach its final destination. However, if the protein fails to attain its native conformation, it will be recognized by UDP-glucose:glycoprotein glucosyltransferase (UGGT), an ER-resident folding sensor consisting of a large non-conserved N-terminal domain presumably involved in recognizing non-native conformations and a smaller highly conserved C-terminal catalytic domain capable of catalyzing a glucosyltransferase reaction using uridyl diphosphate-glucose (UDP-Glc) as a substrate (5). As a result, a single Glc is added back to deglucosylated *N*-glycans of the incompletely/mis-folded protein, permitting its reassociation with CNX/CRT and their associated proteins for another round of assisted folding. The alternate reactions of GII and UGGT drive many cycles of dissociation and reassociation of CNX/CRT with an incompletely/mis-folded glycoprotein [widely known as the CNX/CRT cycle (6)], till the protein attains its native conformation (Fig. 1.2). It is worthy to mention that the budding

yeast (*Saccharomyces* cerevisiae), which is widely used for studying the ERAD process, lacks the CNX/CRT-UGGT system due to the presence of a catalytically inactive UGGT homolog (7).

A Conserved CRT-UGGT System Regulates Glycoprotein Folding in *Arabidopsis*

The *Arabidopsis* genome encodes only one UGGT homolog, and its physiological function was inadvertently found in a study for identifying additional signaling proteins of the plant steroid hormones, brassinosteroids (BR) (8). A genetic screening for extragenic suppressors of an *Arabidopsis* dwarf mutant *brassinosteroid-insensitive 1-9* (*bri1-9*) led to the discovery of *Arabidopsis* UGGT (also known as EBS1 for EMS mutagenized bri1 suppressor 1, Table 1.2) (8). BRI1 is a cell surface-localized leucine-rich-repeat receptor-like-kinase that function as a BR receptor and contains a single transmembrane domain and 14 putative N-glycosylation sites in its N-terminal extracellular domain (9). The mutant bri1-9, carrying a Ser662-Phe mutation in the BR-binding domain (10), was found to be retained in the ER by an EBS1/AtUGGT-dependent mechanism and subsequently degraded by a plant ERAD process (8, 11). Loss-of-function mutations in EBS1/UGGT compromise such an ER-retention mechanism and allow some bri1-9 proteins to escape from the ER to reach the plasma membrane, resulting in phenotypic suppression of the dwarfism of the *bri1-9* mutant. The same genetic screen also identified CRT3 (12), a unique member of the *Arabidopsis* CNX/CRT family consisting of two CNXs and three CRTs, which actually retains bri1-9 via the CRT3-$GlcMan_9GlcNac_2$ binding (Table 1.2). Both UGGT and CRT3 were also identified from two other independent genetic screens aiming to identify key regulators of the plant innate immune response to a bacterial translational elongation factor EF-Tu (13,

14). Interestingly, while loss-of-function mutations in AtUGGT/CRT3 led to restoring partial sensitivity to BRs, *atuggt/crt3* mutants were insensitive to elf18, a biologically active epitope of EF-Tu. Further studies showed that both UGGT and CRT3 are absolutely required for the correct folding of EFR (EF-Tu Receptor) (15), a BRI1-like receptor-like kinase that binds elf18/EF-Tu to initiate a plant defense process (16). The importance of *N*-glycan-mediated folding control was further supported by discoveries that loss-of-function mutations in STT3A, a OST subunit, and GII resulted in significant reduction of the EFR protein abundance, presumably caused by incomplete folding and subsequent degradation (17-19).

Calreticulin Participates in Multiple Biological Processes in Cell

Besides its role in the glycoprotein quality control, CRT is shown to play a role in many biological processes in a variety of subcellular compartments. It contains a sugar-binding N-globular domain, a central proline-rich arm-like P-domain and a C-terminal domain that is responsible for Ca^{2+} binding (20). Ca^{2+} signaling affects a series of biological processes including gene expression, neuronal excitability, cell differentiation, stress response, etc. The ER is the major Ca^{2+} storage organelle in cell. ER-localized Calreticulin is essential for Ca^{2+} homeostasis as its C-terminal region can bind multiple Ca^{2+} with low affinity but high capacity (21). For instance, CRT knockout mice result in embryonic lethality due to development and gene expression failure in early cardiogenesis (22). Besides, ER-localized CRT participates in cell differential pathways via its regulation of Ca^{2+} homeostasis and it has been reported that adipocyte differentiation is inhibited by overexpression of CRT *in vivo* (23). In addition, CRT mediates cellular stress response via balancing ER and intracellular Ca^{2+} level. One

example is that osmotic stress in the renal epithelial cells decreases the expression of CRT and over-expression of CRT but not a CRT mutant lacking the C-terminal region results in poor viability of these cells in hypertonic environment (24, 25). Notably, other cellular stress conditions including Ca^{2+} depletion may result in CRT translocation to cell surface and this ER-to-cell-surface translocation is not restricted to CRT but involves other ER-resident proteins (26-28). Though the mechanism of this stress-induced cell-surface ER-protein recruitment remains elusive.

It has been long known that CRT is an ER-resident protein, however, CRT also plays a variety of roles in cell surface, cytoplasm and extracellular matrix. The cell surface CRT exposure via protein translocation is an essential step to target the immunogenic cell death (29, 30). Extracellular CRT expression is shown to increase the wound repair rate in several animal model studies (31). Cytosolic-exposed CRT was reported to play a role in cell adhesion and gene expression though the mechanism behind is not clear yet (32, 33).

Compared with the well-studied mammalian CRT, our knowledge on the physiological functions of plant CRTs is rather limited. Most of the plant CRT studies have been mainly focused on the regulatory role in intracellular Ca^{2+} homeostasis. For example, it was reported that the *Arabidopsis* CRT1 (AtCRT1) expressed in CRT-deficient mouse embryonic fibroblasts could rescue the decreased Ca^{2+} level and deficient protein folding phenotypes (34). Yet the plant CRTs have some unique features in regulating plant growth and other physiological events. For example, CRT expression level is elevated in reproductive organs and early embryos in maize, barley, *Arabidopsis* and several other plants and this elevation might be correlated with changes in Ca^{2+} homeostasis in plant

reproduction process (35-38). In addition, plant CRTs participate in many stress response including cold, drought and pathogen response (13, 39-42).

Both mammals and plants contain multiple CRTs. Besides the well-understood CRT1 that involves in a wide range of cellular processes mentioned above, mammalian genome encodes a CRT2 that is highly expressed in testis with unknown function (43-45). Many plant species including *Arabidopsis* have three CRTs that are classified into two functional groups: CRT1/CRT2 and CRT3 based on sequence alignment and phylogeny analysis (12, 46, 47). The *Arabidopsis* CRT1/CRT2 and CRT3 share similar sugar-binding N-domain and the central P-domain. However, their C-terminal domains and their co-expression profiles are quite distinct. CRT1 and CRT2, similar to the mammalian CRT1, have an acidic C-terminal domain and are co-expressed with known ER chaperones and folding catalysts, whereas CRT3 has a C-terminal domain enriched with basic residues and is co-expressed with genes involved in plant stress responses (12, 48).

The distinct groups of CRTs (CRT1/2 and CRT3) perform both similar and unique functions in plant cells. On one hand, it was mentioned before that an AtCRT1 could substitute the role of mouse CRT in Ca^{2+} storage and protein folding, and a recent study demonstrate that AtCRT3 could also restore the function of mammalian CRT1 in $crt^{-/-}$ mouse embryonic fibroblasts (48), indicating the similarity between the two groups. On the other hand, the expression of both AtCRT1 and AtCRT2 can be induced by an ER stress inducer tunicamycin while AtCRT3 has no such induction. Additionally, AtCRT1 and AtCRT2 could complement the double mutant of *Δcrt1Δcrt2* while AtCRT3 fails to do so. Recent studies showed that AtCRT3 but not the other CRTs is the key ER retention factor for a mutated brassinosteroid receptor BRI1 allele (bri1-9) and a

pathogen-defense related pattern recognition receptor EFR (12, 13). In a recent study, AtCRT2 was reported to contain a dual regulatory role in plant defense against pathogens and this function is not through the EFR-mediated pathway (49).

N-glycan Independent Quality Control

In addition to the glycan-dependent ER retention system, the ER is equipped with additional retention systems to prevent export of misfolded proteins, especially those non-glycosylated ones. One system uses the family of ER-localized HSP70 proteins (known as BiPs), which have a N-terminal ATP-binding domain and a C-terminal substrate-binding domain that recognizes and binds to exposed hydrophobic patches of incompletely/mis-folded proteins in an ATP-dependent manner (50). The *Arabidopsis* has three BiP homologs, AtBiP1, AtBiP2 and AtBiP3, all of which were known to exhibit higher levels of gene expression under ER stresses (51). In *Arabidopsis*, BiPs were shown to bind both bri1-9 and bri1-5, another mutant variant of BRI1 carrying a Cys69Tyr mutation that destroys a disulfide bridge crucial for the structural integrity of the BR receptor, and were thought to contribute for the ER retention of the two mutant BR receptors (8, 52). BiPs and their associated factors ERdj3B (an *Arabidopsis* ER-localized DNAJ homolog) and SDF2 (the *Arabidopsis* homolog of the murine stromal cell-derived factor 2) are also involved in the biogenesis/folding control of EFR (53). BiPs were also known to interact with the orphan heavy chain of a murine IgG1 antibody or an assembly defective form of the trimeric vacuolar storage protein phaseolin in transgenic tobacco plants (54, 55). Another glycan-independent ER retention mechanism relies on mixed disulfide bridges between incompletely/mis-folded proteins with PDIs and related ER-localized oxidoreductases (56-58). The *Arabidopsis* genome encodes 13

PDI-like proteins (59), none of which has been implicated in retaining misfolded proteins. However, a recent study on bri1-5 carrying an orphan cysteine residue (Cys62) suggested involvement of a thiol-mediated retention system in keeping the mutant BR receptor in the ER (52). Further biochemical studies are needed to verify this prediction and to identify one or more PDIs that form the predicted mixed disulfide bridge with the orphan Cys62 residue.

Degradation of Terminally Misfolded Proteins via ERAD

Marking of a Terminally Misfolded Glycoprotein for ERAD

A protein that fails to attain its native conformation within a given time window is eliminated by ERAD (60). One of the key events in ERQC is to terminate a futile folding cycle and to deliver an irreparable misfolded protein into the ERAD pathway. Although little is known about the marking mechanism for irreparable non-glycosylated ERAD clients, recent studies indicated that removal of the terminal α1,2-Man residue from the C-branch of *N*-glycan (Fig. 1.2), catalyzed by homologous to mannosidase 1 (Htm1) in yeast and ER-degradation enhancing α-mannosidase-like proteins (EDEMs) in mammals, is required for generating the ERAD signal, an exposed α1,6 Man residue on an N-linked glycan (Fig. 1.1B) (61, 62). The *Arabidopsis* genome encodes at least two homologs of the yeast Htm1/mammalian EDEMs [known as MNS4 and MNS5 (63)] but their involvement in a plant ERAD process awaits functional investigation. Nevertheless, recent genetic screening for *Arabidopsis* mutants defective in ERAD of bri1-5/bri1-9 and subsequent molecular cloning and biochemical studies indicated that the glycan ERAD signal is well conserved in plants (11, 64). Loss-of-function mutations in either EBS3 and

EBS4 (homologs of the yeast/mammal ALG9 and ALG12, respectively) prevent complete assembly of the *N*-glycan precursor (Fig. 1.1, Table 1.2), resulting in glycosylation of the two ER-retained mutant BR receptor with truncated *N*-glycan lacking the α1,6-Man residue that would function as the ERAD signal and consequential inhibition of ERAD of bri1-5/bri1-9. In contrast, forcing the addition of the missing α1,6 Man residue to Dol-PP-$Man_6GlcNAc_2$ by overexpression of EBS4/ALG12 in an *Arabidopsis ebs3/alg9 bri1-9* mutant promoted the ERAD of bri1-9 (Fig. 1.1A) (64). Similarly, the ERAD of bri1-9 was presumably accelerated when its N-linked glycans carried a different exposed α1,6 Man residue (the inner α1,6 Man) (64) caused by a loss-of-function mutation in ALG3 that adds an α1,3 Man to the inner α1,6-Man (Fig. 1.1A) (65, 66). The exposed inner α1,6 Man residue was shown to function as an alternative ERAD signal in both yeast and mammalian cells (62, 67).

Recruitment of ERAD Substrates

The *N*-glycan ERAD signal is decoded by one or two ER luminal lectins, osteosarcoma 9 (OS9, also known as Yos9 in yeast) and XTP3-Transactivated protein B (XTP3-B) (Fig. 1.3) (68). Yos9 and its mammalian homologs contain the mannose-6-phosphate receptor homology (MRH) domain that specifically recognizes and binds *N*-glycans with an exposed α1,6 Man residue (67). In addition to OS-9/Yos9, selection of an ERAD client requires another ER resident protein, Hrd3 (HMG-CoA reductase degradation 3) in yeast and Sel1L (Suppressor of lin-12-Like) in mammals (69), a type I transmembrane protein with a large ER luminal domain consisting of multiple copies of the tetratricopeptide repeat motif. It was believed that Hrd3/Sel1L, exhibiting high affinity binding to exposed hydrophobic amino acid residues on misfolded proteins, makes the initial selection of a

potential ERAD client, which is subsequently inspected by OS-9/Yos9 for the presence of an *N*-glycan ERAD signal (Fig. 1.3) (70, 71). Such a bipartite ERAD signal of a misfolded domain plus an α1,6-Man-exposed *N*-glycan ensures degradation of only terminally misfolded glycoproteins but not folding intermediates carrying *N*-glycans with no exposed α1,6 Man residue.

The *Arabidopsis* genome has two *Hrd3/Sel1L* homologous genes, *AtSel1A* (also known as *EBS5 or HRD3A* or) and *AtSel1B* (also known as *HRD3B,* an apparent pseudogene) and just one *OS9/Yos9* homolog, *AtOS9* (also known as *EBS6*) (72-75) (Table 1.2). AtSel1A/EBS5 complemented the ERAD-defect of the yeast Δ*hrd3* mutant assayed by ERAD of a mutant variant of carboxypeptidase Y (CPY*) (73), a commonly used ERAD substrate for many ERAD studies in yeast. By contrast, AtOS9 failed to rescue the defective ERAD of CPY* when expressed in a Δ *yos9* yeast strain (72). Interestingly, a chimeric AtOS9-Yos9 protein consisting of the full-length AtOS9 and the Yos9's C-terminal region (amino acids of 277–542) promoted CPY* degradation in Δ *yos9* yeast cells (72), suggesting that the MRH domain is interchangeable but the Yos9's C-terminal domain might be crucial for interacting with other components of the yeast ERAD machinery. Loss-of-function mutations in either AtSel1A/EBS5 or AtOS9/EBS6 inhibit ERAD of bri1-5, bri1-9, misfolded EFR (in an *ebs1/uggt* mutant background), and/or the transgenically expressed MLO-1 (72-75), mutant variant of barley powdery resistance o (MLO) that carries a single amino acid change in the cytoplasmic region and was previously shown to be an ERAD substrate (76). As expected, AtSel1A/EBS5 and AtOS9/EBS6 physically interacted with bri1-9 or bri1-5 in a tobacco transient expression system or an *in vitro* pull-down assay (72, 74). Consistent with what was known in yeast

and mammalian cells, AtSel1A/EBS5 binds AtOS9/EBS and seems to be required for maintaining the stability of AtOS9/EBS6 (72, 74). These results strongly suggested that the selection mechanism for a terminally misfolded glycoprotein for ERAD is conserved in *Arabidopsis*. It is important to point out that *Arabidopsis* mutants of AtSel1A/EBS6 or AtOS9/EBS6 are hypersensitive to NaCl-induced salt stress, suggesting a relationship between a cellular stress response and an environmental stress pathway (72, 75). It is quite possible that environmental stresses lead to decreased folding efficiency and increased accumulation of misfolded proteins in the ER, which require a highly efficient ERAD system for their removal to maintain ER homeostasis.

Ubiquitination of Chosen ERAD Substrates

Hrd3/Sel1L and Yos9/OS9 not only select irreparable misfolded glycoproteins but also bring the chosen ERAD substrates to the membrane-anchored ERAD complexes responsible for ubiquitination and retrotranslocation. The central component of these ERAD complexes is a polytopic membrane protein with a RING finger-type ubiquitin ligase (E3) activity exposed to the cytosolic surface of the ER membrane, which not only ubiquitinates ERAD substrates but also connects to various ER luminal/cytosolic adapters (69). Yeast contains at least two distinct E3 ligases, 6 transmembrane-spanning Hrd1 (HMG-CoA reductase degradation) and 14-transmembrane-spanning Doa10 (Degradation of alpha2), that ubiquitinate three different types of ERAD substrates differing in the location of folding lesions: $ERAD_L$ (lesion in the ER luminal area), $ERAD_M$ (lesion in the transmembrane segment), and $ERAD_C$ (lesion in the cytosolic domain) (77, 78). The Hrd1 complex ubiquitinates $ERAD_{L/M}$ substrates while the Doa10 complex deals with $ERAD_C$ clients. Mammals have at least 9 membrane-bound ERAD

E3 ligases (79), including two Hrd1 homologs (HRD1 and gp78), one Doa10 homolog (TEB4), and several other RING-type E3 ligases such as RING membrane-anchor 1 (RMA1) (80), whose founding member was initially discovered in *Arabidopsis* (81).

The *Arabidopsis* genome encodes two Hrd1 homologs (AtHrd1a and AtHrd1b) (73, 82), at least two Doa10 homologs (Doa10A/At4g34100 and Doa10B/At4g32670) (75), and three homologs of RMA1, AtRMA1-AtRMA3 that were shown to be localized to the ER and exhibit *in vitro* E3 ubiquitin ligase activity (Table 1.1) (83), but it remains unclear if plants use distinct E3 ligases to removal different classes of ERAD substrates. Loss-of-function mutations in AtHrd1a or AtHrd1b had no detectable effect on bri1-5/bri1-9 degradation, but simultaneous elimination of the two Hrd1 homologs inhibited degradation of the two mutant BR receptors, indicating that AtHrd1a and AtHrd1b function redundantly in a plant ERAD pathway (73). By contrast, the role of the two Doa10 homologs in the plant ERAD pathway remains unknown. Two recent genetic studies revealed important regulator roles of Doa10A (also known as SUD1 for SUPPRESSOR OF DRY2 DEFECTS1 or CER9 for ECERIFERUM9) in the cuticle lipid biosynthesis and in controlling the activity but not the protein level of an *Arabidopsis* HMG-CoA reductase (84, 85). Further studies are needed to determine if the *Arabidopsis* Doa10A is indeed involved in an ERAD pathway that regulates the protein abundance of key regulatory factors or metabolic enzymes involved in the cuticle lipid biosynthesis. Unlike yeast but similar to mammals, plants have additional membrane-anchored RING-type E3 ligases for ERAD. For example, the three *Arabidopsis* RMA1 homologs (Rma1H1) and a hot pepper (*Capsicum annuum*) Rma1H1 are involved in the degradation of a cell surface water channel to regulate its plasma membrane level (86). A

recent study also suggested that a legume (*Medicago truncatula*) homolog of RMA1 seems to play a role in the regulation of biosynthesis of plant defense compounds, triterpene saponins that share the same biosynthetic precursors with sterols, through regulated degradation of HMG-CoA reductase (87).

In a typical ubiquitination reaction, ubiquitin is attached to a substrate through a three-step process consisting of activation, conjugation, and ligation catalyzed by an ubiquitin-activating enzyme (E1), ubiquitin-conjugating enzyme (E2), and E3 (88). In yeast, the Hrd1/Doa10 E3 ligases work together with a membrane-anchored E2 (Ubc6) and two cytosolic E2s (Ubc1 and Ubc7) that are recruited to the ER membrane by an ER anchor protein Cue1 (69), which also activates both E2 and E3 (89, 90). *Arabidopsis* has a total of 37 E2 enzymes (91), including one potential Ubc1 homolog (UBC27), three putative homologs of Ubc7 known to be the cognate E2 for Hrd1 (UBC7 UBC13, and UBC14), and three likely homologs of Ubc6 associated mainly with Doa10 (UBC32, UBC33, and UBC34 each having a predicted transmembrane domain at their C-termini) (75), but our understanding of the roles of these potential ERAD-participating E2s in the plant ERAD process is extremely limited. One of the *Arabidopsis* Ubc6-like E2 gene, *UBC32*, was recently found to be induced by salt, drought, and ER stress (92). Interestingly, the *Arabidopsis ubc32* mutant seedlings are more tolerant whereas *UBC32*-overexpressing transgenic *Arabidopsis* lines are more sensitive to salt and ER stress (92). The observed salt tolerance of the *ubc32* mutant is in contrast to the reduced salt tolerance of other known *Arabidopsis* ERAD mutants, including *ebs5/hrd3a*, *ebs6/os9*, and *hrd1ahrd1b* (72, 75, 82). This discrepancy might be explained by different ERAD substrates being degraded by different E3 ligase complexes: $ERAD_{L/M}$ substrates by AtHrd1a/AtHrd1b in

association with cytosolic E2s and $ERAD_C$ substrates by Doa10 using membrane-anchored E2s. Indeed, UBC32 was found to interact with *Arabidopsis* Doa10B and to stimulate the ubiquitination and degradation of a known ERAD substrate MLO-12, another variant of MLO carrying a single amino acid change in its cytosolic domain (76), in a tobacco leaf transient expression experiment (92). However, the tobacco result was quite different from the results obtained with the yeast MLO experiment showing that the ERAD of MLO-12 plus two other mutant MLOs (all carrying a cytosolic mutation) used the Ubc7-Hrd1 pathway but was unaffected by either *ubc6* or *doa10* deletion in yeast (76). Such inconsistency might be simply caused by heterologous expression of $ERAD_C$ substrates in two different eukaryotic systems. Nevertheless, UBC32 was implicated in the Hrd1-mediated degradation of bri1-9 (a presumed $ERAD_L$ substrate) as the *ubc32* mutation partially inhibited the degradation of the mutant BR receptor and weakly suppressed the corresponding dwarf phenotype (92). The partial inhibition could be attributed to a redundant role of UBC32 with its two close homologs or the potential *Arabidopsis* homologs of Ubc1/Ubc7. However, blast searches failed to find a single homolog of the yeast *Cue1* gene from published sequences of plant genomes and expressed sequence tags (our unpublished results), suggesting that plant ERAD processes might exclusively rely on ER-anchored membrane E2s. Alternatively, plants could recruit cytosolic E2s to the membrane-anchored E3 complexes via yet unknown recruiting factors that share no sequence homology but are functionally similar to Cue1.

The ubiquitination of ERAD substrates, especially those lacking *N*-glycan degradation signals, by the Hrd1 complex requires two additional adapters: U1-Snp1 associating-1 (Usa1; HERP in mammals), an ER membrane protein containing a ubiquitin-like (UBL)

motif near it N-terminus and two predicted transmembrane domains in the middle, and Der1 (degradation in the ER; Derlins for Der1-like proteins in mammals), another integral ER membrane protein with four transmembrane segments (93). Usa1 is thought to regulate the stability and/or oligomerization of Hrd1 and to recruit Der1 to the Hrd1 complex (77, 94-96), while Der1 is believed to function either as a receptor for soluble non-glycosylated ERAD substrates or a potential retrotranslocation channel (97-99). The *Arabidopsis* contains no homolog of Usa1/HERP1 but its genome encodes three Der1 homologs whose functional involvement in a plant ERAD pathway awaits detailed genetic and biochemical investigations (100). An earlier study showed that at least two maize Der1 homologs could complement the yeast Δ *der1* mutant, suggesting a potential role for a plant Der1 homolog in an ERAD pathway; however, there is no genetic evidence for proving the hypothesis (100).

Retrotranslocation of ERAD Substrates

Because the catalytic domains of the ERAD-participating E2s and E3s are on the cytosolic surface of the ER membrane, ERAD substrates need to undergo retrotranslocation for ubiquitination and to access the cytosolic proteasome system for their degradation. However, the molecular nature of this retrotranslocon remains controversial (101). It was previously thought that the Sec61 translocon, which imports nascent polypeptides into the ER lumen during protein biosynthesis, is responsible for retrotranslocation ERAD substrates through the ER membrane (102, 103). Other studies suggested that the yeast Der1 and its mammalian orthologs Derlins are the suspected retrotranslocon (98, 99). A recent study, however, showed that the E3 ligase Hrd1 itself could serve as the retrotranslocation channel for $ERAD_L$ substrates (95). It is quite

possible that all three proteins are capable of retrotranslocation different ERAD substrates involving different adapter proteins.

Compared to the knowledge gained from the yeast and mammalian studies, we know almost nothing about the retrotranslocation step of a plant ERAD pathway. Several earlier studies did suggest the existence of a retrotranslocon in plant cells to move ERAD substrates into the cytosol. A confocal microscopic analysis of subcellular localization of a fusion protein between green fluorescent protein (GFP) with the P-domain of a maize CRT in tobacco leaf protoplasts suggested a retrotransport route from the ER to the cytosol (104). In addition, a series of studies revealed that the A chain (known as RTA) of a ribosome-inactivating toxin, ricin that is normally produced as a dimeric protein of RTA covalently linked to a galactose-binding B chain via a single intramolecular disulfide bond and stored in the central vacuole of the endosperm cells of castor bean (*Ricinus communis*), was detected to be deglycosylated and eventual degraded in the cytosol when expressed alone in tobacco leaf protoplasts (105-107). It is important to mention that ricin and a few other plant toxins were known to exploit the ERAD pathway to reach their cytosolic targets after being internalized by mammalian cells and retrograde-transported from the cell surface to the ER (108). In both yeast and mammalian systems, retrotranslocation of ERAD substrates was driven by ubiquitination (109); however, a recent RTA study using plant protoplasts showed that retrotranslocation is independent of ubiquitination as the lysine-lacking (hence non-ubiquitinated) variant of RTA could still be retrotranslocated from the ER into the cytosol (106), suggesting that the ubiquitination-retrotranslocation coupling might be substrate-dependent.

Substrate Extraction, Processing, and Delivery to the Proteasome

Without regard to the identity of the actual retrotranslocons, ubiquitinated ERAD clients are extracted from the ER lumen ($ERAD_L$ substrates) or ER membrane ($ERAD_{M/C}$ substrates) by a trimeric complex consisting of a homohexameric Cdc48 (p97 or valosin-containing protein in mammals), an AAA-type ATPase and its two substrate-recruiting factors Ufd1 and Npl4 (each having a ubiquitin-binding domain) (110). The $(CDC48)_6$-Ufd-Npl4 complex itself is recruited to the Hrd1/Doa10 E3 complexes by Ubx2 (VIMP for p97/VCP-interacting membrane protein in mammals), one of the 7 ubiquitin regulatory X (UBX) domain-containing proteins in yeast (13 UBX proteins in mammals) (111-113). The current working model posits that extracted ERAD substrates are further processed through antagonistic interactions between an U-box-containing E4 multiubiquitination enzyme Ufd2 and a WD40 repeat-containing protein Ufd3 with unknown enzyme activity plus a deubiquitylating enzyme Otu1, and/or through deglycosylation by the cytoplasmic peptide:*N*-glycanase Png1 (114). The processed ERAD substrates were subsequently delivered to the cytosolic proteasome by Cdc48 in association with two ubiquitin receptors Rad23 and Dsk2, each containing a UBL domain that interacts directly with the cytosolic proteasome and a polyubiquitin-interacting ubiquitin-associated (UBA) domain (114).

The *Arabidopsis* genome encodes three Cdc48 homologs, AtCDC48A, AtCDC48B, and AtCDC48C (115). AtCDC48A was able to complement a yeast *cdc48* mutant (116) and was shown to play a role in the ERAD of a mutant form of MLO and a mutant variant of the *Arabidopsis* vacuolar carboxypeptidase carrying the same Gly-Arg mutation as the yeast CPY* and in the retrotranslocation of RTA and the orphan subunit (RCA A) of

another castor bean toxin agglutinin in plant cells (76, 107, 117). AtCDC48A is likely to be recruited to the ER membrane by UBX-containing proteins as the *Arabidopsis* genome encodes a total of 15 UBX-containing proteins (known as AtPUXs; Table 1.1), some of which were shown to interact with AtCDC48A (118, 119). It remains to be determined which of the 15 AtPUX proteins are actually involved in recruiting an AtCDC48 to the ER membrane-anchored E3 ligase complexes and play a role in degrading known plant ERAD substrates. Our BLAST searches using the known ERAD components of yeast and mammals as query identified multiple homologs of the Ufd1, Ufd2, Ufd3, Npl4, Rad23, Dsk2 but only a single PNGase homolog in *Arabidopsis* (Table 1.1). The functional involvement of these potential ERAD components in an *Arabidopsis* ERAD process remains unknown except AtPNG1, which was recently shown to contain the suspected PNGase activity and could stimulate the degradation of two mutant variants of RTA in an *N*-glycan-dependent manner in yeast cells (120, 121).

Conclusion

Thanks to the rapid progress in recent years for identifying molecular components of plant ERQC/ERAD systems and studying their biochemical functions, we now have a better understanding of the whole protein quality control system in the plant ER. Take *Arabidopsis* as an example: it contains a conserved GII-UGGT-mediated CNX/CRT cycle in retaining incomplete/mis-folded glycoproteins and other chaperones for the glycan-independent folding monitoring and it has a variety of conserved ERAD components that function inside the ER lumen to promote the degradation of several known plant ERAD substrates including two mutant BR receptors. Using reverse genetic

approaches, we have identified candidate ERAD genes in the *Arabidopsis* genome (Table 1.1). The convenient T-DNA insertional mutant and RNAi-mediated knockdown libraries in *Arabidopsis* certainly provide study materials to pursue additional knowledge on these putative ERAD components and their functions. In addition, transgenic *Arabidopsis* lines expressing carefully engineered substrates of glycosylated/non-glycosylated $ERAD_C$/$ERAD_M$ coupled with forward genetic screens and reverse genetic studies will reveal if *Arabidopsis* has several distinct ERAD subpathways using different E3 ligases and adapter proteins that recruits distinct ERAD clients. Similarly, genetic screens for enhancers/suppressors of the *Arabidopsis* wax mutant *cer9* [defective in Doa10A (84)] or *drought hypersensitive 2* mutant [that led to independent discovery of Doa10A (85)] could uncover additional ERAD components, reveal unique features of the plant ERAD processes, and a better understanding of the regulatory function of the plant ERAD system in biosynthetic processes. Proteomic studies with the existing *Arabidopsis* mutants of the ERAD E3 ligases could lead to the discovery of additional biochemical pathways and/or physiological processes regulated by the plant ERAD machinery.

Rationales

Comprehensive studies in yeast and mammalian cells have led to a better understanding of the ERQC/ERAD systems and we have taken advantages of these studies to predict and identify the plant ERQC/ERAD proteins. Despite the rapid progress in recent years, our understanding of the plant ERQC/ERAD processes remains rather limited. Because plants have unique physiological and biological needs, one essential question is whether a forward genetic approach in *Arabidopsis* can identify novel ERQC/ERAD components

that have not yet been characterized in other eukaryotic systems. Chapter 3 will introduce a novel, plant-specific gene named AtEBS7 that was identified in a forward genetic screen that we previously reported (8, 11). EBS7 is a highly conserved gene in the plant lineage and AtEBS7 is responsible for the degradation of several known *Arabidopsis* ERAD substrates including two mutated BRI1 allele and the incomplete/misfolded EFR. In addition, EBS7 participates in the salt and ER stress response, consistent with the former reports about the relationship between ER and environment stress responses (72, 75, 82). The discovery of EBS7 may shed light on the existence of a plant-unique ERAD pathway that is required to handle the specific physiological needs.

Another question in the plant ERQC/ERAD field is whether the combination of the *Arabidopsis* genetics with cutting-edge biochemical studies could reveal novel biochemical functions of known or predicted ERQC/ERAD components and provide satisfactory answers to questions in the general ERQC/ERAD research field. In fact, *Arabidopsis* has proved to be a convenient model to study the *in vivo* function of ERQC/ERAD components. The deletion of essential ERQC/ERAD components may lead to the disruption of protein quality control systems and cause early embryonic lethality in animal models (22, 122). The T-DNA insertional knockout lines for the corresponding *Arabidopsis* genes however, are vital in normal growth conditions despite their deficiency in protein folding and quality control processes (8, 12). Thus the discoveries in *Arabidopsis* provide us a possible way to study the physiological function of these essential genes in a live model using genetics. In Chapter 2, we used this convenience to pursue the physiological function of one important chaperone Calreticulin (CRT) in regulating the folding process of incomplete/misfolded bri1-9 *in vivo*. Our results

illustrated five amino acids and a conserved C-terminal basic tetrapeptide that are indispensable for the chaperone function of AtCRT3.

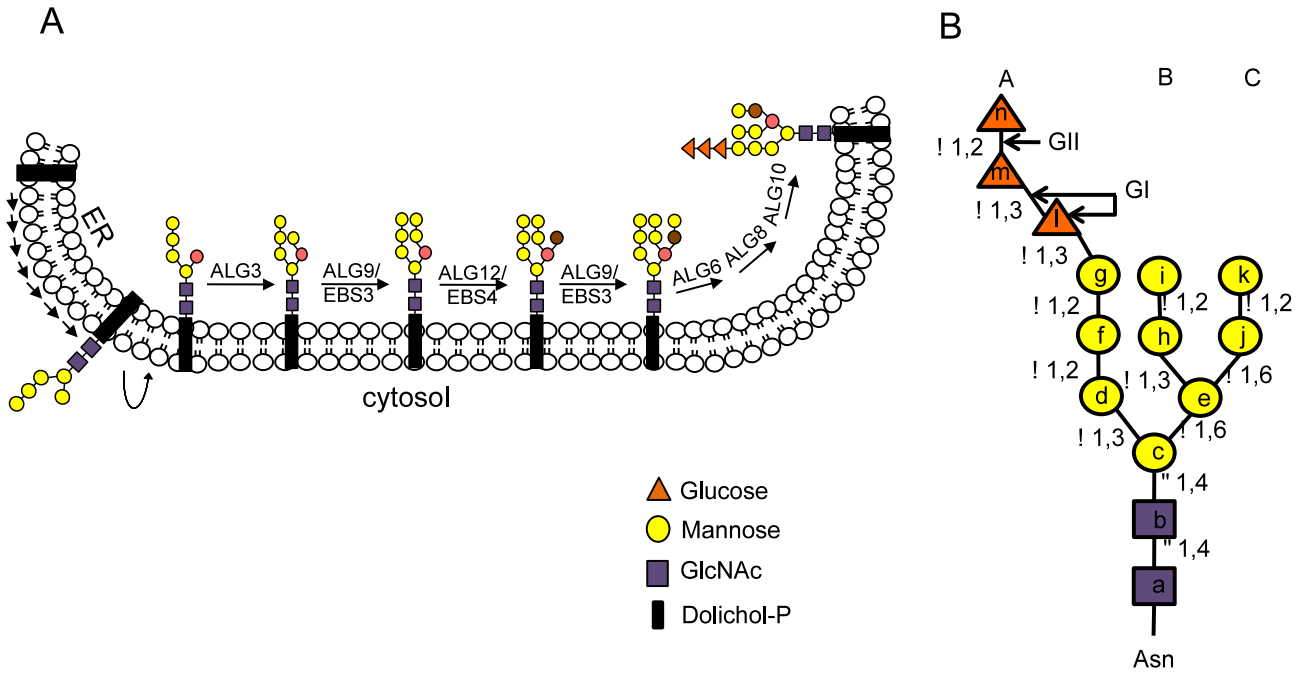

Figure 1.1. N-glycan precursor assembly process in ER

(A) Stepwise assembly of *N*-glycan precursor on the ER membrane. The assembly of the *N*-glycan precursor starts at the cytosolic face of the ER membrane by adding two GlcNAc and five Man residues to the membrane-anchored Dol-PP linker. The resulting Dol-PP-$Man_5GlcNAc_2$ flips over into the ER lumen. Four Man residues are sequentially added to the flipped Dol-PP-$Man_5GlcNAc_2$ by three mannosyltransferases named asparagine-linked glycosylation proteins (ALGs) ALG3, ALG9 (known as EBS3 in *Arabidopsis*) and ALG12 (known as EBS4 in *Arabidopsis*) with the ALG9 catalyzing two reactions of adding the terminal α1,2 Man residues on the middle and right branches. Three Glc residues are subsequently added to the right branch, generating the 14-sugar precursor, Dol-PP-$Glc_3Man_9GlcNAc_2$. Two α1,6 Man residues are marked by brown and salmon color. The Dol-PP linker and different sugar residues are indicated.

(B) The structure of N-linked $Glc_3Man_9GlcNac_2$ glycan with three dimannose branches (branch A, B and C). Lower case letters inside sugar residues represent the order of sugar addition. The sugar linkage bonds and enzymes (GI, GII) that remove the three Glc residues are indicated.

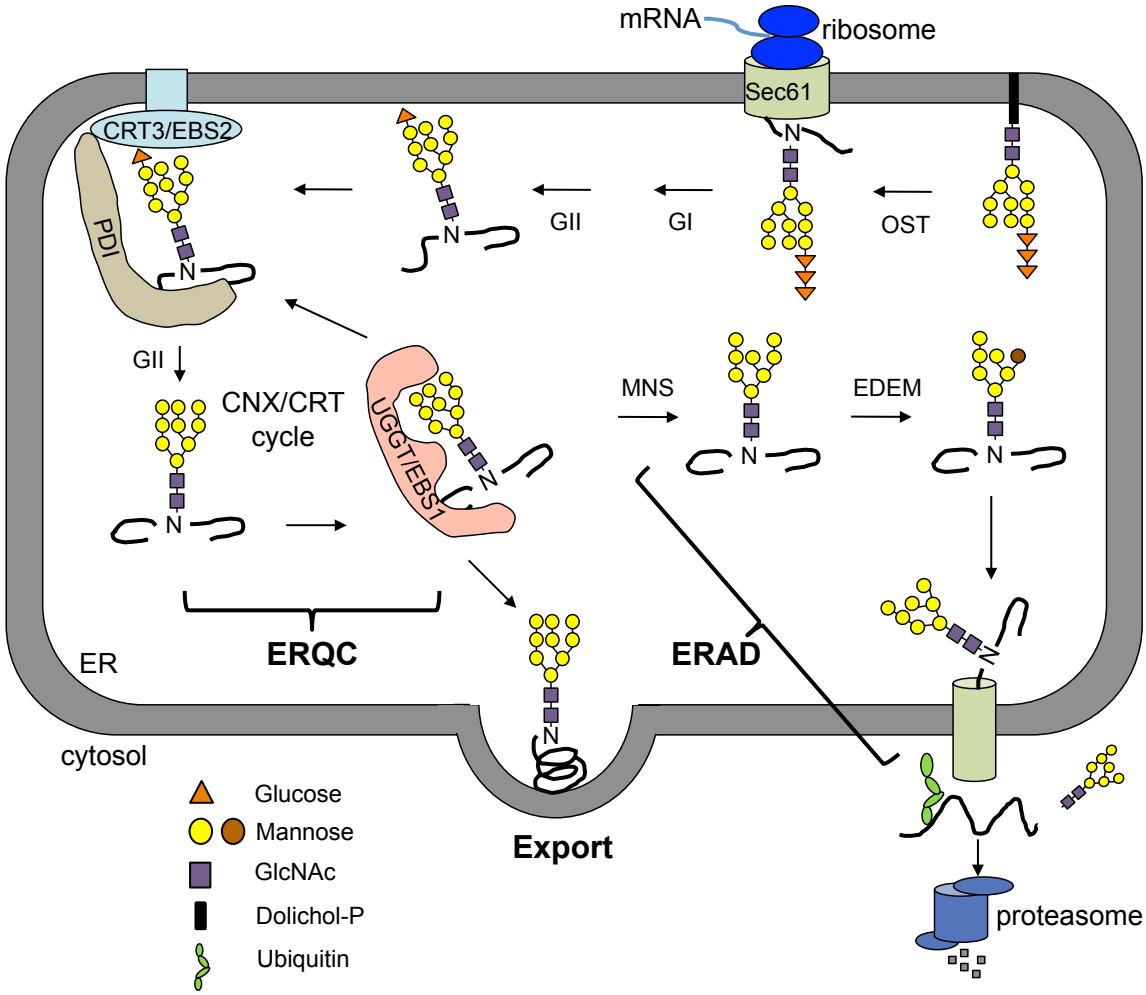

Figure 1.2. An overview of the ERQC/ERAD system.
Two Glc residues on the *N*-glycan of a nascent polypeptide are rapidly trimmed by GI and GII right after being transferred from the Dol-PP-linker. The resulting monoglucosylated *N*-glycans bind the two ER lectins CNX and CRT chaperone-assisted folding. The removal of this last Glc by GII releases a mature polypeptide from CNX/CRT. A correctly folded protein can leave the ER while an incompletely/mis-folded glycoprotein is recognized by UGGT (known as EBS1 in *Arabidopsis*) that adds back a Glc residue to the A branch, permitting its reassociation with CNX/CRT. A glycoprotein that fails to gain its native structure within a certain time window is removed from the folding cycle via sequential trimming of the two terminal α1,2 Man residues of the B and C branch by MNS1 (an ER-localized α1,2-Mannosidase, known as MNS3 in *Arabidopsis*) and Htm1/EDEM. A terminally misfolded glycoprotein with α1,6 Man-exposed glycan is selected to enter the ERAD pathway.

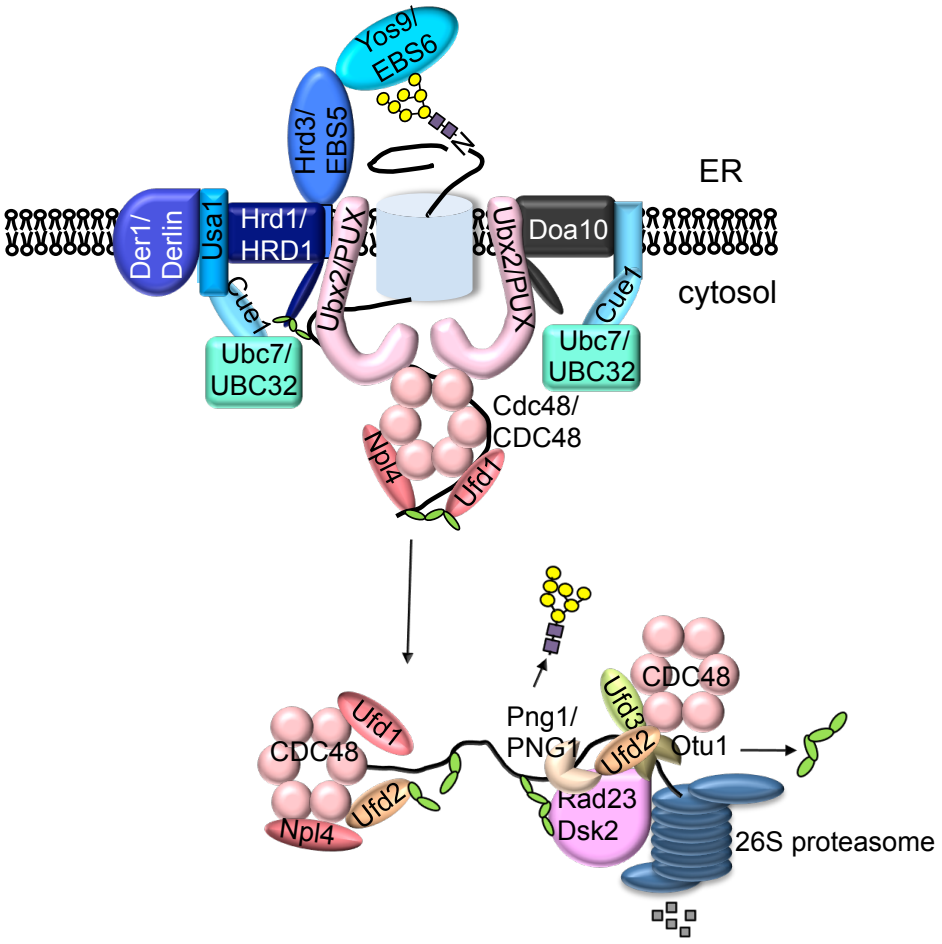

Figure 1.3. A model of ERAD system

An ERAD client that has lesion in membrane-embedded segment ($ERAD_M$) or in ER lumen region ($ERAD_L$) is recruit by Hrd3 (EBS5 in *Arabidopsis*) and Yos9 (EBS6/OS9 in *Arabidopsis*) to the membrane-anchored E3 ligase Hrd1 (AtHrd1a and AtHrd1b in *Arabidopsis*) complex that also contains Cue1, Ubc6 (UBC32 in *Arabidopsis*), Usa1 and Der1. An ERAD substrate with a folding lesion in the cytosolic domain ($ERAD_C$ is recruited to a different ER membrane-anchored E3 ligase complex that contains Doa10 and Ubc6 (or Cue1/Ubc7). The two E3 ligase complexes share similar components on the cytosolic side of the ER membrane, including the substrate-extracting Cdc48-Ufd1-Npl4 trimeric complex and its membrane recruitment factor Ubx2 (one or more AtPUX proteins in *Arabidopsis*). An extracted polyubiquitinated ERAD substrate is processed by Ufd2, Ufd3, Otu1, and/or Png1 (AtPNG1 in *Arabidopsis*), delivered to the cytosolic proteasome with help of Dsk2 and Rad23, and eventually proteolyzed by the 26S proteasome.

Table 1.1. A list of known/predicted components of the *Arabidopsis* ERAD system.

Yeast/Human name	*Arabidopsis* name	Accession number	Reference
Hrd1/HRD1	HRD1A	At3g16090	(73)
	HRD1B	At1g65040	
Hrd3/SEL1L	EBS5/HRD3A	At1g18260	(73)
	HRD3B	At1g73570	
Yos9/OS-9	EBS6/OS9	At5g35080	(72, 74)
Der1/DERLIN	DER1	At4g29330	(100)
	DER2.1	At4g04860	(123)
	DER2.2	At4g21810	(124)
Ubc6/UBE2J1	UBC32	At3g17000	(91, 92)
	UBC33	At5g50430	
	UBC34	At1g17280	
Htm1/EDEM	MNS4	At5g43710	(63)
	MNS5	At1g27520	
Doa10/TEB4	SUD1/CER9/DOA10A	At4g34100	(75, 84, 85)
	DOA10B	At4g32670	
RMA1	RMA1	At4g03510	(81, 83)
	RMA2	At4g28270	
	RMA3	At4g27470	
Ubx2/ERASIN	PUX1	At3g27310	(118, 119)
	PUX2	At2g01650	(125, 126)
	PUX3	At4g22150	
	PUX4	At4g04210	
	PUX5	At4g15410	
	PUX6	At3g21660	
	PUX7	At1g14570	
	PUX8/SAY1	At4g11740	
	PUX9	At4g00752	
	PUX10	At4g10790	
	PUX11	At2g43210	
	PUX12	At3g23605	
	PUX13	At4g23040	
	PUX14	At4g14250	
	PUX15	At1g59550	
Cdc48/p97	CDC48A	At3g09840	(115)
	CDC48B	At2g03670	
	CDC48C	At3g01610	
Npl4/NPL4		At2g47970	
		At3g63000	
Ufd1/UFD1	UFD1	At2g21270	(127)
		At4g38930	
		At2g29070	
		At4g15420	

Ufd2/UFD2		At5g15400	(128)
Png1/PNG1	PNG1	At5g49570	(121)
Rad23/RAD23	RAD23A	At1g16190	(129)
	RAD23B	At1g79650	
	RAD23C	At3g02540	
	RAD23D	At5g38470	

Table 1.2. A list of EBS genes identified in the suppressor screening for *bri1-9*

Yeast/Human name	*Arabidopsis* name	Accession number	Reference
UGGT	EBS1/UGGT	At1g71220	(73)
CRT	EBS2/CRT3	At1g08450	(73)
ALG9	EBS3	At1g16900	(72, 74)
ALG12	EBS4	At1g02145	(100)
Hrd3/SEL1L	EBS5/HRD3A	At1g18260	(73)
	HRD3B	At1g73570	
Yos9/OS-9	EBS6/OS9	At5g35080	(72, 74)

CHAPTER 2
CHARACTERIZATION OF CRITICAL RESIDUES FOR THE LECTIN FUNCTION OF *ARABIDOPSIS* CALRETICULIN 3 IN THE RETENTION OF RECEPTOR-LIKE-KINASES IN THE ENDOPLASMIC RETICULUM

Abstract

Calreticulin (CRT) is a highly conserved chaperone-like lectin that regulates Ca^{2+} homeostasis and participates in protein quality control in the endoplasmic reticulum (ER). CRT and its ER membrane-anchored homolog calnexin (CNX) share a three-domain structure composed of a sugar-binding β-sandwich globular N-domain, an extended central proline-rich P-domain, and an acidic C-domain. *In vitro* biochemical studies coupled with crystallographic analysis of recombinant CRT proteins have identified amino acid residues in the globular N-domain critical for its lectin function. However, no study verifying these *in vitro* findings in a living organism has been reported so far. Many plant species contain more than two CRTs that form two distinct groups: CRT1/CRT2 and CRT3. Previous studies on plant CRTs were focused on their Ca^{2+}-binding function, yet recent studies revealed a crucial role for the *Arabidopsis* CRT3 in ER retention of a mutant brassinosteroid receptor, brassinosteroid-insensitive 1-9 (bri1-9) and in complete folding of a plant immunity receptor EF-Tu Receptor (EFR). Despite these discoveries, little is known about the molecular basis of the functional specification of distinct CRTs. In this study, we used an *Arabidopsis* insertional mutant of CRT3, *ebs2-8* (*EMS*

mutagenized bri1 suppressor 2-8), in the *bri1-9* background as a convenient genetic system and investigate the physiological importance of amino acid residues of a predicted sugar-binding site of an *Arabidopsis* CRT in a plant protein quality-control process. Our results provided an *in vivo* genetic confirmation for the critical role of the five conserved amino acid residues in the predicted lectin site of a plant CRT for retaining structurally imperfect glycoprotein in the ER. Besides, we identified a highly conserved basic tetrapeptide $Arg^{392}Arg^{393}Arg^{394}Lys^{395}$ on the C terminus of CRT3 that is essential for its retention function.

Introduction

Calreticulin (CRT) is a chaperone-like lectin that regulates intracellular Ca^{2+} homeostasis and functions as a key component of a protein quality control mechanism in the endoplasmic reticulum (ER) (20). The protein quality control function is mediated by the N-globular domain of the two ER lectins, whereas the regulatory role in Ca^{2+} homeostasis is unique to CRT due to its acidic C-terminal domain rich in acidic residues responsible for low affinity but high capacity Ca^{2+}-binding (21). CRT and its membrane-anchored homolog calnexin (CNX) specifically recognize and bind newly synthesized and incompletely/mis-folded glycoproteins through their monoglucosylated asparagine (Asn or N)-linked glycans $Glc_1Man_9GlcNac_2$ (Glc, Man and GlcNac denoting glucose, mannose and N-acetylglucosamin, respectively), which are generated by sequential trimming of two glucose residues from the preassembled 14-sugar oligosaccharide $Glc_3Man_9GlcNac_2$ containing three covalently-linked glucose residues on one of its three mannose branches (4). The removal of the last glucose residue by a unique glucosidase

releases these glycoproteins from binding CRT/CNX, while reglucosylation by an ER protein folding sensor, UDP-glucose:glycoprotein glucosyltransferase (UGGT) that is capable of discriminating native glycoproteins from their incompletely/mis-folded counterparts, permitting another round of CRT/CNX binding (130). It is thought that repeated actions of the glucosidase and UGGT drive cycles of dissociation and reassociation of client glycoproteins with CRT/CNX, a process widely known as "the CRT/CNX cycle" (4).

CRT and CNX share a three-domain structural organization consisting of a sugar-binding β-sandwich N-globular domain, a central proline-rich P-domain and a C-terminal domain. The previously reported crystal structure of CNX identified the carbohydrate binding sites on the concave β sheet of the N-globular domain (131). The following mutagenesis study confirmed that these amino acids are dispensable for the molecular chaperone function of CNX but are essential for its oligosaccharide binding capability (132). Based on the homology between CNX and CRT, sugar-binding sites that are critical for the lection function of CRT were identified and confirmed by both *in vitro* biochemical and crystallographic analysis (133-135). However, these findings have not been verified in a living organism probably due to the embryonic lethality of CRT knockout mice.

Both mammals and plants contain multiple CRTs. In addition to its roles in regulating intracellular Ca^{2+} homeostasis and participating in a quality control process, the mammalian CRT1 is a multifaceted protein that is involved in a wide range of cellular processes at many different cellular locations, including the cytosol, the nucleus, the plasma membrane and the extracellular matrix (20). By contrast, little is known about the physiological function of the mammalian CRT2 that is highly expressed in testis and does

not bind Ca^{2+} (43-45). Many plant species including *Arabidopsis* have three CRTs that are classified into two functional groups: CRT1/CRT2 and CRT3 based on sequence alignment and phylogeny analysis (12, 46, 47). The *Arabidopsis* CRT1/CRT2 and CRT3 share similar sugar-binding N-domain and the central P-domain. In fact, previous reports suggested that these two domains are interchangeable between the two CRT groups (12). However, their C-terminal domains and their co-expression profiles are quite distinct. CRT1 and CRT2, similar to the mammalian CRT1, have an acidic C-terminal domain and are co-expressed with known ER chaperones and folding catalysts, whereas CRT3 has a C-terminal domain enriched with basic residues such as histidine (His or H), arginine (Arg or R) and lysine (Lys or K) and is co-expressed with genes involved in plant stress responses (12, 48). Compared with the well-studied mammalian CRT1, our knowledge on the physiological functions of plant CRTs is rather limited. Most of the plant CRT studies have been mainly focused on the regulatory role in intracellular Ca^{2+} homeostasis for the CRT1/CRT2 family with occasional reports suggesting their chaperone function (136, 137).

Several recent genetic studies in *Arabidopsis* have revealed a unique role of CRT3 in the quality control of two receptor-like kinases (8, 13, 14). The first one is EF-Tu Receptor (EFR) that binds the bacterial translational elongation factor Tu to triggers a plant innate immunity response (16), and the second one is a mutant variant of BRassinosteroid-Insensitive I (BRI1) that functions as the receptor for brassinosteroids (BRs) to initiate a phosphorylation-mediated signaling cascade critical for normal plant growth (9, 138). Loss-of-function mutations in CRT3 or UGGT cause misfolding and subsequent degradation of EFR, thus making *Arabidopsis crt3* or *uggt* mutants insensitive to EF-Tu

or its biologically active epitope elf18 (13, 14). By contrast, neither *crt3* nor *uggt* mutations has any detectable effect on the wild-type BRI1 protein (8, 12). Instead, loss-of-function *crt3* (also known as *ebs2* for *EMS mutagenized bri1 suppressor 2*) and *uggt* (also known as *ebs1*) mutations were recovered in a genetic screen for extragenic suppressors of a weak *Arabidopsis* dwarf mutant *bri1-9* carrying a Ser662-Phe mutation in the ligand-binding domain of BRI1 (8, 12). These studies revealed that bri1-9 is a structurally misfolded but functionally competent BR receptor that is retained in the ER partly by the UGGT-CRT3-mediated quality control system. Loss-of-function *ebs1/uggt* and *ebs2/uggt* mutations destroy this system, permitting export of almost 50% bri1-9 proteins to the plasma membrane where the mutant BR receptor initiates a BR signaling cascade to promote plant growth.

Despite high sequence similarity with CRT3 and their coexpression patterns with known ER chaperones and folding enzymes, neither CRT1 nor CRT2 plays a role in retaining bri1-9 in the ER. Neither CRT1 nor CRT2 interacts with bri1-9, and simultaneous elimination of CRT1 and CRT2 fails to suppress the *bri1-9* mutation (12). To investigate the biochemical basis of the apparent functional difference between CRT1/CRT2 and CRT3, we previously used two chimeric transgene constructs of *CRT1* and *CRT3* to show that the C-terminal domain of the *Arabidopsis* CRT3 is essential for its quality control function that retains bri1-9 in the ER. A chimeric CRT protein, CRT1NP::CRT3C consisting of the N- and P-domains of CRT1 and the C-domain of CRT3, was able to complement the T-DNA insertional *ebs2-8* mutation, whereas a reciprocal chimeric CRT3NP::CRT1C protein failed to complement the same mutation (12).

In the current study, we utilized the *Arabidopsis* CRT3 mutant as a model system to pursue which functional domain is responsible for the specificity of CRT3 over other CRTs. We identified and tested two clusters of basic residues of the CRT3′s C-terminal domain for retaining the mutant BR receptor in the ER and for completing the folding process of the *Arabidopsis* immunity receptor EFR. Besides, we combined site-directed mutagenesis and transgenic complementation experiments to investigate the physiological significance of several amino acid residues of a predicted sugar-binding site of an *Arabidopsis* CRT in a plant protein quality-control process.

Results

Comparison of *Arabidopsis* CRT3 with other CRTs

In this study, we used the T-DNA insertional *ebs2-8* mutant as a convenient genetic system to investigate the physiological importance of several amino acid residues of a predicted sugar-binding site of an *Arabidopsis* CRT in a plant protein quality-control process. Our previous studies showed that loss-of-function mutations in a plant-specific CRT, CRT3, suppress a unique *Arabidopsis* dwarf mutation, *brassinosteroid-insensitive 1–9* (*bri1-9*) of the plant brassinosteroid (BR) receptor BRI1, which keeps a structurally imperfect but biochemically competent BR receptor in the ER via a CRT3–bri1-9 binding (8, 12). In order to find potential lectin binding sites in *Arabidopsis* CRT3 (AtCRT3), we did a sequence alignment of the three *Arabidopsis* CRTs, a rice CRT3 homolog, with two mammalian CRTs (mCRT and HsCRT) (Fig. 2.1). It has been previously reported that six amino acid residues in mouse CRT were considered as carbohydrate binding sites (133, 135). Among them, Tyr118 (Y118), Lys120 (K120), Tyr137 (Y137), Met140

(M140), Asp144 (D144) are highly conserved between mammalian and plant species. Although the last lectin-binding site in mouse and human CRT is aspartic acid (Asp317) while in plant species it is glutamic acid (Glu327), these two amino acids are very similar in all. Molecular modeling of a 3-D structure of CRT3 also supported the hypothesis that these six conserved amino acids may directly involve in binding monoglucosylated N-glycan (Fig. 2.2A-B). Besides, we picked Asp169 (D169) as the seventh candidate as its corresponding residue in a mammalian CNX was shown to be involved in glucose binding (131).

Detecting the functional importance of predicted lectin-binding sites in AtCRT3 *in vivo*

To verify the physiological importance of these residues in the predicted lectin function of CRT3, we performed site-directed mutagenesis experiments to mutate each of these residues to alanine (A) or phenylalanine (F) in a genomic *CRT3* transgene (*gCRT3*) that could complement a null *ebs2* mutation (12). We reasoned that, if these conserved residues are involved in binding monoglucosylated N-glycans of the ER-retained bri1-9, their mutations should destroy the 'bri1-9-retention' activity of CRT3 and their corresponding *CRT3* transgenes should fail to complement an *ebs2* mutation in the *bri1-9* background. To test our hypothesis, we individually transformed each of the mutant *gCRT3* transgenes into the *Arabidopsis ebs2-8 bri1-9* double mutant that carries a T-DNA insertional allele of CRT3 with the DNA being inserted in the second intron (12).

Because a missense mutation of a key residue in CRT3 could lead to protein misfolding and subsequent ER-associated degradation (ERAD) (12), we performed an immunoblotting experiment to ensure that each of the mutant *gCRT3* transgenes did lead

to accumulation of detectable amounts of CRT3 in the transgenic *ebs2-8 bri1-9* plants. As shown in Fig. 2.3A, each representative transgenic line did accumulate CRT3 at a level equal to or higher than that of the wild-type or the *bri1-9* mutant, indicating that the introduced mutations did not lead to significant degradation of the mutant CRT3 proteins. We first analyzed the overall plant morphology to determine whether a mutant gCRT3 transgene was able to complement the *ebs2-8* mutation in the *ebs2-8 bri1-9* double mutant. As shown in Fig. 2.3B, all introduced mutant *gCRT3* transgenes except *gCRT3 (Y137F)* and *gCRT3(D169A)* failed to rescue the *ebs2-8* mutation, as the morphology of the corresponding representative transgenic plants were indistinguishable from that of *ebs2-8 bri1-9*. In addition to the morphological analysis, we also performed a convenient biochemical assay, widely known as endoglycosidase (Endo-H) sensitivity assay, which can directly assess the 'bri1-9-retention' activity of various mutant CRT3 proteins (12). Endo-H only removes the high-mannose-type (HM) N-glycans on the ER-localized glycoprotein but cannot cut Golgi-processed complex-type (CT) N-glycans. Consistently with our previous study (8, 12), the wild-type BRI1 is largely Endo H-resistant, the mutant bri1-9 protein is extremely sensitive to the Endo-H treatment, and the *ebs2-8* mutation compromises the ER retention of bri1-9, allowing its ER export and plasma membrane targeting. As expected from their plant morphological phenotypes, the Endo-H-resistant band of bri1-9 was still detectable in all *ebs2-8 bri1-9*-like *gCRT3* transgenic plants but became almost undetectable in the phenotypically rescued *ebs2-8 bri1-9 gCRT3(D169A)* and *ebs2-8 bri1-9 gCRT3(Y137F)* transgenic plants (Fig. 2.4A-B). These results further confirmed that the D169A/Y137F-mutated CRT3 could still retain bri1-9 in the ER.

Identification of two positively charged tetrapeptides that may contribute to the client specificity of different CRTs

Although the N-terminal parts of AtCRT1, AtCRT2 and AtCRT3 are relatively conserved, their C terminuses are quite distinct. One of the major differences between CRT1/2 and CRT3 is the net charge of their C-domains with CRT1/CRT2 being rich in acidic residues and CRT3 being rich in basic residues (12). We decided to investigate the effects of mutating basic residues on the quality control function of the *Arabidopsis* CRT3. Sequence alignment of CRT3 homologs of other plant species identified at least two clusters of positively charged residues. The first basic tetrapeptide $Arg^{392}Arg^{393}Arg^{394}Lys^{395}$ (referred hereinafter as RRRK or simply R3K) is highly conserved among CRT3 homologs with occasional substitutions at the last residue, while the second tetrapeptide $Arg^{401}Arg^{402}Arg^{403}Arg^{404}$ (referred hereinafter as RRRR or simply R4) is less conserved but within a region that has > 50% positively charged residues (Fig. 2.5).

A conserved positively charged tetrapeptides RRRK is essential for AtCRT3 to retain the misfolded bri1-9 in ER

We performed PCR-based site-directed mutagenesis with a genomic *gCRT3* transgene, to mutate each basic residue of the two chosen tetrapeptides to either the acidic residue glutamate (E) or the non-charged small residue alanine (A). We first examined the morphology of the resulting transgenic plants for each mutant $gCRT3^{M}$ transgene. We reasoned that if an RRRK-EEEE (R3K-E4), RRRK-AAAA (R3K-A4), RRRR-EEEE (R4-E4), or RRRR-AAAA (R4-A4) mutation destroys the "bri1-9-retainner" function of CRT3, we would expect that the corresponding $gCRT3^{M}$ transgene should fail to rescue

the *ebs2-8* mutation and the corresponding *gCRT3^{M} ebs2-8 bri1-9* transgenic plants should be morphologically similar to the *ebs2-8 bri1-9* double mutant. Otherwise, the resulting transgenic mutants should be phenotypically similar to the *bri1-9* single mutant. As shown in Fig. 2.6A, the *gCRT3^{M} (R3K-E4) ebs2-8 bri1-9* and *gCRT3^{M} (R3K-A4) ebs2-8 bri1-9* transgenic mutants were morphologically similar to *ebs2-8 bri1-9*, whereas the *gCRT3^{M} (R4-E4) ebs2-8 bri1-9* or *gCRT3^{M} (R4-A4) ebs2-8 bri1-9* transgenic plants are phenotypically similar to the *bri1-9* single mutant. Because substitution of certain amino acid residues in a secretory/membrane protein may lead to misfolding and subsequent ER-associated degradation (8, 12), which could explain why the CRT3^{M} (R3K-E4) or CRT3^{M} (R3K-A4) failed to complement the *ebs2-8* mutation, we performed an immunoblot assay to analyze the CRT3^{M} abundance in selected transgenic lines. As shown in Fig. 2.6B, representative transgenic lines accumulated more CRT3^{M} protein than the wild-type CRT3 in wild type or the *bri1-9* single mutant. The increased abundance of CRT3^{M} compared with the endogenous CRT3 might be caused by multiple insertions of a *gCRT3^{M}* transgene or insertion of a *gCRT3^{M}* transgene into a more active chromatin region of the *Arabidopsis* genome. Thus, we concluded that the first basic tetrapeptide R3K is essential but the second basic tetrapeptide R4 is dispensable for the "bri1-9-retention" activity of CRT3.

We performed the Endo-H assay to further confirm our conclusion. Fig. 2.7 shows that no Endo-H resistant band was detected in *bri1-9* or the *gCRT3^{M} (R3K-E4) ebs2-8 bri1-9* or *gCRT3^{M} (R3K-A4) ebs2-8 bri1-9* transgenic lines, suggesting that CRT3^{M} (R4-E4) or CRT3^{M} (R4-A4) was still capable of retaining bri1-9 in the ER. By contrast, both Endo-H-resistant and Endo-H-sensitive forms of bri1-9 were detected in the parental *ebs2-8*

bri1-9 double mutant and the two *gCRT3^{M} (R4-E4/A4) ebs2-8 bri1-9* transgenic lines, indicating that the CRT3^{M} (R3K-E4/A4) lost the "bri1-9-retention" activity. These results therefore provided a biochemical confirmation for the above conclusion.

Correct folding of EFR requires the conserved positively charged tetrapeptides RRRK but not RRRR in AtCRT3

Recent studies have also implicated an essential role of CRT3 in ensuring the correct folding of a BRI1-like receptor kinase EFR (13, 14), which functions as a cell surface-localized receptor for the bacterial translational elongation factor Tu (EF-Tu) to trigger a plant innate immunity response (16). Loss-of-function *crt3* mutations result in incomplete folding and subsequent ER-associated degradation of EFR (13). We were therefore interested in knowing whether the conserved basic residue cluster RRRK is also critical for the quality control function of CRT3 in facilitating the complete folding of EFR. The total protein extracts of the wild type, *bri1-9*, *ebs1-3 bri1-9*, *ebs2-8 bri1-9* and 4 representative *gCRT3^{M}* transgenic lines were analyzed for the abundance of EFR. Consistent with the previous reports (13, 14), no EFR protein was detectable in either *ebs1-3 bri1-9* or *ebs2-8 bri1-9* double mutants, although the immunity receptor was readily detected in the wild-type control or *bri1-9* (Fig. 2.8A). Importantly, while the wild-type level of EFR was detected in the *gCRT3^{M} ebs2-8 bri1-9* transgenic plants expressing the mutant CRT3^{M} (R4-E4) or CRT3^{M} (R4-A4) protein, no EFR was detectable in the two other transgenic lines expressing CRT3^{M}(R3K-E4) or CRT3^{M}(R3K-A4) (Fig. 2.8A).

It is possible that the second site mutations (R4-E4 and R4-A4) had an effect on the "folding facilitator" function of CRT3 but inhibits the subsequent degradation step of the

ER quality control system, which could also lead to detectable amount of EFR in the corresponding transgenic *gCRT3*^{M} *ebs2-8 bri1-9* mutants. If this were true, we would expect that the EFR proteins accumulated in the *gCRT3*^{M}*(R4-E4) ebs2-8 bri1-9* or *gCRT3*^{M}*(R4-A4) ebs2-8 bri1-9* transgenic mutants should remain misfolded and thus be non-functional in response to EF-Tu or its biologically active peptides such as elf18 (139). To investigate this possibility, we performed a simple elf18 sensitivity assay that relies on the inhibitory effect of the EF-Tu-derived peptide on seedling growth(139). As shown in Fig. 2.8B, the *ebs2-8 bri1-9* double mutant and the *gCRT3*^{M}*(R3K-E4) ebs2-8 bri1-9* and *gCRT3*^{M}*(R3K-A4) ebs2-8 bri1-9* transgenic lines could continue to grow after 10-d growth in the presence of 100 nM elf18, whereas the growth of the other two *gCRT3*^{M} *ebs2-8 bri1-9* transgenic lines were completely inhibited by the elf18 treatment, similar to the wild-type control and the *bri1-9* single mutant. This result indicated that the EFR protein is likely transported to the plasma membrane to be a functional receptor to sense elf18. Indeed, an Endo-H assay (Fig. 2.8C) revealed that the EFR protein is largely resistant to the Endo-H treatment in the *gCRT3*^{M} *(R4-E4) ebs2-8 bri1-9* and *gCRT3*^{M} *(R4-A4) ebs2-8 bri1-9* transgenic lines, which was similar to the EFR in wild type or *bri1-9* plants.

Discussion

In this study, we combined site-directed-mutagenesis and transgenic complementation experiments to investigate the physiological importance of seven conserved amino acid residues of the predicted lectin site of a plant CRT for retaining structurally imperfect but biochemically competent glycoprotein in the ER. Six out of seven conserved amino acids

(Y118, K120, Y137, M140, D144 and E327) are essential for the proper retention of bri1-9. Consistently with earlier *in vitro* studies and a recent structural analysis (133, 135), the D169A mutation had no detectable effect on the CRT3 function, indicating that the mutant CRT3 (D169A) largely maintains the 'bri1-9-retaining' activity of the wild-type CRT3. Interestingly, our study also suggested that the aromatic ring of the Y137 residue is more important than its hydroxyl group for the biological function of CRT3, as Y137A transgenic plant fell to rescue the *ebs2-8* mutation while the Y137F trasngene could complement the loss-of-function of a wild-type *AtCRT3* in retaining bri1-9 in ER. While our result is similar to an earlier *in vitro* study that revealed reduced but not abolished sugar-binding activity by the Y–F mutation (133), it is inconsistent with the recent structural analysis suggesting an essential role of the hydroxyl group in forming a key hydrogen bond with the glucose moiety of a monoglucosylated N-glycan (135). A structural analysis of a sugar-bound AtCRT3 is needed to determine the exact contributions of the two functional groups of the polar aromatic residue for glucose binding. Given the fact that the sugar-binding N-domain and the central P-domain are interchangeable between CRT3 and CRT1/CRT2 in *Arabidopsis* (12), our conclusion on the roles of the five conserved residues also applies to the other two *Arabidopsis* CRTs and other plant CRTs that have diverse functions in plant growth/development and stress responses (137).

In addition, we identified two basic tetrapeptides of the C-terminal domain in AtCRT3 and detected their importance for the quality control function of the protein. Our results showed that the first and more conserved basic residue cluster of RRRK is essential but the second less conserved basic tetrapeptide RRRR is dispensable for the quality control

function of CRT3 to retain bri1-9 in the ER and to facilitate the complete folding of EFR. However, these residues in RRRK are unlikely to be directly involved in binding monoglucosylated N-glycans as recent structural analyses and the above mutagenesis experiments indicated that the key residues for its lectin function are on the concave surface of the N-terminal globular domain largely formed by a sandwich of a sevenstranded concave β-sheet and a six-stranded convex β-sheet (133-135, 140). Given a recent discovery showing Ca^{2+}-dependent interactions between the lectin-binding N-globular domain and the acidic C-terminal domain (141), it is quite possible that the conserved basic residue cluster (RRRK) might play a similar structural role in stabilizing the β-sandwich N-globular domain critical for its lectin function. Alternatively, the highly conserved basic tetrapeptide RRRK might be involved in creating a protein-binding surface for interaction with amino acids of its client proteins (140). A third possibility is that the positively charged amino residues of the RRRK tetrapeptide might interact with negatively charged phospholipids on the ER membrane, thus regulating the sub-organelle distribution of CRT3 for its quality control function for transmembrane receptor-like kinases such as bri1-9 and EFR. Biochemical and biophysical studies of wild-type and mutant C-terminal domains of CRT3 and crystallographic analysis of the full-length CRT3 protein will certainly lead to a better understanding of the unique biochemical function of the basic C-domain of the plant-specific CRT.

Materials and Methods

Plant materials, growth conditions

Arabidopsis thaliana ecotype Columbia-0 (Col-0) is the parental line for all mutants and transgenic plants described in this study. The T-DNA insertional mutant of CRT3 (*ebs2-8/SALK_051336*) was obtained from the *Arabidopsis* Biological Resource Center at the Ohio State University. Methods for seed sterilization and conditions for plant growth were described previously (142).

elf18 sensitivity assay

For the elf18-induced seedling growth inhibition assay, seedling were germinated and grown on half-strength Murashige and Skoog (MS) agar medium for 7 d and were subsequently submerged in half-strength MS liquid medium containing 100 nM elf18 for 10 d before photographing (13).

Plasmids construction and Generation of Transgenic Plants

The g*CRT3* construct *pPZP222-pCRT3::gCRT3-cCRT3* plasmid was previously described (12). We used this plasmid as the template and performed PCR-based mutagenesis using the Stratagene's QuickChange® site-directed mutagenesis kit (Stratagene) to make the following mutations: $R^{392}R^{393}R^{394}K^{395}$ to EEEE (R3K-E4) or AAAA (R3K-A4) and $R^{401}R^{402}R^{403}R^{404}$ to EEEE (R4-E4) or AAAA (R4-A4). The resulting mutant $gCRT3^{M}$ transgenes were individually transformed into the *Arabidopsis ebs2-8 bri1-9* double mutant by the *Agrobacterium*-mediated vacuum infiltration (143).

Endo H treatment and immunoblot

Two-week-old *Arabidopsis* seedlings were ground in liquid N_2, dissolved in 2× SDS buffer, boiled for 10 min and centrifuged at 12,000 × g for 10 min to remove cellular debris. The supernatants were incubated with or without 1,000 U of Endo Hf (P0703,

New England Biolabs) in the supplied G5 buffer at 37°C for 1.5 h. The resulting protein samples were separated by 7% (for detecting bri1-9 or EFR) or 10% SDS/PAGE (for detecting CRT3/CRT3^{M}), and analyzed by immunoblotting with antibodies raised against the C-terminal domain of CRT3 (12), BRI1 (144) and EFR (74).

Figure 2.1. Sequence alignment of *Arabidopsis* CRT3 with other CRTs
Sequence alignment of CRTs from *Arabidopsis thaliana* (*At*), *Oryza sativa* (*Os*), *Mus musculus* (*m*), and *Homo sapiens* (*Hs*). Multiple sequence alignments of amino acid residues of AtCRT3 (NP_563816), OsCRT3 (BAC06263), AtCRT1 (NP_176030), AtCRT2 (NP_172392), mCRT (AAH03453), and HsCRT (AAB51176) were performed using the ClustalW program (http://mobyle.pasteur.fr/cgi-bin/portal.py). Aligned sequences were color-shaded at a BoxShade 3.31 web server (http://mobyle.pasteur.fr/cgi-bin/portal.py). Residues identical in at least four proteins are shaded in red while similar amino acid residues are shaded in cyan. Diamonds indicate residues predicted to be involved in N-glycan binding. The N-globular domain, the central P-domain, and the C-terminal domain are indicated by blue box, green underline, and yellow box, respectively.

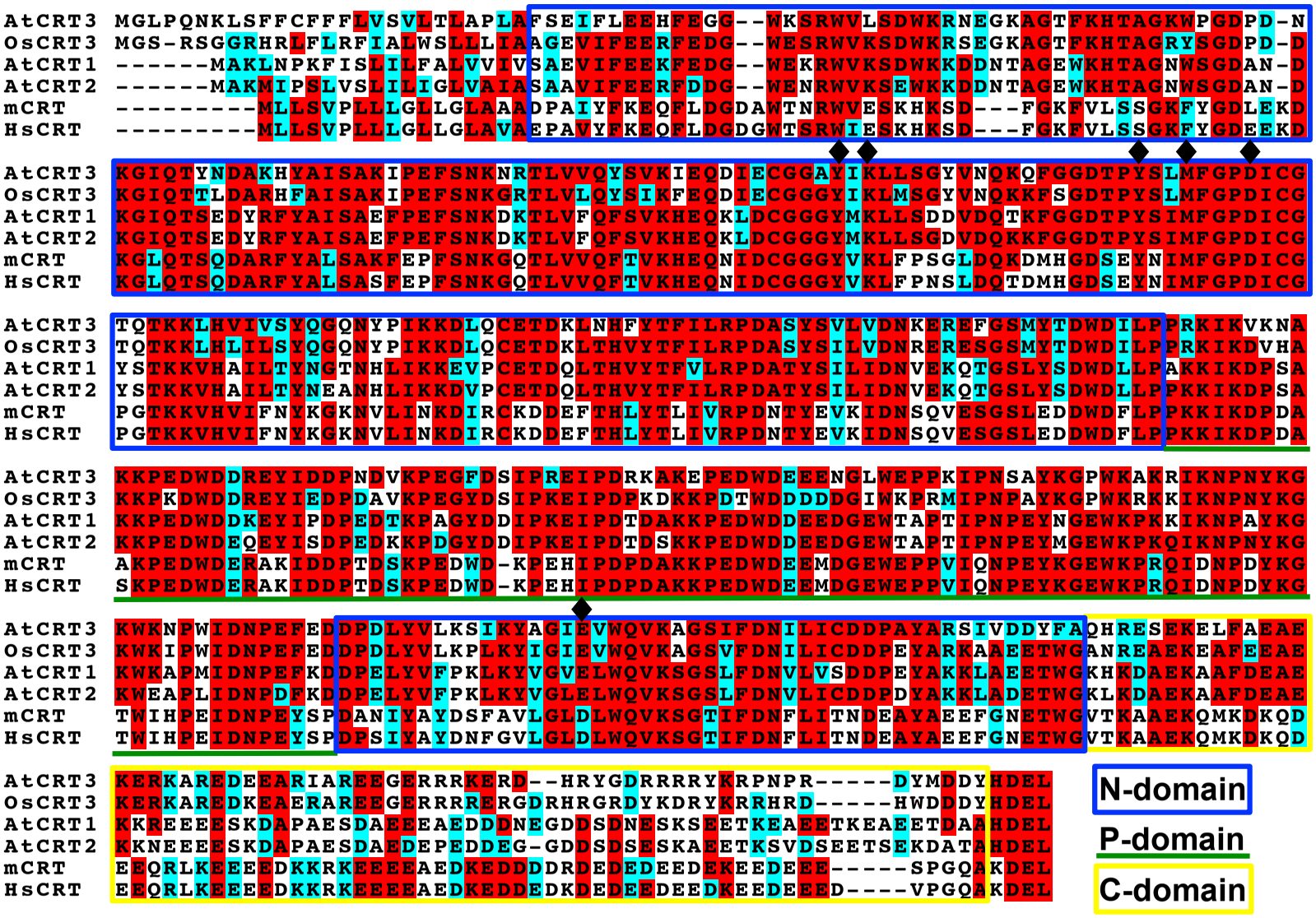
AtCRT3 MGLPQNKLSFFCFFFLVSVLTLAPLAFSEIFLEEHFEGG--WKSRWVLSDWKRNEGKAGTFKHTAGKWPGDPD-N
OsCRT3 MGS-RSGGRHRLFLRFIALWSLLLIAAGEVIFEERFEDG--WESRWVKSDWKRSEGKAGTFKHTAGRYSGDPD-D
AtCRT1 ------MAKLNPKFISLILFALVVIVSAEVIFEEKFEDG--WEKRWVKSDWKKDDNTAGEWKHTAGNWSGDAN-D
AtCRT2 ------MAKMIPSLVSLILIGLVAIASAAVIFEERFDDG--WENRWVKSEWKKDDNTAGEWKHTAGNWSGDAN-D
mCRT ---------MLLSVPLLLGLLGLAAADPAIYFKEQFLDGDAWTNRWVESKHKSD---FGKFVLSSGKFYGDLEKD
HsCRT ---------MLLSVPLLLGLLGLAVAEPAVYFKEQFLDGDGWTSRWIESKHKSD---FGKFVLSSGKFYGDEEKD
AtCRT3 KGIQTYNDAKHYAISAKIPEFSNKNRTLVVQYSVKIEQDIECGGAYIKLLSGYVNQKQFGGDTPYSLMFGPDICG
OsCRT3 KGIQTTLDARHFAISAKIPEFSNKGRTLVLQYSIKFEQDIECGGGYIKLMSGYVNQKKFSGDTPYSLMFGPDICG
AtCRT1 KGIQTSEDYRFYAISAEFPEFSNKDKTLVFQFSVKHEQKLDCGGGYMKLLSDDVDQTKFGGDTPYSIMFGPDICG
AtCRT2 KGIQTSEDYRFYAISAEFPEFSNKDKTLVFQFSVKHEQKLDCGGGYMKLLSGDVDQKKFGGDTPYSIMFGPDICG
mCRT KGLQTSQDARFYALSAKFEPFSNKGQTLVVQFTVKHEQNIDCGGGYVKLFPSGLDQKDMHGDSEYNIMFGPDICG
HsCRT KGLQTSQDARFYALSASFEPFSNKGQTLVVQFTVKHEQNIDCGGGYVKLFPNSLDQTDMHGDSEYNIMFGPDICG
AtCRT3 TQTKKLHVIVSYQGQNYPIKKDLQCETDKLNHFYTFILRPDASYSVLVDNKEREFGSMYTDWDILPPRKIKVKNA
OsCRT3 TQTKKLHLILSYQGQNYPIKKDLQCETDKLTHVYTFILRPDASYSILVDNRERESGSMYTDWDILPPRKIKDVHA
AtCRT1 YSTKKVHAILTYNGTNHLIKKEVPCETDQLTHVYTFVLRPDATYSILIDNVEKQTGSLYSDWDLLPAKKIKDPSA
AtCRT2 YSTKKVHAILTYNEANHLIKKDVPCETDQLTHVYTFILRPDATYSILIDNVEKQTGSLYSDWDLLPPKKIKDPSA
mCRT PGTKKVHVIFNYKGKNVLINKDIRCKDDEFTHLYTLIVRPDNTYEVKIDNSQVESGSLEDDWDFLPPKKIKDPDA
HsCRT PGTKKVHVIFNYKGKNVLINKDIRCKDDEFTHLYTLIVRPDNTYEVKIDNSQVESGSLEDDWDFLPPKKIKDPDA
AtCRT3 KKPEDWDDREYIDDPNDVKPEGFDSIPREIPDRKAKEPEDWDEEENGLWEPPKIPNSAYKGPWKAKRIKNPNYKG
OsCRT3 KKPKDWDDREYIEDPDAVKPEGYDSIPKEIPDPKDKKPDTWDDDDDGIWKPRMIPNPAYKGPWKRKKIKNPNYKG
AtCRT1 KKPEDWDDKEYIPDPEDTKPAGYDDIPKEIPDTDAKKPEDWDDEEDGEWTAPTIPNPEYNGEWKPKKIKNPAYKG
AtCRT2 KKPEDWDEQEYISDPEDKKPDGYDDIPKEIPDTDSKKPEDWDDEEDGEWTAPTIPNPEYMGEWKPKQIKNPNYKG
mCRT AKPEDWDERAKIDDPTDSKPEDWD-KPEHIPDPDAKKPEDWDEEMDGEWEPPVIQNPEYKGEWKPRQIDNPDYKG
HsCRT SKPEDWDERAKIDDPTDSKPEDWD-KPEHIPDPDAKKPEDWDEEMDGEWEPPVIQNPEYKGEWKPRQIDNPDYKG
AtCRT3 KWKNPWIDNPEFEDDPDLYVLKSIKYAGIEVWQVKAGSIFDNILICDDPAYARSIVDDYFAQHRESEKELFAEAE
OsCRT3 KWKIPWIDNPEFEDDPDLYVLKPLKYIGIEVWQVKAGSVFDNILICDDPEYARKAAEETWGANREAEKEAFEEAE
AtCRT1 KWKAPMIDNPEFKDDPELYVFPKLKYVGVELWQVKSGSLFDNVLVSDDPEYAKKLAEETWGKHKDAEKAAFDEAE
AtCRT2 KWEAPLIDNPDFKDDPELYVFPKLKYVGLELWQVKSGSLFDNVLICDDPDYAKKLADETWGKLKDAEKAAFDEAE
mCRT TWIHPEIDNPEYSPDANIYAYDSFAVLGLDLWQVKSGTIFDNFLITNDEAYAEEFGNETWGVTKAAEKQMKDKQD
HsCRT TWIHPEIDNPEYSPDPSIYAYDNFGVLGLDLWQVKSGTIFDNFLITNDEAYAEEFGNETWGVTKAAEKQMKDKQD
AtCRT3 KERKAREDEEARIAREEGERRRKERD--HRYGDRRRRYKRPNPR-----DYMDDYHDEL
OsCRT3 KERKAREDKEAERAREEGERRRRERGDRHRGRDYKDRYKRRHRD-----HWDDDYHDEL
AtCRT1 KKREEEESKDAPAESDAEEEAEDDDNEGDDSDNESKSEETKEAEETKEAEETDAAHDEL
AtCRT2 KKNEEEESKDAPAESDAEDEPEDDEG-GDDSDSESKAEETKSVDSEETSEKDATAHDEL
mCRT EEQRLKEEEEDKKRKEEEEAEDKEDDDDRDEDEDEEDEKEEDEEE-----SPGQAKDEL
HsCRT EEQRLKEEEEDKKRKEEEEAEDKEDDEDKDEDEEDEEDKEEDEEED----VPGQAKDEL
N-domain
P-domain
C-domain

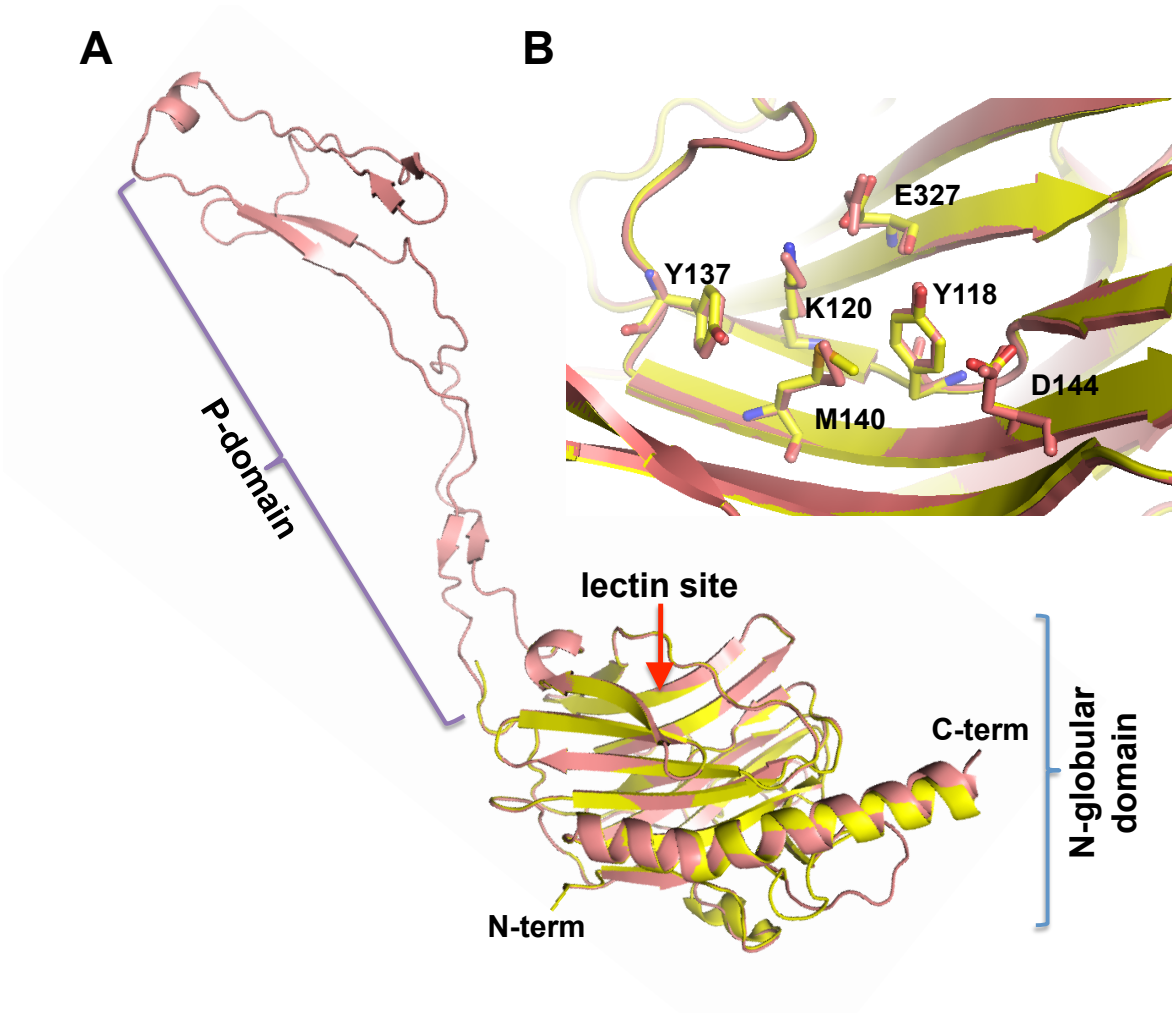

Figure 2.2. Molecular modeling of a 3-D structure of AtCRT3 based on mCRT
(A) Superimposition of the N-globular domain of the mCRT structure (pdb code 30oW; yellow) and the predicted 3-D structural model of AtCRT3 (salmon). The N- and P-domains, the predicted lectin site, and two termini are indicated.
(B) A close-up view of the sugar-binding site revealing similar positioning of key amino acid residues of the predicted lectin sites of mCRT and AtCRT3. The numbers shown are amino acid residue positions of AtCRT3.

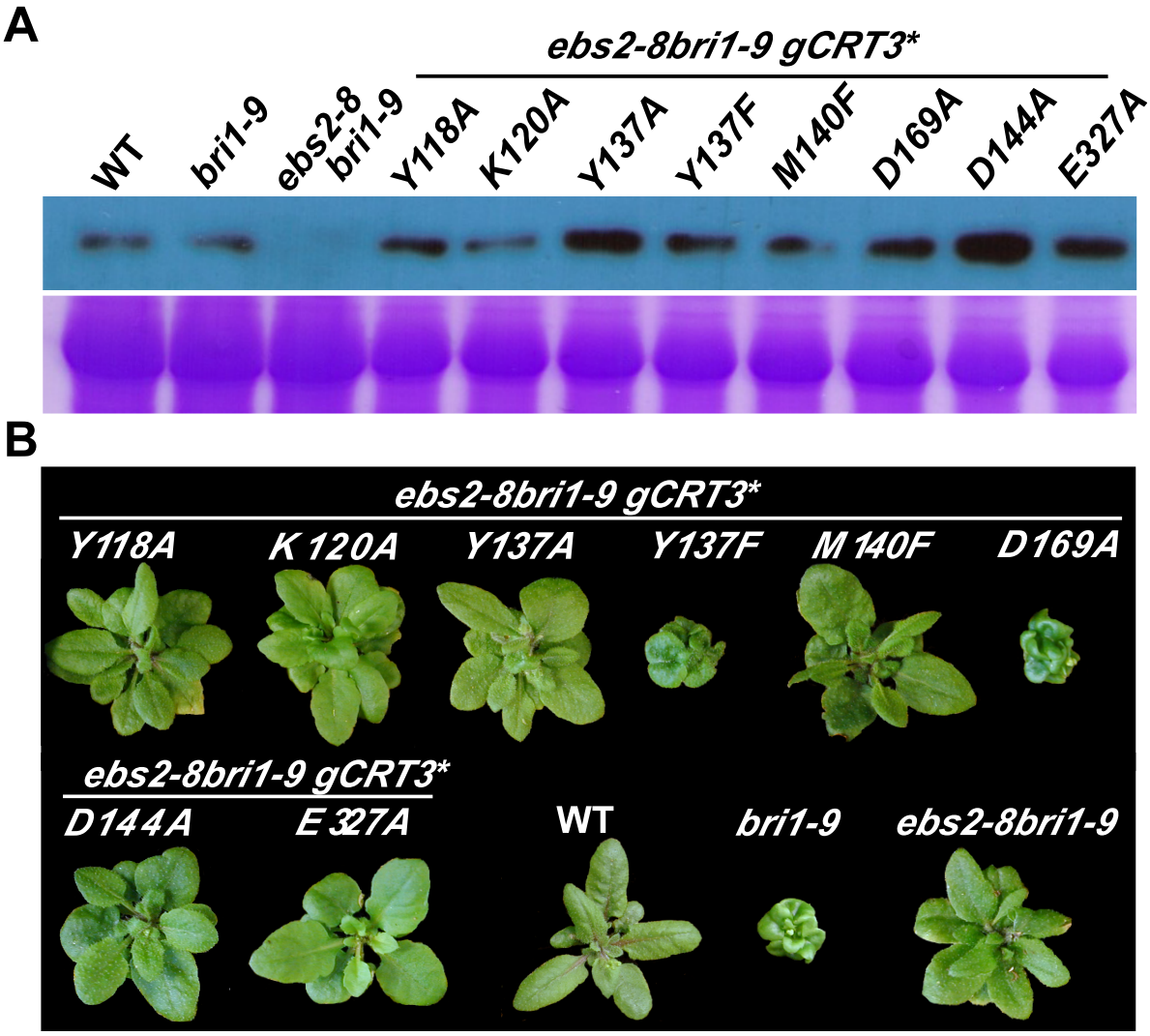

Figure 2.3. *gCRTM transgene containing mutations of Y118A, K120A, Y137A, M140F, D144A or E327A fail to complement a loss-of-function mutation in the T-DNA insertional *ebs2* plant**

(A) Immunoblot analysis of CRT3 in the wild-type (WT), *bri1-9*, *ebs2-8 bri1-9*, and 8 representative *ebs2-8 bri1-9 gCRT3** transgenic lines (* substitutes for each of the eight italicized amino acid mutations listed beneath the line), each carrying a mutant *gCRT3* transgene containing one of the following amino acid changes: Y118A, K120A, Y137A, Y137F, M140F, D169A, D144A, and E327A. Total protein extracts from 5-week-old soil-grown plants were separated by 10% SDS–PAGE and analyzed by immunoblotting using anti-CRT3 antibody. Coomassie-blue-stained SDS–PAGE gel is shown to serve as a loading control.

(B) Images of 5-week-old soil-grown plants of WT, *bri1-9*, *ebs2-8 bri19*, and 8 representative *gCRT3* ebs2-8 bri1-9* transgenic lines shown in (A).

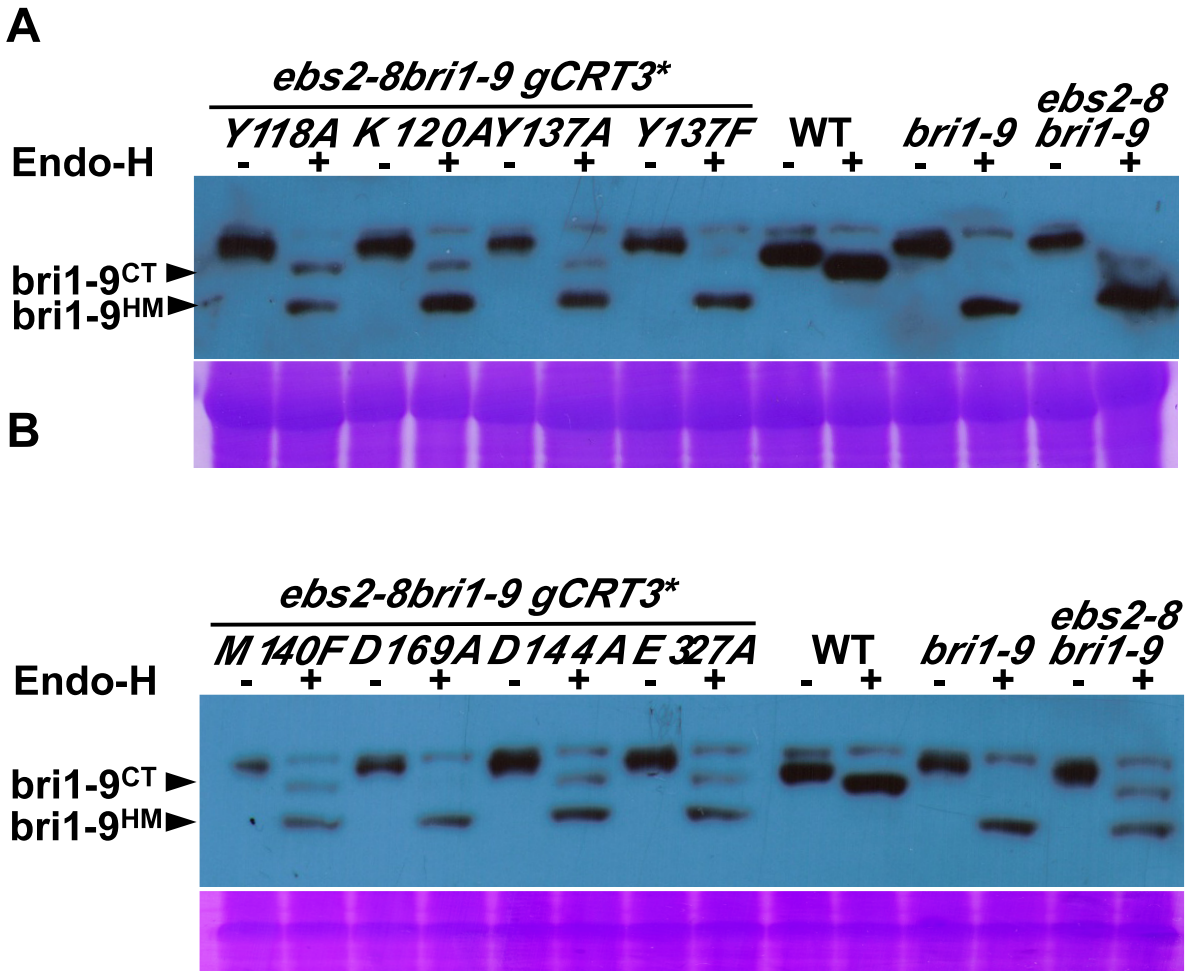

Figure 2.4. The Endo-H sensitivity of BRI1 in WT, bri1-9, ebs2-8 bri1-9 and 8 representative ebs2-8 bri1-9 gCRT3* lines shown in Fig. 2.3 B

(A, B) Equal amounts of total proteins extracted from rosette leaves of 5-week-old plants were treated with 1 µl Endo Hf for 1.5 h at 37°C, separated by 10% SDS–PAGE, and analyzed by either Coomassie-blue-staining (to serve as a loading control) or by immunoblotting with anti-BRI1 antibody.

Figure 2.5. Sequence alignment of the *Arabidopsis* CRT3 and its plant homologs. Amino acid sequence alignment of *Arabidopsis* CRT3 and its plant homologs was performed using the ClustalW program at Mobyle web tool (http://mobyle.pasteur.fr/cgi-bin/portal.py). Names and accession numbers of the CRT3 homologs used for analyses are as follows: AtCRT3 (NP_563816; At: *Arabidopsis thaliana*), BrCRT3 (translated from nucleotide sequences EX116073.1, EX026998.1 and EX117522.1, *Br*: *Brassica rapa*), VvCRT3 (translated from nucleotide sequence XM_002276397.1, *Vv*: *Vitis vinifera*), MtCRT3 (translated from nucleotide sequence BT052978.1, *Mt*: *Medicago truncatula*), OsCRT3 (BAC06263; *Os*: *Oryza sativa*), GhCRT3 (translated from nucleotide sequence DT563804.1; *Gh*: *Gossypium hirsutum*) MdCRT3 (translated from nucleotide sequences CN943087.1 and CV082227.1; *Md*: *Malus domestica*), SmCRT3 (translated from nucleotide sequence FE490612.1 and FE490611.1; *Sm*: *Selaginella moellendorffii*), AfCRT3 (translated from nucleotide sequences DR940519.1 and DT750168.1, *Af*: *Aquilegia formosa*), PtCRT3 (translated from nucleotide sequences BF777977.1, CO198952.1 and CO158387.1; *Pt*: *Pinus taeda*), ZmCRT3 (translated from nucleotide sequence AY105822; *Zm*: *Zea mays*), HvCRT3 (translated from nucleotide sequence AK248906.1; *Hv*: *Hordeum vulgare*) and TaCRT3 (EF452301.1; *Ta*: *Triticum aestivum*). Aligned amino acid sequences were shaded using the BoxShade 3.31 web server (http://mobyle.pasteur.fr/cgi-bin/portal.py). Residues identical in more than 8 sequences are shaded in red and similar ones are shaded in cyan. Two basic tetrapeptides in the C terminus of AtCRT3 are marked by blue bar, and the region that has > 50% basic residues is indicated by a green box.

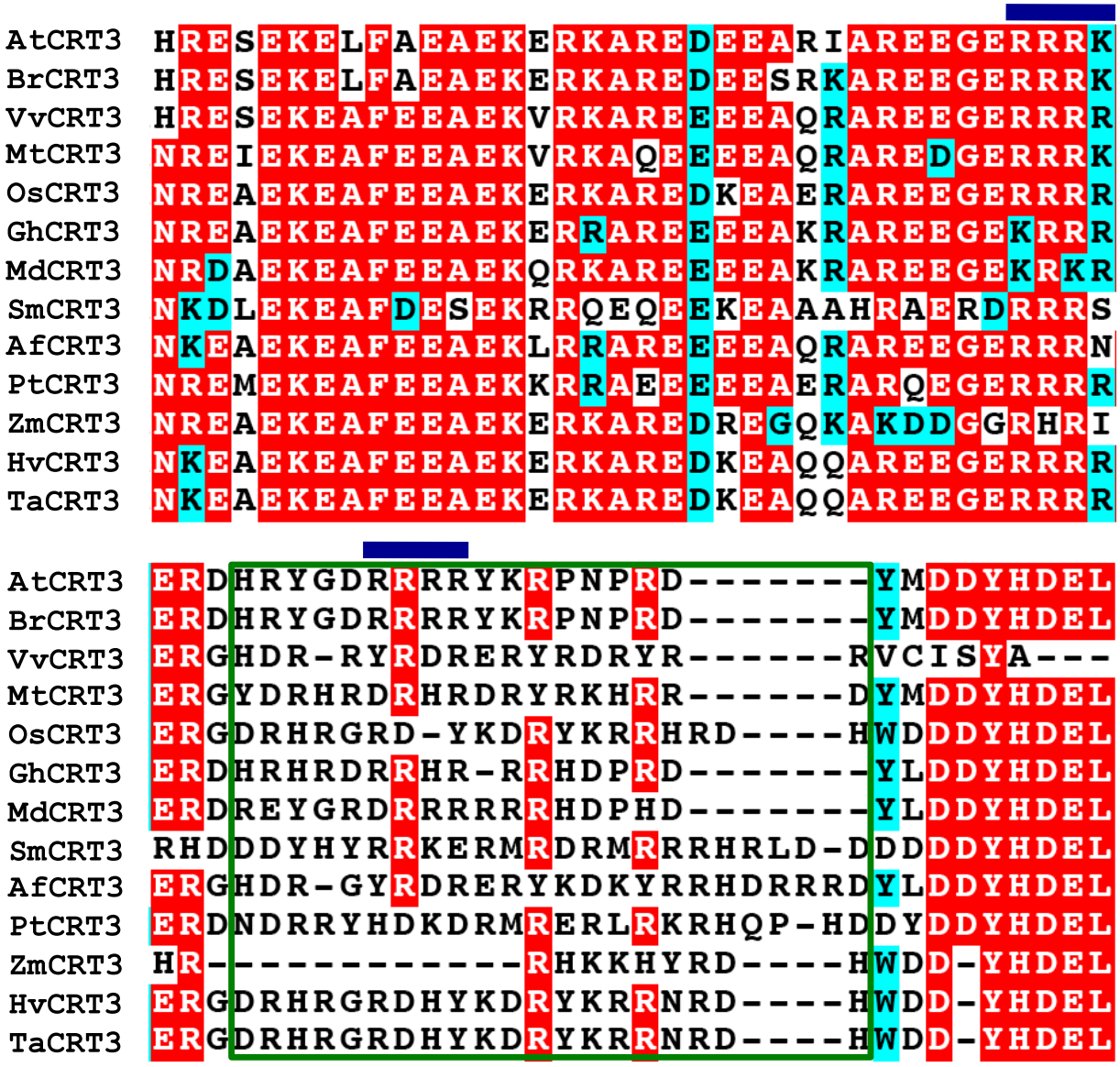
AtCRT3 HRESEKELFAEAEKERKAREDEEARIAREEGERRRK
BrCRT3 HRESEKELFAEAEKERKAREDEESRKAREEGERRRK
VvCRT3 HRESEKEAFEEAEKVRKAREEEEAQRAREEGERRRR
MtCRT3 NREIEKEAFEEAEKVRKAQEEEEAQRAREDGERRRK
OsCRT3 NREAEKEAFEEAEKERKAREDKEAERAREEGERRRR
GhCRT3 NREAEKEAFEEAEKERRAREEEEAKRAREEGEKRRR
MdCRT3 NRDAEKEAFEEAEKQRKAREEEEAKRAREEGEKRKR
SmCRT3 NKDLEKEAFDESEKRRQEQEEKEAAAHRAERDRRRS
AfCRT3 NKEAEKEAFEEAEKLRRAREEEEAQRAREEGERRRN
PtCRT3 NREMEKEAFEEAEKKRRAEEEEEAERARQEGERRRR
ZmCRT3 NREAEKEAFEEAEKERKAREDREGQKAKDDGGRHRI
HvCRT3 NKEAEKEAFEEAEKERKAREDKEAQQAREEGERRRR
TaCRT3 NKEAEKEAFEEAEKERKAREDKEAQQAREEGERRRR
AtCRT3 ERDHRYGDRRRRYKRPNPRD-------YMDDYHDEL
BrCRT3 ERDHRYGDRRRRYKRPNPRD-------YMDDYHDEL
VvCRT3 ERGHDR-RYRDRERYRDRYR------RVCISYA---
MtCRT3 ERGYDRHRDRHRDRYRKHRR------DYMDDYHDEL
OsCRT3 ERGDRHRGRD-YKDRYKRRHRD----HWDDDYHDEL
GhCRT3 ERDHRHRDRRHR-RRHDPRD-------YLDDYHDEL
MdCRT3 ERDREYGRDRRRRRRHDPHD-------YLDDYHDEL
SmCRT3 RHDDDYHYRRKERMRDRMRRRHRLD-DDDDDYHDEL
AfCRT3 ERGHDR-GYRDRERYKDKYRRHDRRRDYLDDYHDEL
PtCRT3 ERDNDRRYHDKDRMRERLRKRHQP-HDDYDDYHDEL
ZmCRT3 HR-----------RHKKHYRD----HWDD-YHDEL
HvCRT3 ERGDRHRGRDHYKDRYKRRNRD----HWDD-YHDEL
TaCRT3 ERGDRHRGRDHYKDRYKRRNRD----HWDD-YHDEL

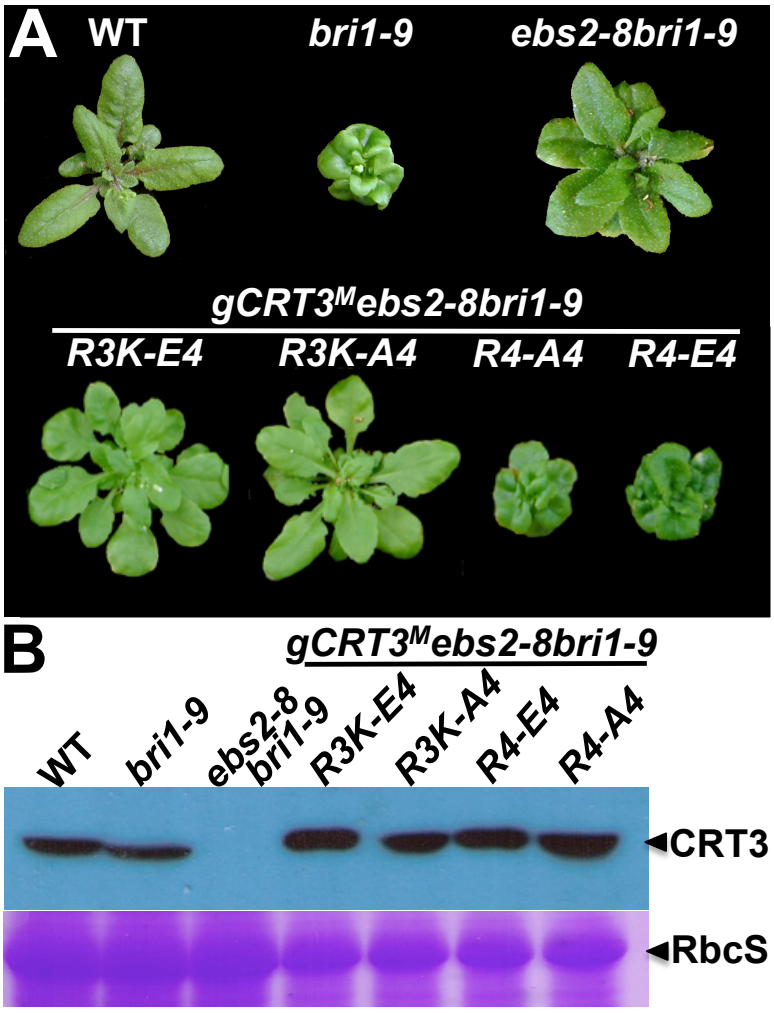

Figure 2.6. Mutations of the basic $Arg^{392}Arg^{393}Arg^{394}Lys^{395}$ tetrapeptide destroy the activity of the *gCRT3M* transgene to rescue a T-DNA insertional *ebs2* mutation.
(**A**) Images of 5-week-old soil-grown plants of wild-type (WT) plant, *bri1-9*, *ebs2-8 bri1-9* and 4 representative $gCRT3^{M}$ *ebs2-8 bri1-9* transgenic lines.
(**B**) Immunoblot analysis of $CRT3^{M}$ abundance in transgenic plants. Total protein extracts of 5-week-old soil-grown plants shown in (**A**) were separated by 10% SDS/PAGE and analyzed by immunoblotting with anti-CRT3 antibody. Coomassie blue staining of a small subunit of the *Arabidopsis* Rubisco gel was used as a loading control. The protein samples of 4 chosen $gCRT3^{M}$ *ebs2-8 bri1-9* transgenic plants were diluted 2 fold before sample loading.

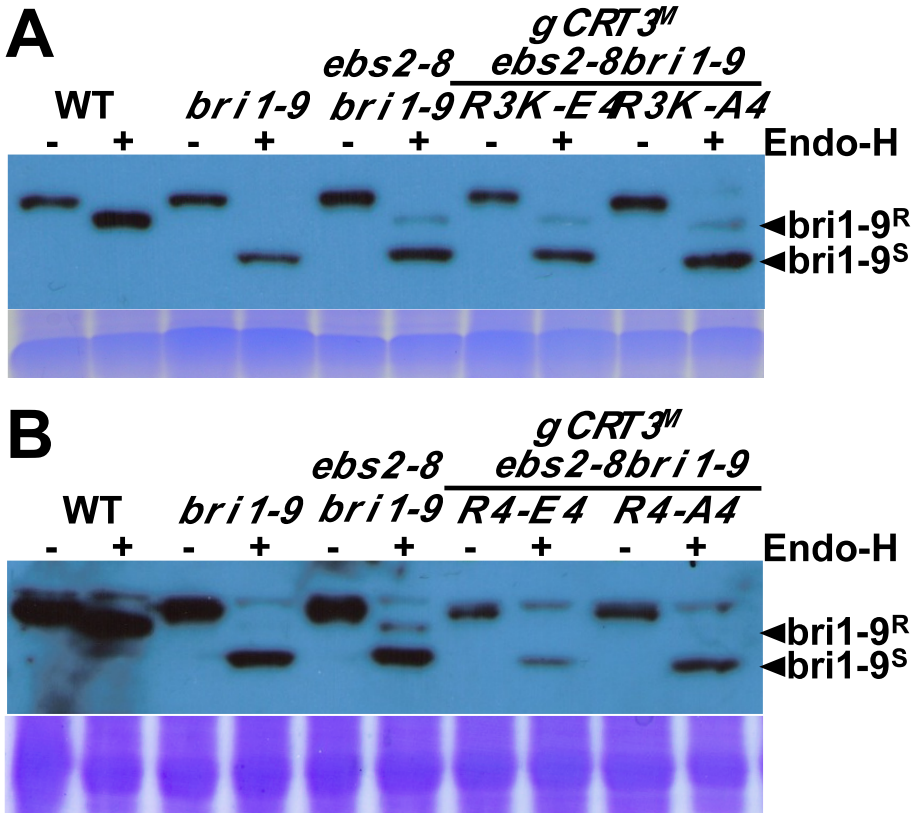

Figure 2.7. The Endo-H sensitivity assay of BRI1 and bri1-9
(A, B) Equal amounts of total proteins extracted from leaves of 5-week-old soil-grown plants shown in Fig.2.6 were treated with (+) or without (−) Endo Hf for 1.5 h at 37°C, separated by 7% SDS/PAGE and analyzed by immunoblotting with an anti-BRI1 antibody. Coomassie blue staining of RbcS serves as a loading control. Arrows indicated the positions of Endo-H-resistant (bri1-9^R) and Endo-H-sensitive bri1-9 (bri1-9^S) forms.

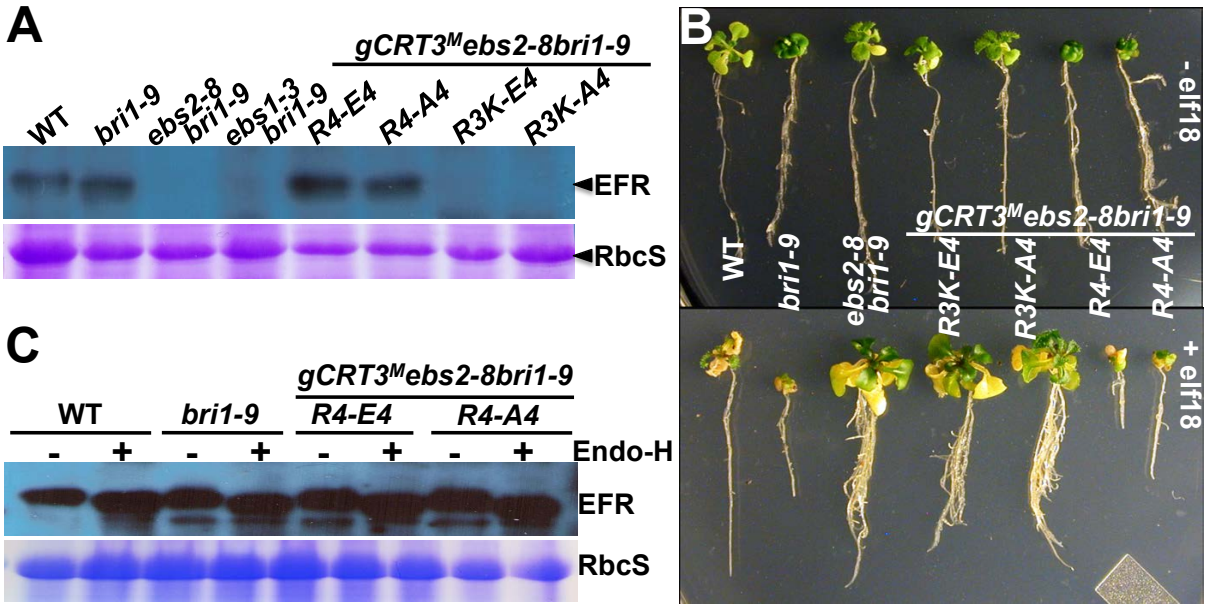

Figure 2.8. The basic tetrapeptide Arg392Arg393Arg394Lys395 of CRT3 is crucial for the complete folding of the plant immunity receptor EFR.

(**A**) An immunoblot analysis of EFR. Total protein extracts from WT, *bri1-9, ebs2-8bri1-9* and 4 selected *gCRT3*^{M} *ebs2-8 bri1-9* transgenic lines were separated by 10% SDS/PAGE and analyzed by immunoblotting with an anti-EFR antibody. Coomassie blue staining of RbcS serves as a loading control.

(**B**) The efl18 growth inhibition assay. Shown here are images of 7-d-old seedlings of WT, *bri1-9, ebs2-8bri1-9* and 4 selected *gCRT3*^{M} *ebs2-8 bri1-9* transgenic lines grown on half-strength MS agar medium (top panel) and 17-d-old seedlings of the same genotypes after 10-d treatment with 100 nM elf18 (bottom panel).

(**C**) The Endo-H assay of EFR. Equal amounts of total proteins extracted from leaves of 5-week-old soil-grown plants were treated with (+) or without (−) Endo Hf for 1.5 h at 37°C, separated by 7% SDS/PAGE and analyzed by immunoblotting with an anti-EFR antibody. Coomassie blue staining of RbcS serves as a loading control.

CHAPTER 3
EBS7 IS A PLANT-SPECIFIC COMPONENT OF A HIGHLY CONSERVED ENDOPLASMIC RETICULUM-ASSOCIATED DEGRADATION SYSTEM IN *ARABIDOPSIS*

Abstract

Endoplasmic reticulum-associated degradation (ERAD) is an essential part of an ER-localized protein quality control system for eliminating terminally-misfolded proteins. Recent studies demonstrated that the ERAD machinery is conserved in yeast, animals, and plants; however, it remains unknown if the plant ERAD system involves plant-specific components. Here we report that the *Arabidopsis EMS-mutagenized bri1 suppressor 7* (*EBS7*) gene encodes an ER membrane-localized ERAD component that is highly conserved in land plants. Loss-of-function *ebs7* mutations prevent ERAD of brassinosteroid-insensitive 1-9 (bri1-9) and bri1-5, two ER-retained mutant variants of the cell surface receptor for brassinosteroids (BRs), causing their accumulation in the ER and consequential leakage to the plasma membrane, which is responsible for restoration of BR sensitivity and phenotypic suppression of the *bri1-9* and *bri1-5* mutants, respectively. EBS7 accumulates under ER stress and its mutations lead to hypersensitivity to ER and salt stresses. EBS7 interacts with the ER membrane-anchored ubiquitin ligase AtHrd1, one of the central components of the *Arabidopsis* ERAD machinery, and an *ebs7* mutation destabilizes AtHrd1 to reduce polyubiquitination of

bri1-9. Taken together, our study not only discovered a plant-specific component of a plant ERAD pathway but also suggested its likely biochemical function.

Introduction

Endoplasmic reticulum-associated degradation (ERAD) is an integral part of an ER-mediated protein quality control system in eukaryotes, which permits export of only correctly-folded proteins but retains misfolded proteins in the ER for repair via additional folding attempts or elimination through ERAD. Genetic and biochemical studies in yeast and mammalian cells have revealed that the core ERAD machinery is highly conserved between yeast and mammals and that ERAD involves 4 tightly-coupled steps: substrate selection, retrotranslocation through the ER membrane, ubiquitination, and proteasome-mediated degradation (60, 145).

As the vast majority of secretory/membrane proteins are glycosylated in the ER, diversion of most ERAD substrates from their futile folding cycles into ERAD is initiated through progressive mannose-trimming of their asparagine-linked glycans (N-glycans) by ER/Golgi-localized class I mannosidases that include Htm1 (homologous to α-mannosidase 1) and its mammalian homologs EDEMs (ER degradation-enhancing α-mannosidase-like proteins) (146). The processed glycoproteins are captured by two ER resident proteins, Yos9 (yeast OS9 homolog) [OS9 (amplified in osteosarcoma 9) in mammals] and Hrd3 (HMG-CoA reductase degradation 3) [SEL1L (Suppressor/Enhancer of Lin-12-like) in mammals], which recognize the mannose-trimmed N-glycans and surface-exposed hydrophobic amino acid residues, respectively (70, 147), and are subsequently delivered to an ER membrane-anchored ubiquitin ligase (E3), which is the core component of the ERAD machinery (93), for polyubiquitination. Yeast has two

known ERAD E3 ligases, Hrd1 and Doa10 (Degradation of alpha2 10), both containing a catalytically-active RING finger domain, while mammals have a large collection of ER membrane-anchored E3 ligases, including Hrd1 and gp78 (a glycoprotein of M_r 78,000) (79). The yeast Hrd1/Doa10-containing ERAD complexes target different substrates with the former ubiquitinating substrates carrying conformational defects in their transmembrane or luminal domains while the latter acting on clients with structural lesions in their cytosolic domains (148). Due to the cytosolic location of the catalytic domain of the E3 ligases and the eventual degradation machinery, proteasome, all ERAD substrates have to retrotranslocate through the ER membrane. It is well known that the retrotranslocation step is tightly coupled with substrate ubiquitination and is powered by AAA-type ATPases [Cdc48 (cell division cycle 48) in yeast and p97 (a protein with a molecular weight of 97,000) in mammals]; however, it remains controversial about the true identity of the retrotranslocon. Earlier studies have implicated the Sec61 (Secretory 61) translocon, Der1 (degradation in the endoplasmic reticulum 1) [derlins (Der1-like proteins) in mammals], and Hrd1 in the retrotranslocation of various ERAD substrates (109). After retrotranslocation, ubiquitinated ERAD substrates are delivered to the cytosolic proteasome with the help of Cdc48/p97 and their associated factors for proteolysis (110). In addition to the above-mentioned proteins, the yeast/mammalian ERAD systems contain several other components, including an ubiquitin-conjugating enzyme (E2), a membrane-anchored E2-recruting factor Cue1 (Coupling of ubiquitin conjugation to ER degradation 1 that has no mammalian homolog), a scaffold protein [the yeast Usa1 (U1-Snp1 associating 1) or mammalian HERP (homocysteine-induced ER protein)] of the E3 ligases, and a membrane-anchored Cdc48-recruiting factor [Ubx2

(ubiquitin regulatory X 2) in yeast or Ubxd8 (UBX domain-containing 8) in mammals] (93).

ERAD has been known to operate in plants for many years (149), but the research on the plant ERAD process has lagged far behind similar studies in yeast and mammalian systems. Recent molecular and genetic studies in the reference plant *Arabidopsis*, especially two *Arabidopsis* dwarf mutants carrying ER-retained mutant variants of the brassinosteroid (BR) receptor BRASSINOSTEROID-INSENSITIVE 1 (BRI1) (8, 52, 150), have revealed that the ERAD system is also conserved in plants [reviewed in (151, 152)]. For example, the ERAD N-glycan signal to mark misfolded glycoproteins in *Arabidopsis* was found to be the same as that in yeast/mammalian cells (11, 64). Both forward and reverse genetic studies have shown that *Arabidopsis* homologs of the yeast/mammalian ERAD components, including Yos9/OS9 (74, 153), Hrd3/Sel1L (73, 75), Hrd1 (73), EDEMs (154), and a membrane-anchored E2 (92), are involved in degrading misfolded glycoproteins. However, it remains unknown if the plant ERAD requires one or more plant-specific components to efficiently degrade terminally-misfolded proteins. In this study, we took a forward genetic approach to identify a novel *Arabidopsis* ERAD mutant, *ems-mutagenized bri1 suppressor 7* (*ebs7*), and subsequently cloned the corresponding *EBS7* gene. We discovered that *EBS7* encodes an ER-localized membrane protein that is highly conserved in land plants but lacks a homolog in yeast or mammals. Our biochemical studies strongly suggested that EBS7 plays a key role in an *Arabidopsis* ERAD process by regulating the protein stability of the *Arabidopsis* Hrd1.

Results

The *ebs7-1* mutation restores BR sensitivity to a BR-insensitive mutant *bri1-9* by blocking the degradation of its mutant BR receptor

We have previously shown that the dwarf phenotype of a BR-insensitive mutant *bri1-9* is caused by ER retention and subsequent ERAD of a structurally-defective yet biochemically-competent BR receptor bri1-9 (8, 64, 150). A genetic screen for extragenic suppressors of the *bri1-9* mutant coupled with a secondary screen for mutants that accumulate bri1-9 not only revealed a conserved ERAD N-glycan signal but also identified several components of an *Arabidopsis* plant ERAD system (73, 74, 151). This study is focused on a new mutant named as *ebs7*-1for *EMS-mutagenized bri1-9 suppressor 7-1*. As shown in Fig. 3.1A, *ebs7-1 bri1-9* accumulates a higher amount of bri1-9 than the parental *bri1-9* mutant (Fig. 3.1A), which is largely caused by attenuated degradation rather than increased biosynthesis of bri1-9 revealed by a simple cycloheximide (CHX)-chase experiment (Fig. 3.1B). Similar to what was observed in other known *Arabidopsis* ERAD mutants (11, 64, 73, 74), accumulation of bri1-9 in the ER likely saturates its ER retention systems, leading to detection of a small percentage of bri1-9 proteins carrying the complex-type (C-type) N-glycans indicative of ER escape, which are resistant to hydrolysis by endoglycosidase H (Endo H) capable of cleaving high-mannose-type (HM-type) N-glycans of ER-localized proteins but not Golgi-processed C-type N-glycans (Fig. 3.1A).

Phenotypically, the *ebs7-1 bri1-9* double mutant has a larger rosette than *bri1-9* (Fig. 3.1C), although its leaves are still as round as that of *bri1-9*. The double mutant also has a longer hypocotyl when grown in the dark and taller inflorescence stem at maturity than those of the parental *bri1-9* mutant (Fig. 3.1, D and E). Consistent with the detection of a

small pool of ER-escaping bri1-9, *ebs7-1 bri1-9* partially regains the BR sensitivity. As shown in Fig. 3.1F, exogenously-applied brassinolide (BL) inhibited the root growth of wild-type and *ebs7-1 bri1-9* in a dose-dependent manner but had a little impact on the root growth of *bri1-9*, a BR-insensitive mutant. The regained BR sensitivity in *ebs7-1 bri1-9* was confirmed by a widely-used biochemical assay that measures BR-induced dephosphorylation of BES1, a key transcription factor of the BR signaling pathway (155). Fig. 3.1G shows that BL had a marginal effect on the BES1 phosphorylation status in *bri1-9* but efficiently and partially dephosphorylated BES1 in wild type and *ebs7-1 bri1-9*, respectively. More importantly, overexpression of EBS2, a limiting component of the bri1-9's ER-retention systems (150), fully retained bri1-9 in the ER and nullified the suppressor activity of the *ebs7-1* mutation on the *bri1-9* mutant (Fig. 3.2, A-B).

The *ebs7-1* mutation inhibits degradation of other known ERAD substrates

To determine if the *ebs7-1* mutation inhibits degradation of other known *Arabidopsis* ERAD clients, we first crossed the *ebs7-1* mutation into another *Arabidopsis* BR-insensitive dwarf mutant, *bri1-5* carrying a different ER-retained mutant BR receptor bri1-5 (52). As shown in Fig. 3.3A, *ebs7-1* suppressed the dwarfism of *bri1-5* (Fig. 3.3A-B, Fig. 3.4A), restored its BR sensitivity (Fig. 3.3C-D), and inhibited the degradation of bri1-5 as revealed by increased bri1-5 abundance and appearance of a small portion of bri1-5 carrying the C-type N-glycans (Fig. 3.3E). The crucial role of EBS7 in ERAD of bri1-5 was further confirmed by identification of two allelic *ebs7* mutations in an independent genetic screen for ERAD mutants of bri1-5 (Fig. 3.4B-C).

We also examined the effect of *ebs7-1* on ERAD of the ER-retained conformer of EFR (EF-Tu receptor), a cell surface-localized leucine-rich-repeat receptor-like kinase that

recognizes and binds the bacterial translational elongation factor EF-Tu to trigger a plant innate immunity response (16). Previous studies demonstrated that the proper folding of EFR requires an *Arabidopsis* ER quality control system consisting of EBS1 and EBS2 and that loss-of-function mutations in EBS1or EBS2 cause EFR misfolding, its ER retention, and subsequent degradation by ERAD (156). We crossed the *ebs7-1* mutation into *ebs1-3 bri1-9* and analyzed the protein abundance of EFR in both *ebs1-3 bri1-9* and *ebs7-1 ebs1-3 bri1-9* mutants using an anti-EFR antibody. As shown in Fig. 3.3F, while no EFR was detected in *ebs1-3 bri1-9*, the protein abundance of EFR in an *ebs1-3 ebs7-1 bri1-9* triple mutant was similar to that of the wild-type, *bri1-9*, or *ebs7-1 bri1-9*, indicating that EBS7 is also required for degrading misfolded EFR. Taken together, our results suggested that EBS7 is a general factor of the *Arabidopsis* ERAD machinery.

Molecular Cloning and Characterization of the *EBS7* Gene

In order to understand how the *ebs7-1* mutation affects the *Arabidopsis* ERAD system, we positionally cloned the *EBS7* gene. PCR-based genetic mapping delimited the *EBS7* locus within an 850-kb region on chromosome 4 (Fig. 3.5A), which includes two candidate genes likely involved in the *Arabidopsis* ERAD process. One (*At4g29330*) encodes a homolog of the yeast protein Der1 (degradation in the ER 1)/mammalian derlins (Der-like proteins) known to be involved in ERAD (98, 99, 157), and the other (*At4g29960*) was known to be co-expressed with many known/predicted ER proteins that include at least three known/predicted ERAD genes, *EBS5* (*At1g18260*), *EBS6* (*At5g35080*), and *DERLIN-2.1* (*At4g21810*) (Fig. 3.6) (158). We PCR-amplified and subsequently sequenced the two candidate genes from the *ebs7-1 bri1-9* mutant. Comparison of the resulting sequences with the published *Arabidopsis* wild-type

sequences detected no mutation in *At4g29330* but identified a G-A mutation in *At4g29960*, which causes a missense mutation of Ala^{131} to Thr. The identity of *At4g29960* being the *EBS7* gene was supported by sequencing analysis of the *At4g29960* gene in two allelic *ebs7* mutants (*ebs7-2* and *ebs7-3*), which were discovered in an independent genetic screen for ERAD mutants in the *bri1-5* genetic background (Fig. 3.4). In both mutants, a G-A mutation was detected, which changes Gly^{74}-Glu in *ebs7-2* and disrupts the correct splicing of the *At4g29960* mRNA, donor of the 3rd intron in *ebs7-3* (Fig. 3.5B). Additional support for *At4g29660* being the *EBS7* gene came from the complementation experiment showing that a genomic construct of *At4G29960* fully rescued the morphological and biochemical phenotypes of the *ebs7-1* mutation (Fig. 3.5, C-E), confirming that *At4G29960* is indeed the *EBS7* gene that is mutated in *ebs7-1*.

EBS7 is a plant-specific protein conserved in land plants

The *EBS7* gene consists of 5 exons plus 4 introns (Fig. 3.5A), encodes a predicted polypeptide of 291 amino acids (Fig. 3.5F), and is expressed in most organs/tissues throughout the entire plant life cycle (Fig. 3.7) (159). Blast searches against GenBank protein databases failed to identify any known protein motif in EBS7 or to discover EBS7 homologs in yeast or animals but did find EBS7 homologs in land plants, including *Physcomitrella* and *Selaginella* (Fig. 3.5F & 3.8). Sequence alignment between EBS7 and its plant homologs identified two major conserved regions, one in the middle and the other at the C-termini (Fig. 3.5F). The annotated At4g29960 protein was predicted to contain three transmembrane segments [http://aramemnon.botanik.uni-koeln.de/, (160)] with the first two (I^{143}AFQLDLFLILKLAAVIFLF^{162} and L^{171}AVLVIFATIIYLYQTGALA^{190} along with a predicted 8-amino acid loop)

corresponding the conserved middle region and the third one (W^{265}WGIVKELQMIVFGFITSLLP^{285}) overlapping with the conserved C-terminus (Fig. 3.5F), suggesting that EBS7 is likely a membrane protein. It should be interesting to point out here that the Ala^{131}, which was mutated to Thr in *ebs7-1*, is not highly conserved among the plant EBS7 homologs, yet the Ala^{131}-Thr mutation significantly reduced the abundance of ebs7-1 (Fig. 3.4). This could be explained by potential misfolding of the ebs7-1 protein and its subsequent degradation. By contrast, Gly^{74}, which is mutated to Glu in *ebs7-2*, is absolutely conserved between EBS7 and its plant homologs (Fig. 3.5F).

EBS7 is an ER-localized membrane protein that accumulates under ER stress

Consistent with the presence of three predicted transmembrane segments, EBS7/At4g29960 was previously identified as a plasma membrane protein by two independent proteomic studies (161, 162). Both studies used the aqueous two-phase partitioning method to obtain the plasma membrane-enriched fraction, which is often contaminated with organellar membrane proteins that include ER proteins. To determine where EBS7 likely localizes, we generated two green fluorescent protein (GFP) fusion constructs (with the GFP tag fused at the N or C-terminus of EBS7) driven by the constitutively active *35S* promoter and transformed the two fusion constructs into the *ebs7 bri1-9* double mutant. Only the *GFP-EBS7* but not *EBS7-GFP* transgene complemented the *ebs7-1* mutation (Fig. 3.9). When the GFP-tagged EBS7 protein was transiently expressed in the tobacco leaf epidermal cells, its subcellular localization pattern overlapped significantly with that of a known ER maker, HDEL (His-Asp-Glu-Leu)-tagged red fluorescent protein (RFP-HDEL) (163), indicating that EBS7 is mainly localizes in the ER (Fig. 3.5G). We also performed a subcellular fractionation experiment

that separated soluble proteins from membrane/microsomal proteins of wild-type *Arabidopsis* seedlings, which were further analyzed by immunoblot using antibodies against EBS2, an ER luminal protein (150), EBS5, an ER-membrane-anchored protein (73), and EBS7. As shown in Fig. 3.5H, while EBS2 was exclusively detected in the soluble fraction, both EBS5 and EBS7 were only detected in the membrane fraction. Taken together, these experiments indicated that EBS7 is an ER-localized membrane protein.

In line with its coexpression pattern with genes encoding ER chaperones/folding enzymes (Fig. 3.6), the protein abundance of EBS7 was increased when the *Arabidopsis* seedlings were treated with tunicamycin (TM) (Fig. 3.10A), an N-glycan biosynthesis inhibitor widely used to induce ER stress (164). ER stresses often lead to activation of an ER stress signaling pathway, widely known as unfolded protein response (UPR) that increases expression of genes encoding ER chaperones, folding enzymes, and ERAD components to mitigate ER stress and maintain ER homeostasis (165, 166).

The *ebs7-1* mutation causes UPR and results in hypersensitivity to ER/salt stresses

Interestingly, the abundance of several known ER resident proteins were significantly elevated in *ebs7-1*, even when seedlings were grown on normal growth medium (Fig. 3.10A), indicating that the *ebs7-1* mutation alone could induce UPR. This finding seems to be consistent with its crucial role in ERAD because a compromised ERAD process would lead to accumulation of misfolded proteins in the ER, which could activate UPR. To examine if the *ebs7-1* mutation alone has any effect on plant growth, we removed the *bri1-9* mutation by crossing the double mutant with the wild-type *Arabidopsis*. Although the *ebs7-1* seedlings exhibited no significant growth phenotype compared to the wild type

control (Fig. 3.10B), they were hypersensitive to low concentration of dithiothreitol (DTT), a reducing agent that can induce ER stress due to its interference with the formation of disulfide bridges important for obtaining native conformations for many proteins (Fig. 3.10B). Consistent with earlier studies of other *Arabidopsis* ERAD mutants (75, 153), *ebs7* mutants displayed increased salt sensitivity. The two allelic *ebs7* mutants had increased ratio of yellow and dead seedlings when grown on growth medium containing 125 mM NaCl, whereas the majority of the wild type or *bri1-5* seedlings remained green (Fig. 3.11).

The *ebs7-1* mutation inhibits bri1-9 ubiquitination

Because an ER membrane-anchored E3 ligase is the central component of an ERAD system (93) and our previous study revealed a redundant function of the two *Arabidopsis* homologs of the yeast Hrd1 in degrading the two ER-retained mutant bri1 proteins (73), we examined if the *ebs7-1* mutation affects the ubiquitination of bri1-9 using transgenic *Arabidopsis* lines expressing GFP-tagged BRI1/bri1-9 (driven by the *BRI1* promoter) in *ebs7-1* or *EBS7*+ background. As shown in Fig. 3.12A, while the GFP-tagged bri1-9 in the *EBS7*+ genetic background was polyubiquitinated, no polyubiquitin signal was detected on the bri1-9-GFP protein immunoprecipitated from the *bri1-9-GFP ebs7-1* transgenic seedlings despite its increased abundance. As expected, the polyubiquitin antibody detected no signal on immunoprecipitated BRI1-GFP. Thus, we concluded that the *ebs7-1* mutation completely blocks the bri1-9 ubiquitination.

EBS7 is important to maintain the stability of AtHrd1

Based on the current ERAD model (145, 152), an ERAD client is recognized and recruited by the two recruitment factors, Hrd3/Sel1L and Yos9/OS9, and subsequently

delivered to the membrane-anchored E3 ligase Hrd1. To test if the *ebs7-1* mutation affects the recruitment step of the bri1-9 ERAD process, we analyzed the interaction of GFP-tagged bri1-9 with EBS5, the functional homolog of Hrd3/Sel1 (73). As shown in Fig. 3.12A, a strong interaction between bri1-9-GFP and EBS5 was detected in the *ebs7-1* mutant. We also examined if the *ebs7-1* mutation might affect the assembly of the AtHrd1 complex that include the two client recruitment factors. As shown in Fig. 3.12B, the interaction between EBS5 and AtHrd1 was unaltered by the *ebs7-1* mutation. Taken together, these results suggested that the *ebs7-1* mutation unlikely affects the ERAD steps upstream of the bri1-9 ubiquitination.

It is quite possible that EBS7 might interact with AtHrd1 to affect its ubiquitination activity towards an ERAD substrate. *Arabidopsis* genome encodes two homologs of the yeast Hrd1, AtHrd1a and AtHrd1b, which were previously shown to be required for ERAD of bri1-9 (73). Indeed, a co-IP experiment with transgenic *Arabidopsis* seedlings expressing GFP-tagged AtHrd1a revealed a strong interaction between AtHrd1a and EBS7 (Fig. 3.12B). We hypothesized that EBS7 might regulate the protein stability or activity of AtHrd1a. Due to lack of an AtHrd1 antibody, it was impossible to directly compare the AtHrd1a abundance between *bri1-5* and *ebs7-1 bri1-5* mutants. Instead, we used independently-generated AtHrd1a-GFP-expressing transgenic *Arabidopsis* lines, which were treated with 180 mM CHX to analyze if the *ebs7-1* mutation reduces the AtHrd1a stability. Fig. 3.12C shows that the AtHrd1a was a quite stable protein in an *EBS7*$^{+}$ background but became quite unstable in the *ebs7-1* mutant, suggesting that EBS7 is important to maintain the protein stability of the ER membrane-anchored E3 ligase. Interestingly, treatment of MG132, a known inhibitor of proteasome, could significantly

increased the AtHrd1a abundance in the *ebs7-1* mutant background but had a marginal effect on that of the *AtHrd1a-GFP EBS7*$^{+}$ transgenic line (Fig. 3.12D). The MG132 experiment not only confirmed the role of EBS7 in maintaining the protein stability of AtHrd1a but also suggested that AtHrd1a in *ebs7-1* is degraded via a proteasome-mediated pathway.

Discussion

EBS7 is a plant-specific ER membrane-anchored component of an *Arabidopsis* ERAD machinery.

Despite rapid progress in understanding the plant ERAD process, it remains unknown if a plant ERAD machinery involves a plant-specific component as all reported studies identified homologs of known components of the yeast/mammalian ERAD pathways [see review in (152)]. In this study, we showed that EBS7 is a plant-specific component of the *Arabidopsis* ERAD machinery. First, all three *ebs7* mutants were isolated in two independent genetic screens for potential *Arabidopsis* ERAD mutants defective in degrading bri1-9 or bri1-5 and our subsequent biochemical experiments confirmed that *ebs7* mutations prevented the degradation of two ER-retained mutant variants of the BR receptor (Fig. 3.1&3.3). Our study revealed that the *ebs7-1* mutation could also block ERAD of a misfolded conformer of an *Arabidopsis* innate immunity receptor, EFR, in an *ebs1* mutant background (Fig. 3.3F). Second, our biochemical assays demonstrated that EBS7 interacts with AtHrd1a (Fig. 3.12B), an ER membrane-anchored E3 ligase that was previously known to function redundantly with its close homolog AtHrd1b in degrading bri1-9 (73), and that the *ebs7-1* mutation inhibits the ubiquitination of the mutant bri1-9 (Fig. 3.12A). Third, The *EBS7* gene was previously shown in multiple microarray

experiments to be coexpressed with genes encoding ERAD components and other ER-localized chaperones/folding catalysts (Fig. 3.6), which was the main reason for its being considered as a candidate gene for our map-based cloning of *EBS7*, and encodes an ER-localized membrane protein that accumulates in response to ER stress (Fig. 3.5G & Fig. 3.10A). Fourth, consistent with what were previously shown for other known *Arabidopsis* ERAD components (75, 153), loss-of-function *ebs7* mutations gave rise to increased sensitivity to ER/salt stresses (Fig. 3.10, B-C; Fig. 3.11). Lastly, BLAST searches against protein databases failed to identify EBS7 homologs in fungi or animals but discovered highly similar proteins in land plants that include *Selaginella* and *Physcomitrella* (Fig. 3.5F & Fig. 3.8).

EBS7 plays an important role in regulating AtHrd1 stability.

Although our data did not exclude the possibility that EBS7 is a necessary factor for the ubiquitin ligase activity of AtHrd1, our study strongly suggested that at least one of the biochemical functions of EBS7 is to regulate the stability of the ER membrane-anchored E3 ligase. Our CHX chasing experiment revealed that the *ebs7-1* mutation significantly increased the degradation rate of AtHrd1a (Fig. 3.12C) while our MG132 assay indicated that a brief treatment of the proteasome inhibitor could dramatically increase the protein abundance of AtHrd1a (Fig. 3.12D). The observed EBS7-AtHrd1a interaction suggested that EBS7 binding could prevent the self-/heterologous ubiquitination activity and subsequent degradation of the *Arabidopsis* ERAD E3 ligase. It is well known that ERAD E3 ligases in both yeast and mammalian cells are regulated by self-/heterologous ubiquitination (167). Alternatively, EBS7 might be needed to assemble the AtHrd1-containing ERAD complex. Although the *ebs7-1* mutation has little effect on the EBS5-

AtHrd1 interaction (Fig. 3.12B), the *ebs7-1* mutation could affect oligomerization of AtHrd1. It is well known that the ER-mediated protein quality control system retains and degrades not only the misfolded proteins but also improperly-assembled polypeptides; and an improperly assembled AtHrd1 could thus be degraded by an AtHrd1-independent ERAD pathway. It is interesting to mention that both the yeast Usa1 and mammalian HERP (homocysteine-induced ER protein) are known to directly interact with the corresponding ER membrane-anchored E3 ligases and are thought to regulate the stability and/or oligomerization of their interacting E3 ligases (94, 168, 169). Despite its lack of sequence homology with Usa1 and HERP, both of which carry an ubiquitin-like domain at their N-termini, EBS7 could be a functional homolog of the yeast Usa1 and mammalian HERP. However, complementation experiments revealed that EBS7 failed to rescue the yeast *Dusa1* mutant and that a HERP transgene driven by the strong *35S* promoter was unable to complement the *Arabidopsis ebs7-1* mutation (Fig. 3.13). It is quite possible that the biochemical mechanism by which EBS7 regulates the stability/oligomerization of the *Arabidopsis* Hrd1 homologs might be different from that of Usa1/HERP's regulation of their interacting ERAD E3 ligases.

The mutant ebs7-1 protein could be a novel-type ERAD substrate.

Our study also suggested that ebs7-1 might be another ERAD substrate that could be used to study the plant ERAD processes. The amino acid Ala^{131}, which was mutated to Thr in *ebs7-1*, is not highly conserved among the plant EBS7 homologs but significantly reduced the abundance of the mutant ebs7-1 protein (Fig. 3.5D), suggesting that the Ala^{131}-Thr mutation does not directly affect the biochemical activity of EBS7 but likely introduces a structural defect to the ER membrane-localized protein. Indeed, the mutant

ebs7-1 could still interact with AtHrd1a when expressed transiently in tobacco leaf epidermal cells (Fig. 3.14) and the abundance of ebs7-1 in the *ebs7-1* mutant could be elevated by treatment with the proteasome inhibitor MG132 (Fig. 3.10A). Unlike the two mutant variants of BRI1 or the misfolded conformer of EFR, which were retained in the ER by the *Arabidopsis* ER quality control systems, ebs7-1 is an ER resident protein (Fig. 3.5G). Thus understanding how ebs7-1 is degraded could provide additional knowledge of the plant ERAD processes. Besides being an ER-resident protein, ebs7-1 might be a so-called "ERAD-C" substrate with its structural lesion in the cytosolic side of the ER membrane (145). While we don't have any experimental data on the topology of EBS7, a bioinformatics analysis, known as TOPCONS [http://topcons.cbr.su.se, (170)], predicted that its N-terminal half, carrying the Ala^{131}-Thr mutation, likely localizes at the cytosolic face of the ER membrane (Fig. 3.15). In yeast, there are at least three different classes of ERAD substrates, ERAD-L, ERAD-M, and ERAD-C carrying structural lesion in the luminal domain, transmembrane segments, or cytosolic region of a misfolded protein, respectively, which are degraded by distinct ERAD machinery involving different ER membrane-localized E3 ligases (77). While the yeast Hrd1 is responsible for degrading ERAD-L and ERAD-M substrate, the removal of ERAD-C clients requires the ubiquitionation activity of another RING-type E3 ligase known as Doa10. Thus, *ebs7-1* could be used to identify components of the AtHrd1-independent ERAD-C machinery in *Arabidopsis*.

Materials and Methods

Plant Materials and Growth Conditions.

Most of the *Arabidopsis* wild-type, mutants and transgenic plants used in the study are in the Columbia-0 (Col-0) ecotype except *bri1-5*, its two allelic *ebs7* suppressors (*ebs7-2* and *ebs7-3*), and a different *bri1-9* mutant (used for mapping the *EBS7* locus), which are all in the Wassilewskija-2 (Ws-2) ecotype. Methods for seed sterilization and plant growth conditions were described previously (142), and the root-growth inhibition assay on BL-containing medium was performed according to a previously described protocol (171).

Map-based cloning of *EBS7*.

The *ebs7-1 bri1-9* mutant (Col-0) was crossed with *bri1-9* (Ws-2) to get the F1 plants. F1 plants were self-fertilized to generate several F2 mapping populations. Genomic DNAs of ~300 *ebs7-1*-like F2 plants were used for PCR-based mapping (see Table 3.1 for major markers used for mapping) to locate the *EBS7* locus within a 850-kb region on the middle of chromosome 4. To sequence candidate genes, genomic DNAs of 4 individual *ebs7-1 bri1-9* plants were extracted, PCR-amplified, sequenced, and compared with the corresponding wild-type genes to detect single-nucleotide polymorphisms.

Plasmid Construction and Generation of Transgenic Plants.

A 3.8-kb genomic fragment of *At4g29960* was amplified from the *Arabidopsis* Col-0 genomic DNA samples using the primer set *gEBS7* (see Table 3.1 for primer sequences) and cloned into *pPZP222* to make the *pPZP222-gEBS7* plasmid. To generate a *p35S:GFP-EBS7* transgene, a 714-bp coding sequence of GFP was amplified from *pBRI1:BRI1-GFP* (172) using the GFPN primer set (Table 3.1) and cloned into the *pCHF1* vector (173) to create a *pCHF1-GFPN* plasmid. The resulting vector was used to generate the translational fusion construct of *GFP-EBS7* with a 876-bp *EBS7* cDNA

fragment amplified from a cDNA preparation of the wild-type *Arabidopsis* (74) using the *GFPN-EBS7* primer set (Table 3.1). To generate the *EBS7-GFP* construct, a 876-bp cDNA fragment of *At4g29960* was amplified from the *Arabidopsis* Col-0 cDNA sample by primer EBS7-GFPC set (Table 3.1) and replaced the bri1-9 fragment in *pBRI1-bri1-9:GFP* to generate *pBRI1:EBS7-GFP*. The *p35S:AtHrd1a-GFP* transgene was created by cloning a 1,479-bp *AtHrd1a* cDNA fragment amplified from the same *Arabidopsis* cDNA preparation using the Hrd1a-GFP primer set (Table 3.1) into the *pCHF1-GFPC* vector, which was created by cloning a 714-bp coding sequence of GFP amplified from *pBRI1-BRI1:GFP* (172) with the GFPC primer set (Table 3.1). All these plasmids were fully sequenced to ensure no PCR-introduced error. The *gEBS2*, *pBRI1-BRI1:GFP*, *pBRI1-bri1-9:GFP*, and *p35S:RFP-HDEL* constructs were previously described (8, 73, 150). To generate *HERP-GFP* construct, a 1176-bp cDNA fragment of the human HERP was amplified from the human 293T cell cDNA library using the primer set HERP-GFP (Table 3.1) and cloned into the pCHF1-GFP vector to generate *p35S: GFP-HERP*. All these transgene constructs were mobilized into the *Agrobacterium* GV3101 strain and the resulting *Agrobacterial* cells were used to transform the flowering *Arabidopsis* wild type or the *ebs7-1* plants by the vacuum infiltration method (143) or to infect tobacco leaves by agroinfiltration (174).

Expression of Fusion Proteins In *E. coli* and Generation of Antibodies.

A 450-bp cDNA fragment encoding a 140AA N-terminal fragment of EBS7 was cloned into *pGEX-4T-1* (GE Healthcare) and *pMAL-c2x* (New England Biolab). The resulting plasmids were transformed into BL21 competent cells (Novagen). The induction and

purification of the glutatione *S*-transferase (GST)-tagged EBS7 [using glutathione sepharose 4B beads (GE Healthcare)] or the maltose-binding protein (MBP)-fused EBS7 [on amylose resin (New England Biolab)] were carried out according to the manufacturers' recommended procedures. The purified GST-EBS7 was sent to Pacific Immunology (www.pacificimmunology.com) for custom antibody production, and the resulting antiserum was used for affinity-purifying the anti-EBS7 antibody using MBP-EBS7 immobilized on Aminolink Plus coupling resin (Thermo Scientific) following the manufacturer's coupling/purification protocols.

Immunoblot, membrane fractionation, and CoIP Experiments. Two-week-old *Arabidopsis* seedlings treated with or without BL (Chemiclones Inc., Canada), CHX (Sigma), TM (Tocris), or MG132 (Sigma) were ground in liquid N2, dissolved in 2X SDS buffer, boiled for 5 min, and centrifuged for 10 minutes. The resulting supernatants were incubated with or without 1000 U of Endo-Hf (NEB) in 1X G5 buffer for 1.5 h at 37 °C or directly loaded onto 7% or 10% SDS-PAGE for separation. After transferring to PVDF membrane (Millipore), separated proteins were analyzed by immunoblot with anti-BES1 (144), anti-BRI1 (175), anti-BiP (at-95, Santa Cruz Biotechnology), anti-maize-CRT (46), anti-PDI (Rose Biotechnology Inc. Winchendon, MA), anti-EBS5 (73), anti-EBS6 (74), anti-EBS7 and anti-GFP (MMs-118P, Covance) antibodies. For coIP experiments, 0.5 gram of *Arabidopsis* seedlings were harvested and ground in liquid nitrogen, dissolved in the protein extraction buffer [50 mM Tris-Cl pH 8.0, 5 mM EDTA, 100 mM NaCl, 10% (v/v) glycerol, 0.4% Triton X-100, a protease inhibitor mix including 0.1 mM phhenylmethylsulphonyl fluoride, 1 μM pepstatin A and 0.5 mg/ml benzamidin hydrochloride, and a deubiquitinase inhibitor 10 mM N-ethylmaleimide].

After filtration through 25μm Miracloth (Calbiochem) to eliminate larger tissue debris, samples were centrifuged at 8000X *g* for 5 min, and the resulting supernatants were incubated with an anti-GFP antibody (TP401, Torry Pines Biolabs) and protein A-agarose beads (Invitrogen) for 8 h at 4ºC to immunoprecipitate GFP-tagged proteins. The immunoprecipitates were washed 4 times with the extraction buffer, boiled with 2X SDS buffer, separated by SDS-PAGE, transferred to PVDF membranes (Millipore), and analyzed by immunoblot with a monoclonal anti-GFP (MMS-118P, Covance), anti-Ubiquitin (P4D1, Santa Cruz Biotechnology), anti-EBS5 (73), or anti-EBS7 antibody. For the cell fractionation experiment, 0.5 gram of 2-week-old seedlings were ground in liquid N2, dissolved in homogenization buffer (protein extraction buffer without 0.4% Triton X-100), and centrifuged for 10 min in 8,000g. The resulting supernatants were collected as total (T) proteins. To separate membrane proteins from soluble proteins, total proteins were centrifuged 100,000 x *g* for 60min, and the resulting supernatants were collected as the soluble fraction (S) while the pellets were dissolved in the protein extraction buffer as the membrane fraction (M). All three protein fractions were mixed with 2X SDS buffer, boiled for 5 min, and separated by 10% SDS-PAGE and analyzed by immunoblot.

Tobacco Transient Expression and Confocal Microscopic Analysis of EBS7-GFP Fusion Proteins.

The *Agrobacterium* cells carrying *p35S:EBS7-GFP* or *p35S:RFP-HDEL* plasmid were mixed and co-infiltrated into leaves of 5-week-old tobacco (*Nicotiana benthamiana*) plants by the agro-infiltration method (174). The subcellular localization patterns of GFP-EBS7 and RFP-HDEL proteins were examined by using a Leica confocal laser-scanning

microscope (TCS SP5 DM6000B) and LAS AF software (Leica Microsystems). GFP and RFP were excited by using 488- and 543-nm laser lights, respectively.

Yeast Complementation Assay.

The Yeast wild-type strains BY4742 and a *Δusa1* deletion mutant strain carrying the pDN436 plasmid encoding a HA-tagged CPY* (which is an ER-retained mutant variant of the yeast vacuolar carboxypeptidase Y) was a gift from A. Chang (University of Michigan, Ann Arbor). The coding sequences of the yeast Usa1 (2.5-kb) and EBS7 (786-bp) were amplified from yeast and *Arabidopsis* using primer sets 352-Usa1 and 352-EBS7 (Table S1), respectively, and cloned into the *pYEp352-ALG9p* expression vector (64) to create *pYEp352-Usa1* and *pYEp352-EBS7* constructs. After fully sequencing to ensure no PCR-introduced error, the two plasmids were transformed into the Δusa1 yeast cells using a previously reported fast transformation method (176). Yeast cultures of the mid-log phase were treated with 100 μg/ml CHX for 0, 45 and 90 min, and were subsequently collected by centrifugation. Collected yeast cells were resuspended in 1X yeast extraction buffer (0.3 M sorbitol, 0.1 M NaCl, 5 mM MgCl2, and 10 mM Tris-Cl pH 7.4), lysed by vortexing with glass beads for 5 min, and boiled for 10 min in 2X SDS sample buffer. Supernatants after centrifugation were separated by 10% SDS-PAGE and analyzed by immunoblot with an anti-HA antibody (10A5, invitrogen).

Figure 3.1. the *ebs7-1* mutation suppresses the dwarf phenotype of *bri1-9* and restores its BR sensitivity by blocking the degradation of bri1-9.

(A) Immunoblot analysis of BRI1/bri1-9. Total proteins of 2-week-old seedlings of wild-type (WT), *bri1-9*, and *ebs7-1 bri1-9* were treated with or without Endo-H, separated by SDS-PAGE, and analyzed by immunoblot with a BRI1 antibody. bri1-9^{HM} and bri1-9^{CT} denotes BRI1/bri1-9 proteins carrying the high-mannose (HM)-type and complex-type (CT) N-glycans.

(B) Immunoblot analysis of the bri1-9 stability. Two-week-old seedlings of *bri1-9* and *ebs7-1 bri1-9* were treated with 180 μM CHX in liquid ½ MS medium for indicated hours, and extracted total proteins were separated by 7% SDS-PAGE and analyzed by immunoblot with the anti-BRI1 antibody.

(C-E) Shown here are 4-week-old light-grown **(C)** and 5-days-old dark-grown **(D)** seedlings, and two-month-old soil-grown plants **(E)** of WT, *bri1-9* and *ebs7-1 bri1-9*.

(F) The BR-induced root inhibition assay. Root lengths of ~ 40 7-d-old seedlings of WT, *bri1-9* and *ebs7-1 bri1-9* grown on half MS medium containing indicated concentrations of BL were measured, and converted into percentage values relative to that of the same genotype seedlings grown on medium without BL. Error bars represent the standard error of 3 independent assays.

(G) The BR-induced BES1 dephosphorylation assay. Total proteins extracted from 2-week-old seedlings of WT, *bri1-9*, and *ebs7-1 bri1-9* treated with or without 1 μM BL were separated by SDS-PAGE and analyzed by immunoblot with an anti-BES1 antibody.

In **(A)**, **(B)**, and **(G)**, coomassie blue staining of the small subunit of the Rubisco (RbcS) on a duplicate gel was used as a loading control.

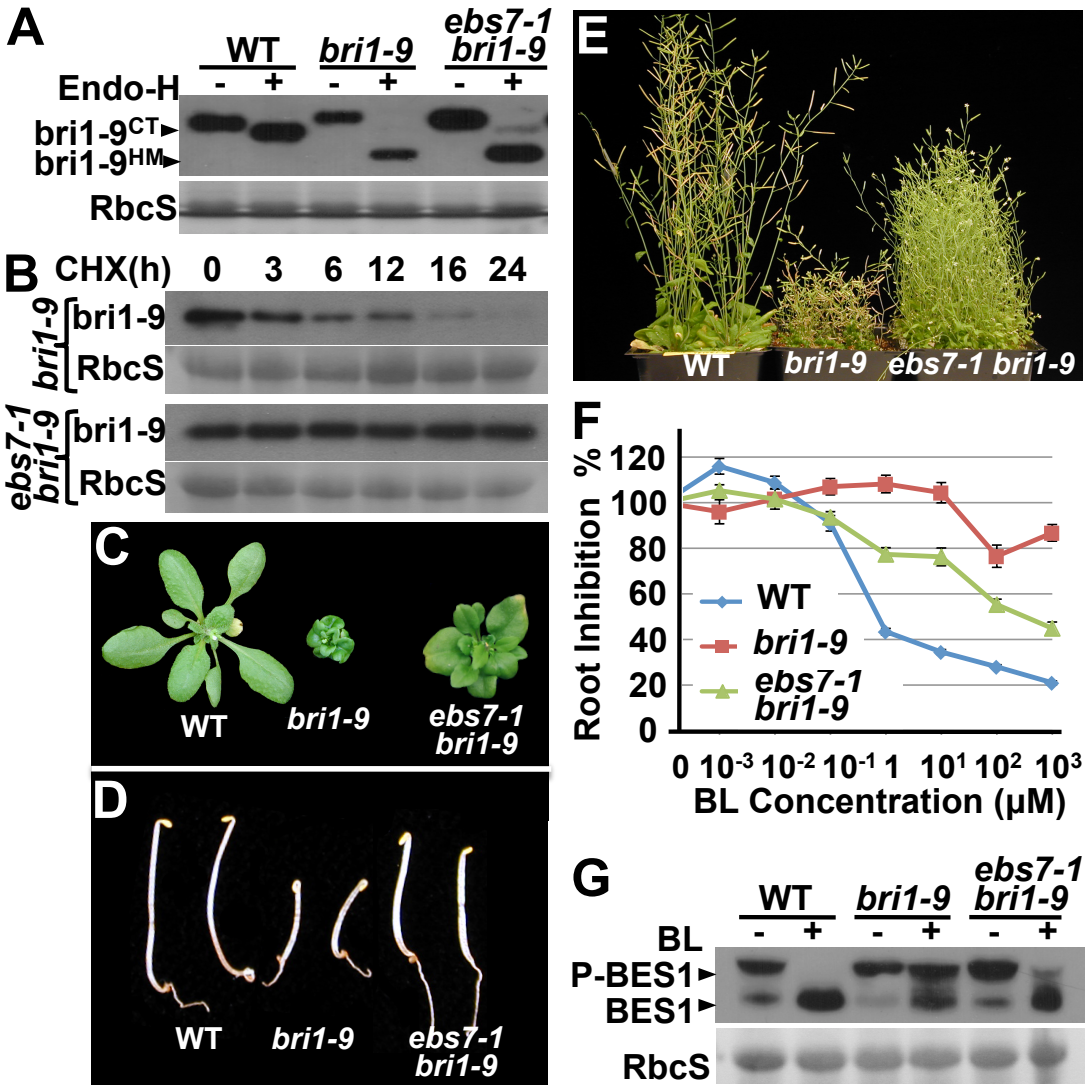
A
WT
bri1-9
ebs7-1 bri1-9
Endo-H
- + - + - +
bri1-9CT
bri1-9HM
RbcS
B
CHX(h) 0 3 6 12 16 24
bri1-9
bri1-9
RbcS
ebs7-1 bri1-9
bri1-9
RbcS
C
WT
bri1-9
ebs7-1 bri1-9
D
WT
bri1-9
ebs7-1 bri1-9
E
WT
bri1-9
ebs7-1 bri1-9
F
Root Inhibition %
120
100
80
60
40
20
0
WT
bri1-9
ebs7-1 bri1-9
0 10-3 10-2 10-1 1 101 102 103
BL Concentration (μM)
G
WT
bri1-9
ebs7-1 bri1-9
BL
- + - + - +
P-BES1
BES1
RbcS

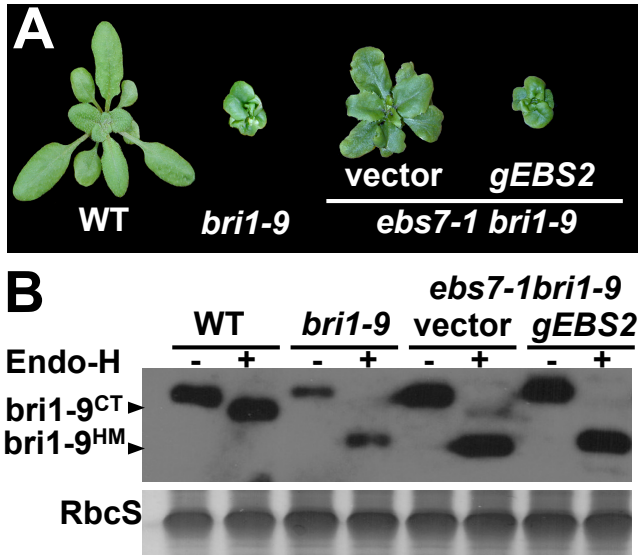

Figure 3.2. Overexpression of *EBS2* nullifies the suppressive effect of the *ebs7-1* mutation on the *bri1-9* dwarfism)

(A) Pictures of 4-week-old soil-growth plants of WT, *bri1-9*, and two transgenic *ebs7-1 bri1-9* mutants carrying an empty vector or a genomic *EBS2* transgene.

(B) Immunoblot analysis of BRI1/bri1-9. Total proteins extracted from 2-week-old seedlings of the genotypes shown in (A) were treated with or without Endo-H, separated by SDS-PAGE, and analyzed by immunoblot with an anti-BRI1 antibody. bri1-9^{HM} and bri1-9^{CT} denotes the BRI1/bri1-9 proteins carrying the high-mannose (HM) and complex type (CT) N-glycans, respectively. Coomassie blue staining of RbcS on a duplicated gel was used as a loading control.

Figure 3.3. The *ebs7-1* mutation inhibits the degradation of bri1-5 and misfolded EFR.

(A-B) Shown here are 4-week-old light-grown **(A)** and 5-days-old dark-grown **(B)** seedlings of WT, *bri1-5* and *ebs7-1 bri1-5*.

(C) The root inhibition assay of WT, *bri1-5* and *ebs7-1 bri1-5* seedlings. Root length of 7-d-old seedlings grown on BL-containing medium were measured and presented as the relative value of average length of BL-treated seedlings to that of the non-treated seedlings of the same genotype. Error bars represent the standard errors for three independent experiments of ~ 40 seedlings/each.

(D) The BES1 dephosphorylation assay. Total protein extracts of 2-week-old seedlings treated with or without 1 μM BL were separated by SDS-PAGE and analyzed by immunoblot with an anti-BES1 antibody.

(E) Immunoblot analysis of the BRI1/bri1-5 abundance. Total proteins of 2-week-old seedlings of WT, *bri1-5* and *ebs7-1 bri1-5* were treated with or without Endo-H, separated by SDS-PAGE, and analyzed by immunoblot with an anti-BRI1 antibody. bri1-5^{HM} and bri1-5^{CT} denotes the BRI1/bri1-5 proteins carrying the HM and CT N-glycans, respectively.

(F) Immunoblot analysis of EFR. Total protein extracts of 2-week-old seedlings of the indicated genotypes were separated by SDS-PAGE and analyzed by immunoblot with an anti-EFR antibody. In (D)-(F), coomassie blue staining of the RbcS band on a duplicate gel served as a loading control.

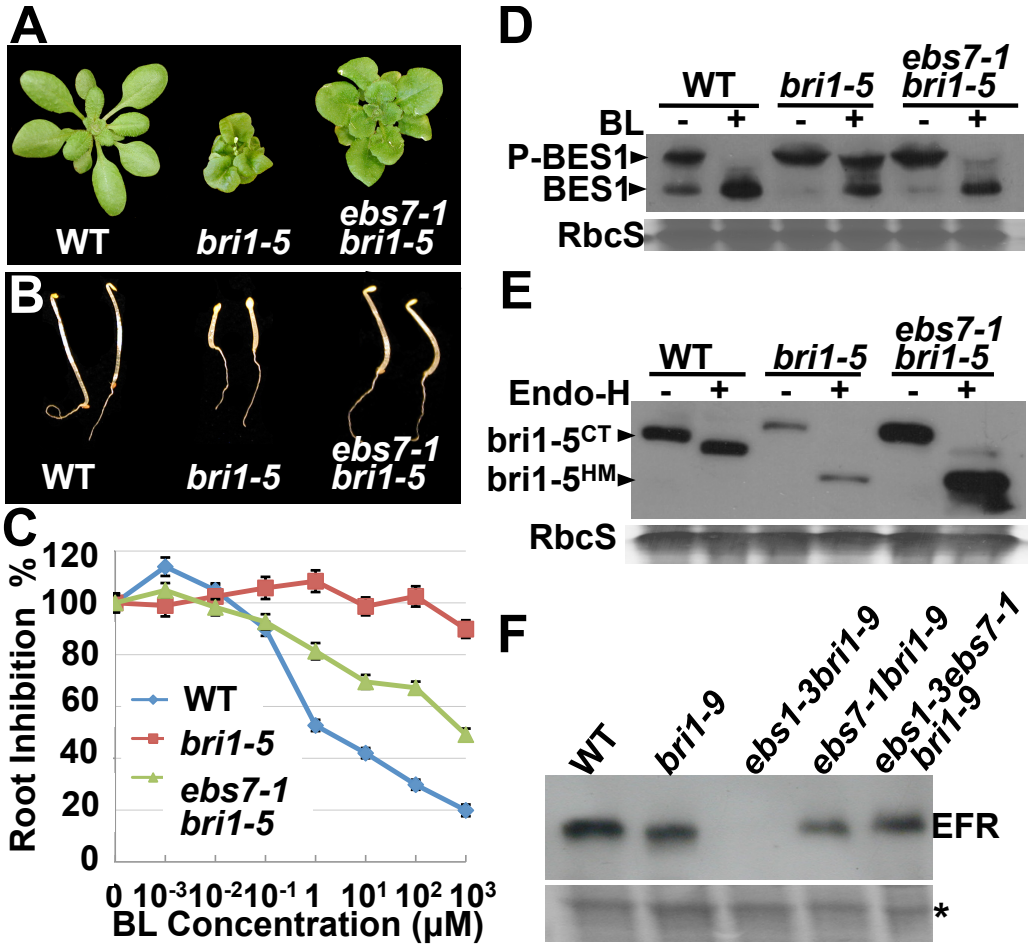
A
WT
bri1-5
ebs7-1
bri1-5
B
WT
bri1-5
ebs7-1
bri1-5
C
Root Inhibition %
120
100
80
60
40
20
0
WT
bri1-5
ebs7-1
bri1-5
0 10-3 10-2 10-1 1 101 102 103
BL Concentration (μM)
D
WT
bri1-5
ebs7-1
bri1-5
BL
- + - + - +
P-BES1
BES1
RbcS
E
WT
bri1-5
ebs7-1
bri1-5
Endo-H
- + - + - +
bri1-5CT
bri1-5HM
RbcS
F
WT
bri1-9
ebs1-3bri1-9
ebs7-1bri1-9
ebs1-3ebs7-1
bri1-9
EFR
*

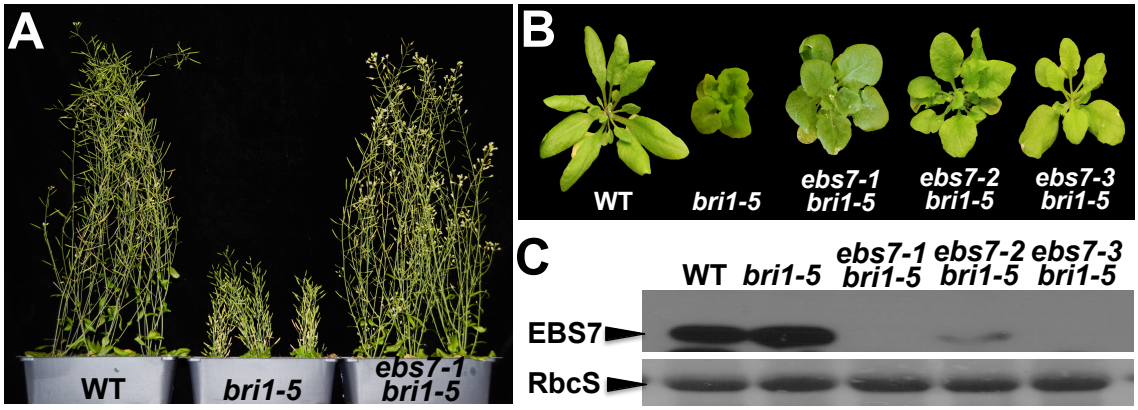

Figure 3.4. Screen for *bri1-5* suppressors identified two additional *ebs7* alleles.
(A) Pictures of 2-month-old soil-growth plants of wild type, *bri1-5*, and *ebs7-1 bri1-9*.
(B) Pictures of 4-week-old plants of WT (Ws-2), *bri1-5*, *ebs7-1 bri1-5*, *ebs7-2 bri1-5*, and *ebs7-3 bri1-5*.
(C) Immunoblot analysis of EBS7 protein. Total proteins extracted from 2-week-old seedlings of the genotypes shown in (B) were separated by SDS-PAGE and analyzed by immunoblot with an affinity purified anti-EBS7 antibody. Coomassie blue staining of the RbcS protein on a duplicated gel serves as a loading control.

Figure 3.5. EBS7 encodes an ER-localized membrane protein that is highly conserved in land plants.

(A) Map-based cloning of *EBS7* gene. The *EBS7* locus was mapped to a ~850-kb region on chromosome 4. The names of the mapping markers and numbers of recombinants are shown above and below the line, respectively. The *EBS7* gene structure is shown with bars denoting exons and lines indicating introns. Arrows show the positions of 3 identified *ebs7* mutations.

(B) The nucleotide changes, predicted molecular defects, and genetic backgrounds of the three *ebs7* alleles.

(C) Shown here are 4-week-old plants of WT, *bri1-9*, and two transgenic *ebs7-1 bri1-9* mutants carrying an empty vector or an *EBS7* genomic transgene.

(D) Immunoblot analysis of EBS7. Total proteins extracted from 2-week-old seedlings of the 4 genotypes shown in **(C)** were separated by SDS-PAGE and analyzed by immunoblot using an anti-EBS7 antibody. Star represents a non-specific band serving as a loading control.

(E) Immunoblot analysis of BRI1/bri1-9. Total proteins from **(D)** were treated with or without Endo-H, separated by SDS-PAGE, and analyzed by immunoblot with anti-BRI1 antibody. bri1-9^{HM} and bri1-9^{CT} denotes BRI1/bri1-9 proteins carrying the HM and CT N-glycans, respectively. Coomassie blue staining of RbcS on a duplicate gel served as the loading control.

(F) Sequence alignment of EBS7 and its representative plant homologs. Alignments of protein sequences of EBS7 (accession #: NP_567837), BdEBS7 (Bd: *Brachypodium distachyon*, XP_003577873), OsEBS7 (Os: *Oryza sativa Japonica*, NP_001053803), PtEBS7 (Pt: *Populus trichocarpa*, XP_002308117), GaEBS7 (Ga: *Genlisea aurea*, EPS72061), AtEBS7 (At for *Amborella trichopoda*, ERN12475), PsEBS7 (Ps: *Picea sitchensis*, ABR16454), and SmEBS7 (Sm: *Selaginella moellendorffii*, XP_002974885) were performed using the ClustalW program (http://mobyle.pasteur.fr/cgi-bin/portal.py). Aligned sequences were color-shaded at a BoxShade 3.31 server (http://mobyle.pasteur.fr/cgi-bin/portal.py). Residues identical in >6 proteins are shaded red while similar residues are shaded cyan. The positions of *ebs7* mutations are indicated by green triangles, while the three predicted transmembrane segments are indicated by blue bars.

(G) The confocal images of tobacco leaf epidermal cells transiently expressing EBS7-GFP (left), RFP-HDEL (middle), and superimposition of GFP and RFP (right).

(H) Immunoblot analysis of EBS7. Total (T), membrane (M), and soluble (S) proteins extracted from 2-week-old seedlings of WT and *ebs7-1* were separated by SDS-PAGE and analyzed by immunoblot with anti-EBS2, anti-EBS5, and anti-EBS7 antibodies.

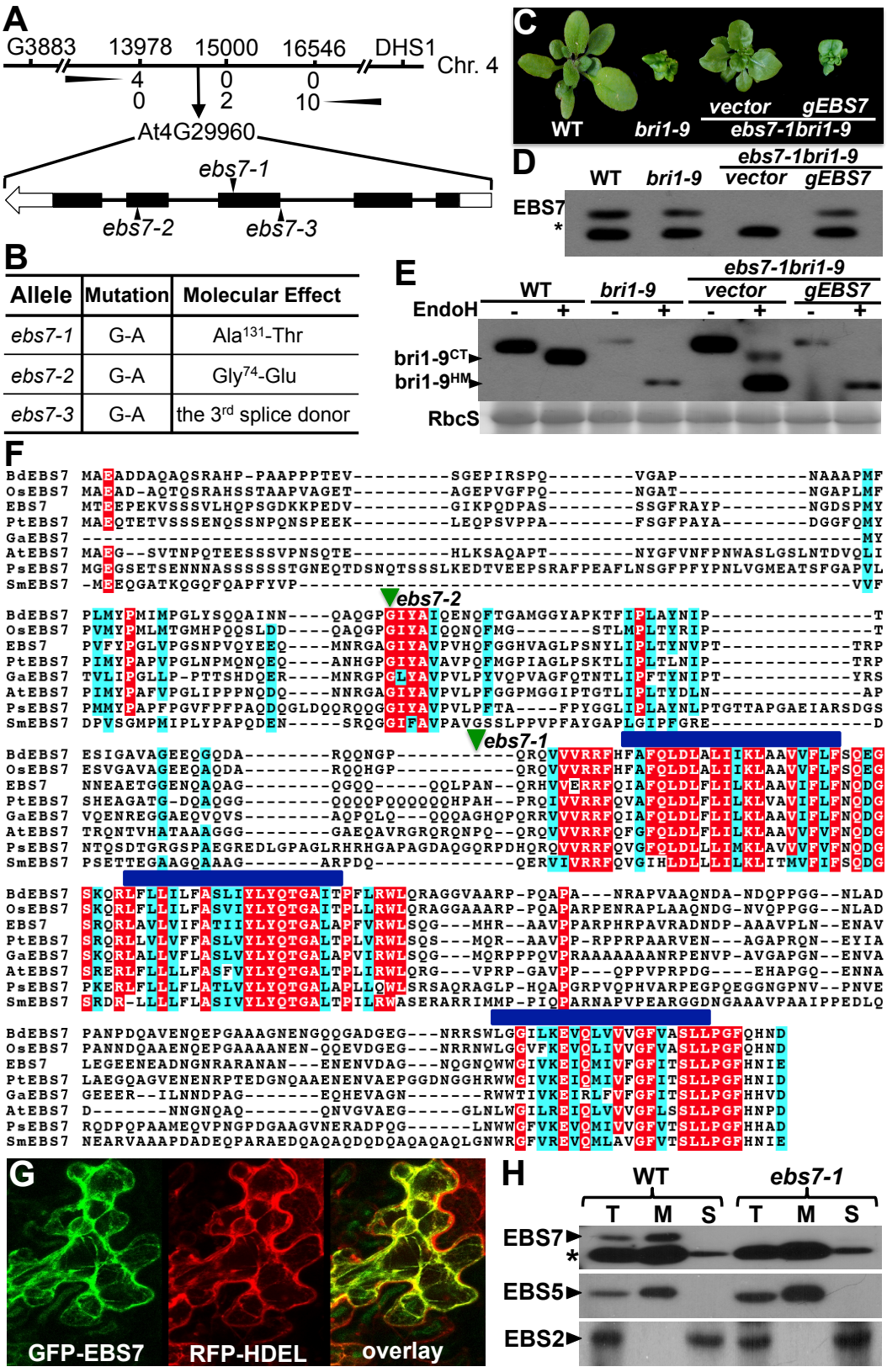
A
G3883
13978
15000
16546
DHS1
Chr. 4
4
0
0
0
2
10
At4G29960
ebs7-1
ebs7-2
ebs7-3
B
Allele | Mutation | Molecular Effect
ebs7-1 | G-A | Ala131-Thr
ebs7-2 | G-A | Gly74-Glu
ebs7-3 | G-A | the 3rd splice donor
C
WT
bri1-9
vector
gEBS7
ebs7-1bri1-9
D
WT
bri1-9
ebs7-1bri1-9
vector
gEBS7
EBS7
*
E
WT
bri1-9
ebs7-1bri1-9
vector
gEBS7
EndoH
- + - + - + - +
bri1-9CT
bri1-9HM
RbcS
F
ebs7-2
ebs7-1
G
GFP-EBS7
RFP-HDEL
overlay
H
WT
ebs7-1
T M S T M S
EBS7
*
EBS5
EBS2

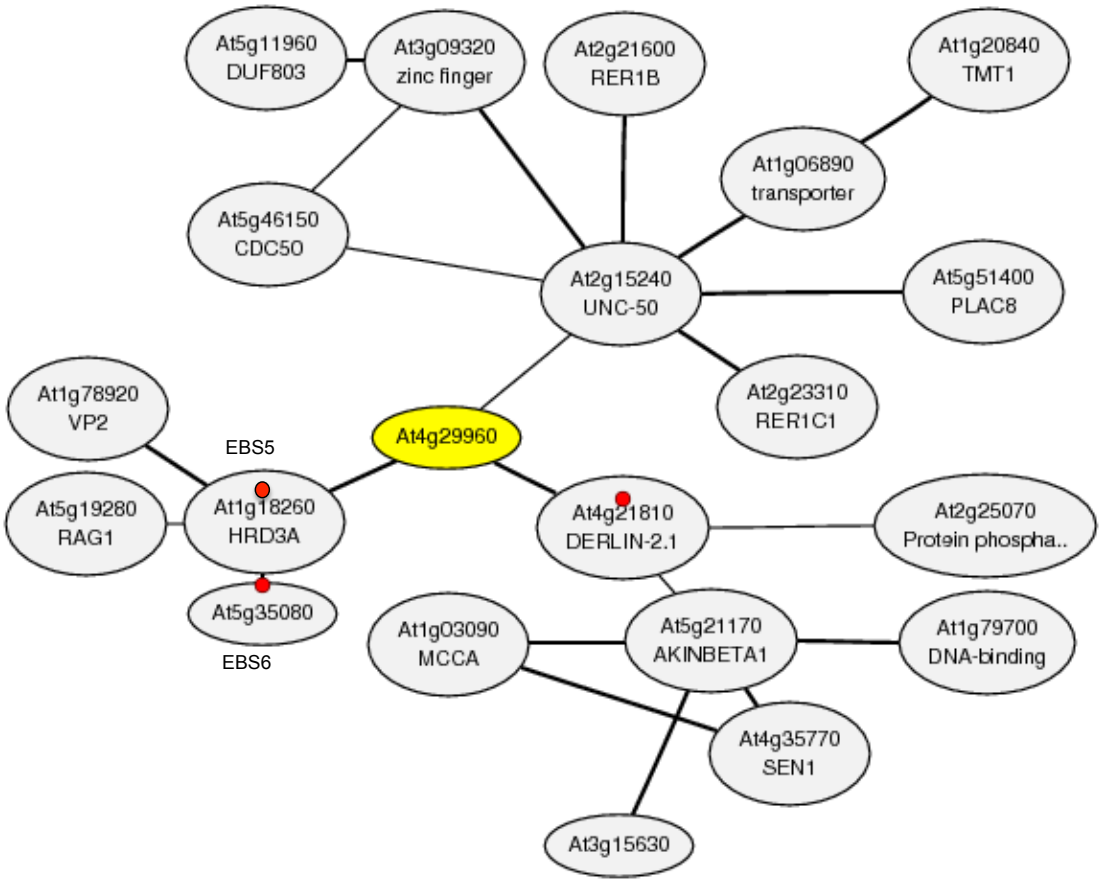

Figure 3.6. At4g29960 is coexpressed with at least three known/predicted ERAD genes.

Shown here is the coexpressed gene network around At4g29960, which was obtained from ATTEDII (http://atted.jp/) using At4g29960 (shaded yellow) as query. The red dots denote genes shown/predicted to be involved in the *Arabidopsis* ERAD process, and black lines link strong (think line) or weakly (thin line) coexpressed genes.

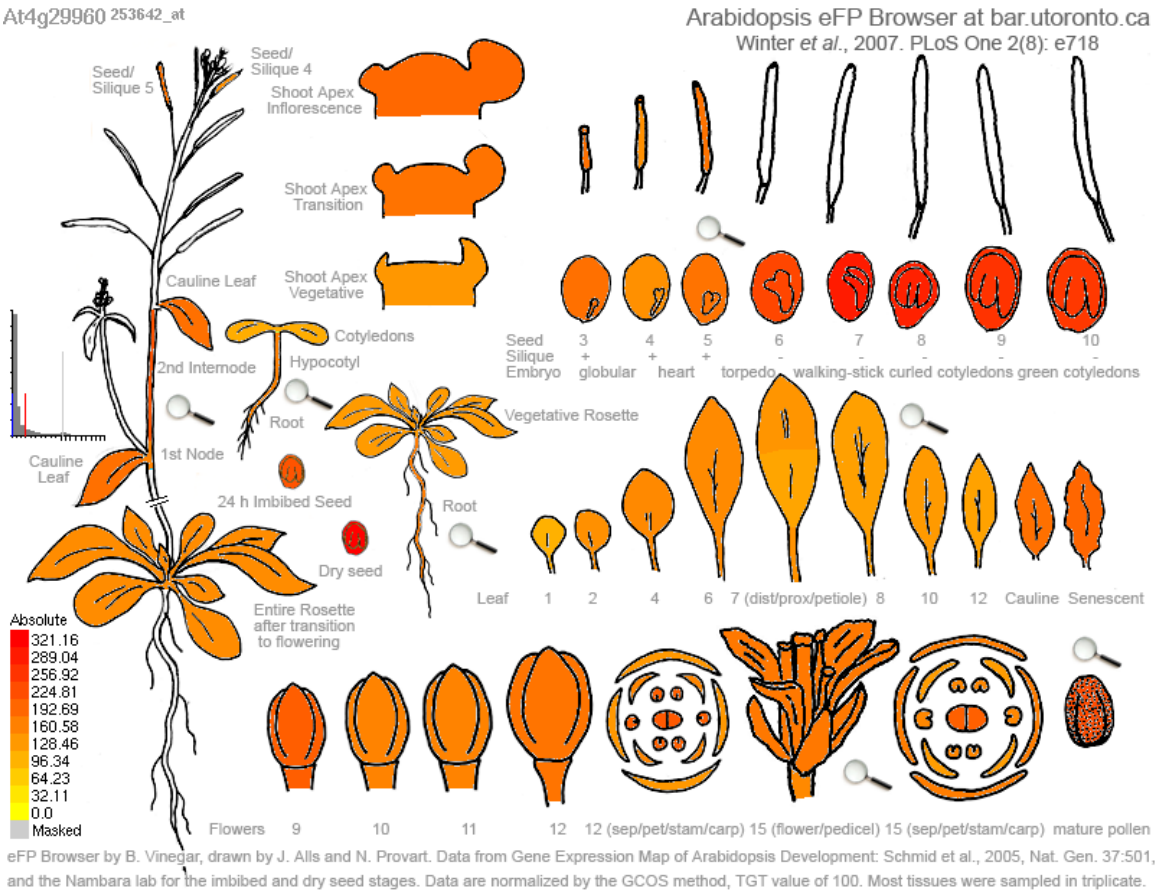

Figure 3.7. EBS7 is a ubiquitously expressed gene in *Arabidopsis*.
Visualization of the expression profile of At4g29960 in different tissues of a growing *Arabidopsis* plants, which was obtained from the *Arabidopsis* eFP browser web server (http://bar.utoronto.ca/efp_*Arabidopsis*/cgi-bin/efpWeb.cgi).

Figure 3.8. The polygenetic tree of EBS7 homologs in land plants.
Names of plant species and accession numbers of the corresponding EBS7 homologs are as follows: *Coffea canephora*, CDP19559.1; *Solanum lycopersicum*, XP_004242818; *Solanum tuberosum*, XP_006361645; *Mimius guttata*, EYU18221.1; *Mimius guttata*, EYU38750.1; *Genlisea aurea*, EPS72061.1; *Arbis alpina*, KFK40291.1; *Brassica napus*, CDY03554.1; *Brassica napus*, CDY43545.1; *Arbis alpina*, KFK29555.1; *Eutrema salsugineum*, XP_006412781.1; *Capsella rubella*, XP_006284250; *Arabidopsis lyrata*, XP_002867378; *Arabidopsis thaliana* (EBS7), NP_567837.1, *Cucumis melo*, XP_008453570.1; *Cucumis sativus*, XP_004146332; *Medicago truncatula*, XP_003595067; *Cicer arietinum*, XP_004487987; *Phaseolus vulgaris*, ESW10771; *Glycine max*, XP_006597064; *Glycine max*, NP_001242739.1; *Vitix vinifera*, XP_002269262; *Ricinus communis*, XP_002527805; *Jatropha curcas*, KDP47202.1; *Populus trichocarpa*, XP_002324697.1; *Populus trichocarpa*, XP_002308117.2; *Theobroma cacao*, XP_007014411.1; *Morus notabilis*, EXB30996.1; *Fragaria vesca subsp. vesca*, XP_004296487.1; *Malus domestica*, XP_008354453; *Prunus persica*, EMJ12895; *Prunus mume* XP_008223885.1; *Eucalyptus grandis*, KCW78661.1; *Citrus sinensis*, KDO61891.1;*Citrus clementina*, XP_006453265; *Setaria italica*, XP_004976735; *Zea mays*, NP_001142664.1; *Soghum bicolor*, XP_002447061; *Zea mays*, NP_001131686.1; *Oryza brachyantha*, XP_006653743; *Oryza sativa* Japonica Group, NP_001053803; *Oryza sativa* Indican Group, i-CAH66780; *Aegilops tauschii*, EMT30053; *Fragria vesca*, XP_004296487; *Triticum urartu*, EMS50749; *Brachypodium distachyon*, XP_003577873; *Phoenix dactylifera*, XP_008781761.1; *Amborella trichopoda*, ERN12475; *Picea sitchensis*, ABR16454; *Selaginella moellendorffii*, XP_002974885; *Physcomitrella patens*, XP_001756855.1.

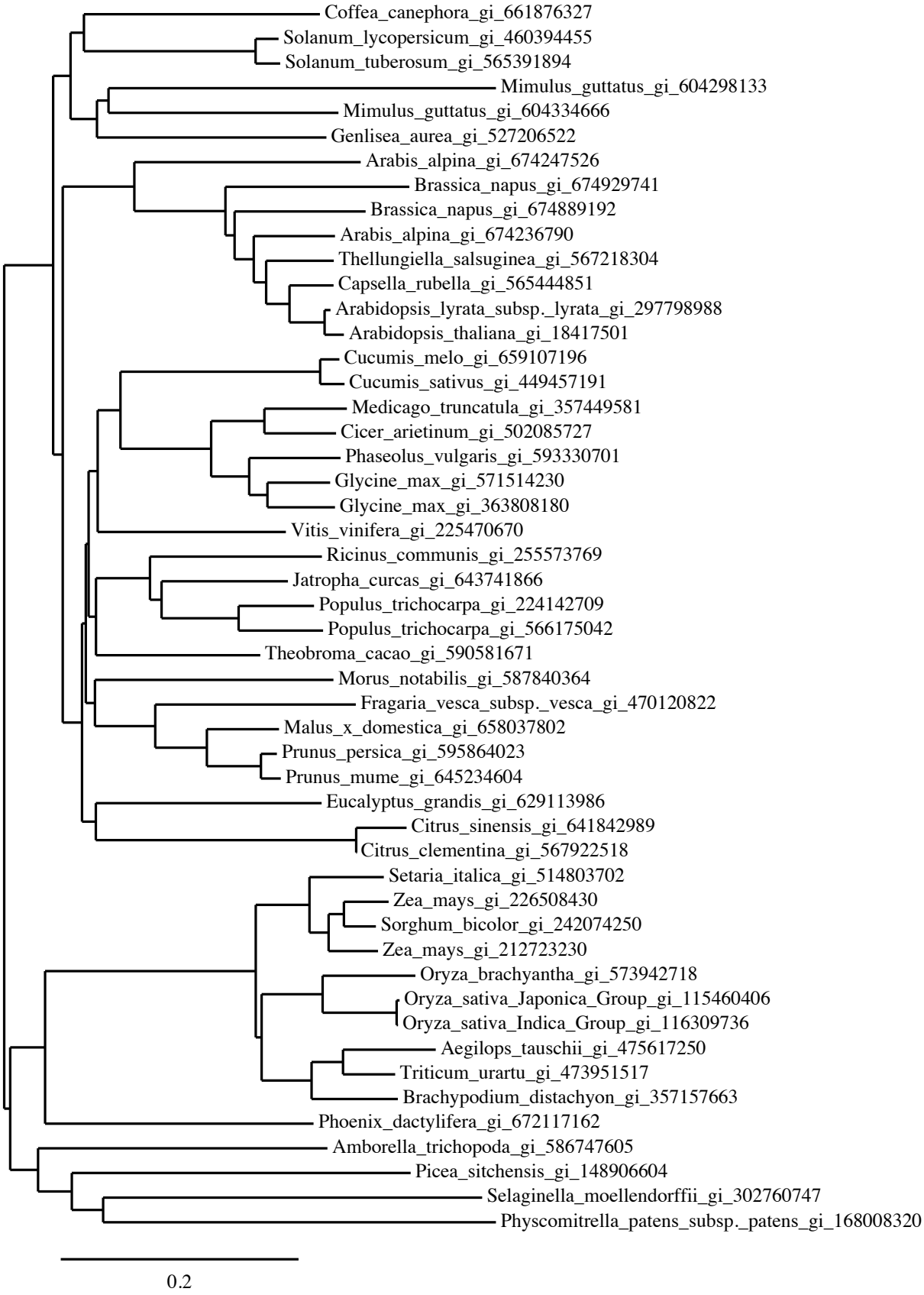
Coffea_canephora_gi_661876327
Solanum_lycopersicum_gi_460394455
Solanum_tuberosum_gi_565391894
Mimulus_guttatus_gi_604298133
Mimulus_guttatus_gi_604334666
Genlisea_aurea_gi_527206522
Arabis_alpina_gi_674247526
Brassica_napus_gi_674929741
Brassica_napus_gi_674889192
Arabis_alpina_gi_674236790
Thellungiella_salsuginea_gi_567218304
Capsella_rubella_gi_565444851
Arabidopsis_lyrata_subsp._lyrata_gi_297798988
Arabidopsis_thaliana_gi_18417501
Cucumis_melo_gi_659107196
Cucumis_sativus_gi_449457191
Medicago_truncatula_gi_357449581
Cicer_arietinum_gi_502085727
Phaseolus_vulgaris_gi_593330701
Glycine_max_gi_571514230
Glycine_max_gi_363808180
Vitis_vinifera_gi_225470670
Ricinus_communis_gi_255573769
Jatropha_curcas_gi_643741866
Populus_trichocarpa_gi_224142709
Populus_trichocarpa_gi_566175042
Theobroma_cacao_gi_590581671
Morus_notabilis_gi_587840364
Fragaria_vesca_subsp._vesca_gi_470120822
Malus_x_domestica_gi_658037802
Prunus_persica_gi_595864023
Prunus_mume_gi_645234604
Eucalyptus_grandis_gi_629113986
Citrus_sinensis_gi_641842989
Citrus_clementina_gi_567922518
Setaria_italica_gi_514803702
Zea_mays_gi_226508430
Sorghum_bicolor_gi_242074250
Zea_mays_gi_212723230
Oryza_brachyantha_gi_573942718
Oryza_sativa_Japonica_Group_gi_115460406
Oryza_sativa_Indica_Group_gi_116309736
Aegilops_tauschii_gi_475617250
Triticum_urartu_gi_473951517
Brachypodium_distachyon_gi_357157663
Phoenix_dactylifera_gi_672117162
Amborella_trichopoda_gi_586747605
Picea_sitchensis_gi_148906604
Selaginella_moellendorffii_gi_302760747
Physcomitrella_patens_subsp._patens_gi_168008320
0.2

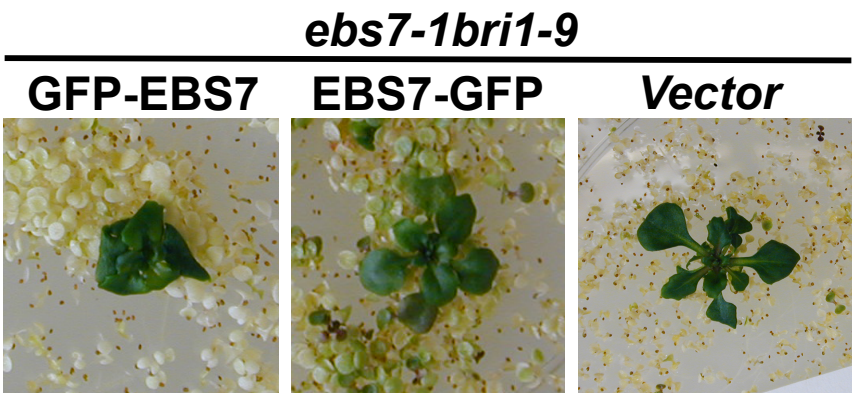

Figure 3.9. Only GFP-EBS7 but not EBS7-GFP rescued the *ebs7-1* mutation.
Shown here are pictures of representative transgenic *ebs7-1 bri1-9* seedlings carrying the *GFP-EBS7*, *EBS7-GFP*, or an empty vector, which were grown on ½ MS medium containing 100 μg kanamycin/mL.

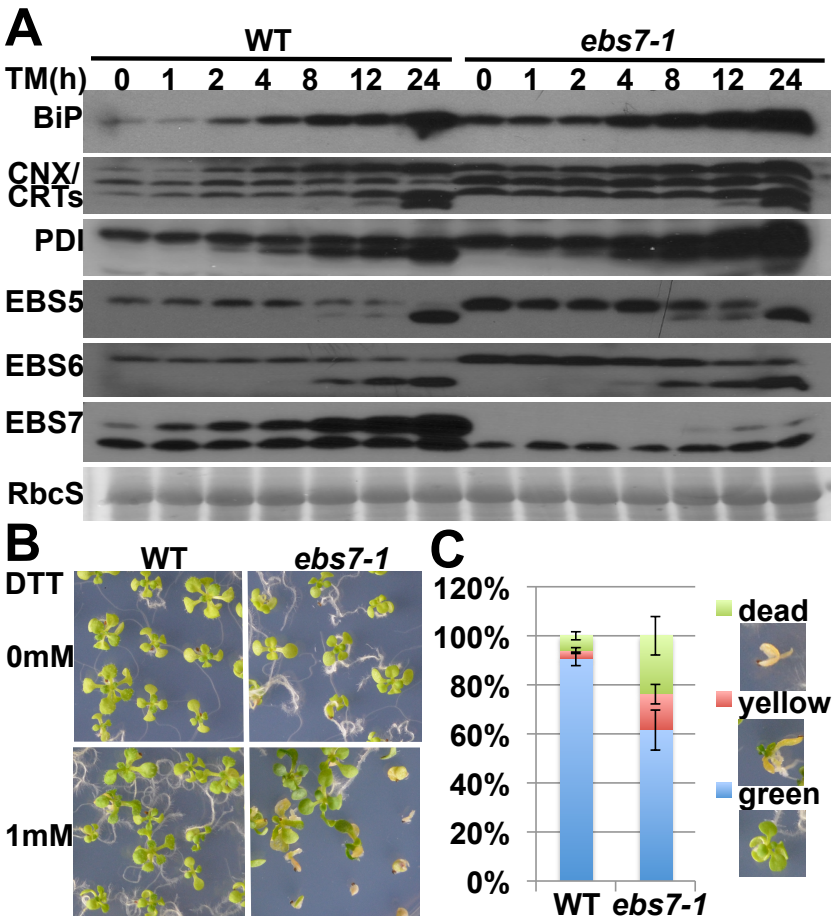

Figure 3.10. The ebs7-1 mutant exhibits constitutive UPR activation and is hypersensitive to ER stress.

(A) Immunoblot analysis of ER proteins. Total proteins of 2-week-old WT and *ebs7-1* seedlings treated with 5μg/mL TM for the indicated hours were separated by SDS-PAGE and assayed by immunoblot with antibodies against BiPs (Binding Immunoglobulin Proteins), PDIs (protein disulfide isomerases), CNX/CRTs (calnexins and calreticulins), EBS5, EBS6, and EBS7. Coomassie blue staining of RbcS on a duplicated gel was used as the loading control.

(B) Shown here are 2-week-old WT and *ebs7-1* seedlings grown on 1/2 MS medium containing 0 or 1 mM DTT.

(C) Quantification analysis of sensitivity to the DTT-induced ER stress. Seedlings being "green", "yellow", or "dead" were counted, and the percentages of each type of seedlings were calculated and shown in the bar graph. Error bar represents standard deviation for 3 independent assays of ~50 seedlings/each.

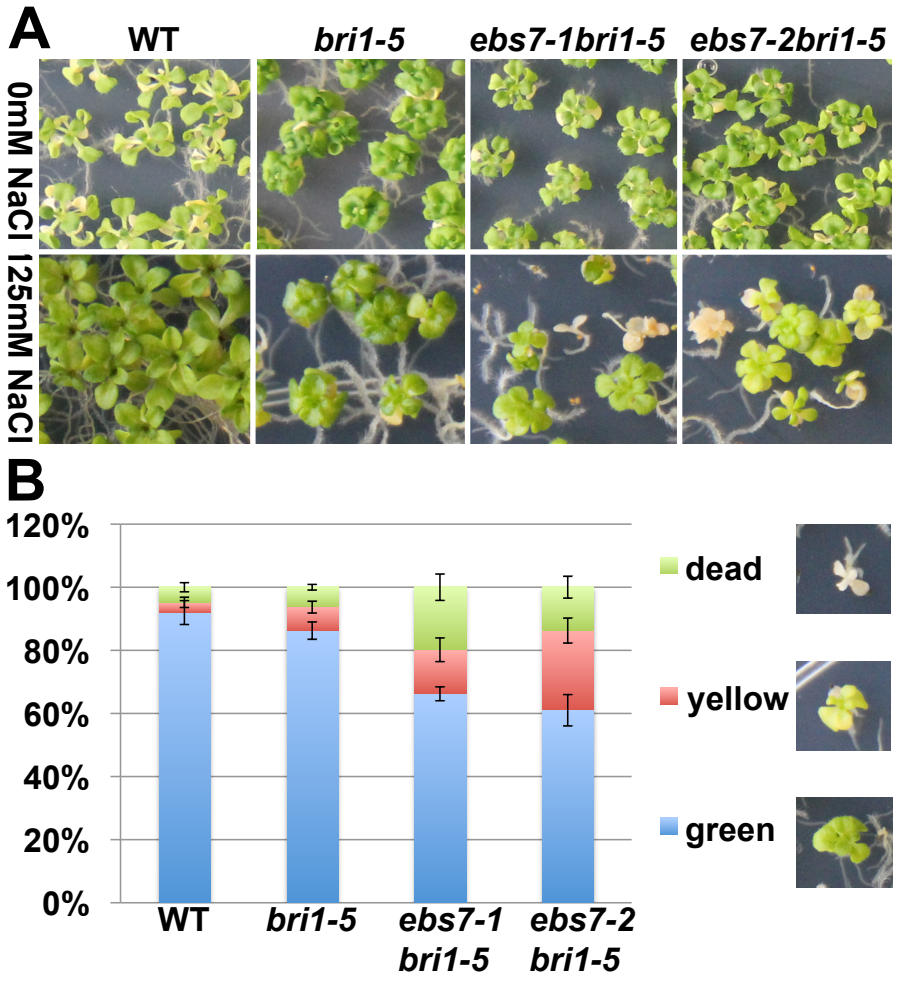

Figure 3.11. The *ebs7* mutations cause hypersensitivity to salt stress.
(A) Shown here are pictures of 2-week-old seedlings of WT, *bri1-5*, *ebs7-1 bri1-5* and *ebs7-2 bri1-5* grown on 1/2 MS medium supplemented with or without 125mM NaCl.
(B) Quantification analysis of sensitivity to the salt stress. Seedlings being "green", "yellow", or "dead" were counted, and the percentages of each type of seedlings were calculated and shown in the bar graph. Error bar represents standard deviation for 3 independent assays of ~50 seedlings/each.

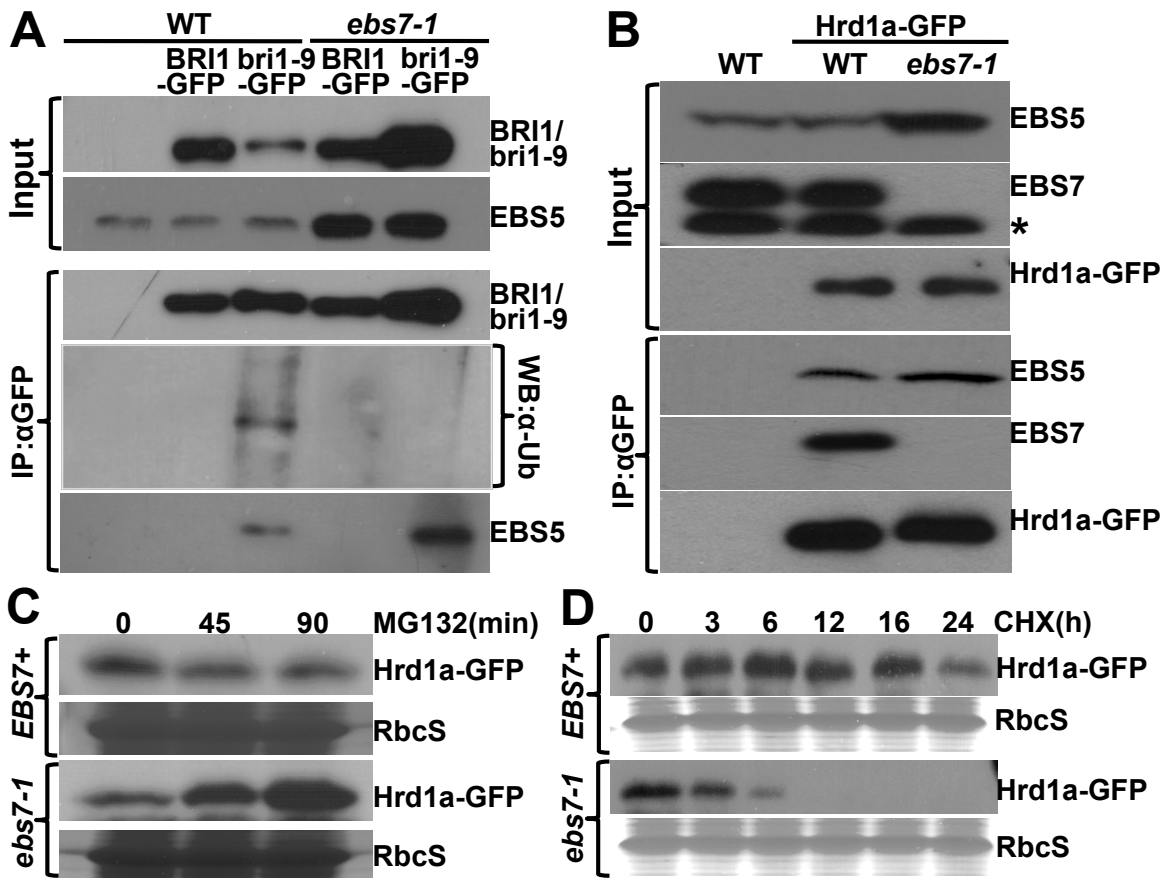

Figure 3.12. EBS7 interacts with AtHrd1a and affects its stability

(A) CoIP of bri1-9 and EBS5. Equal amounts of total proteins and anti-GFP immunoprecipitates from WT or transgenic plants were separated by SDS-PAGE and analyzed by immunoblot with anti-GFP, anti-Ubiquitin and anti-EBS5 antibodies.

(B) CoIP of EBS7, AtHrd1a, and EBS5. Equal amounts of total protein extracts and anti-GFP immunoprecipitates from WT or transgenic *Arabidopsis* plants were separated by SDS-PAGE and analyzed by immunoblot with anti-GFP, anti-EBS7 and anti-EBS5 antibodies.

(C) Immunoblot analysis of AtHrd1a-GFP. Total proteins of 2-week-old AtHrd1-GFP-expressing transgenic seedlings treated with 80μM MG132 for different durations were separated by SDS-PAGE and analyzed by immunoblot with a GFP antibody.

(D) Immunoblot analysis of the AtHrd1a-GFP stability. Total proteins extracted from 2-week-old seedlings treated with 180μM CHX in 1/2 liquid MS medium for the indicated durations were separated by SDS-PAGE and assayed by immunoblot with an anti-GFP antibody. In **(C)** and **(D)**, coomassie blue staining of RbcS on a duplicate gel served as a loading control.

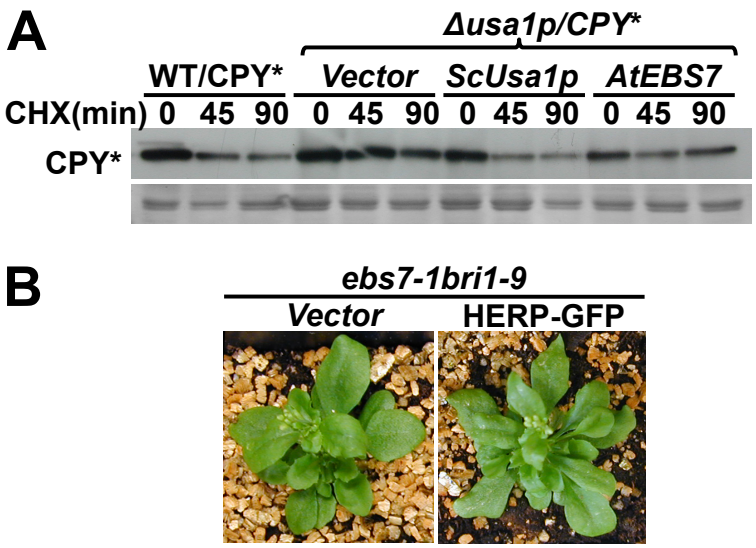

Figure 3.13. EBS7 is not a functional homolog of the yeast Usa1 or the mammalian HERP

(A) Immunoblot analysis of the protein abundance of CPY* in the yeast BY4742 and *Δusa1* strains carrying the indicated expression plasmids. Coomassie blue staining of an unknown major yeast protein on a duplicate gel serves as the loading control.

(B) Shown here are pictures of 4-week-old soil-grown plants of two representative transgenic *ebs7-1 bri1-9* plants carrying the empty vector or the *p35S:HERP-DFP* transgene.

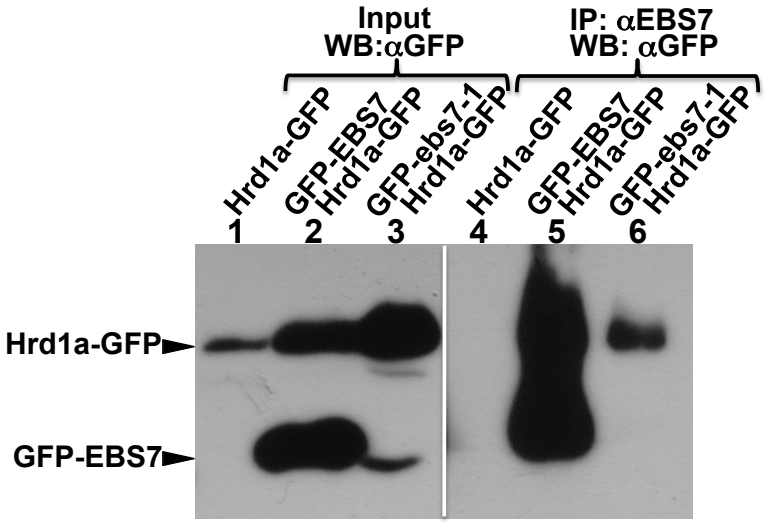

Figure 3.14. The mutant ebs7-1 protein could still interact with AtHrd1a.
Total proteins from tobacco leaves infiltrated with *Agrobacteria* cells carrying *p35S:Hrd1a-GFP* alone or with *p35S:GFP-EBS7* or its mutant variant *p35S:GFP-ebs7-1* were either directly separated by SDS-PAGE and analyzed by immunoblot using a monoclonal anti-GFP antibody (**Input/WB:aGFP**) or incubated with anti-EBS7 antibodies and protein A sepharose beads to precipitate GFP-EBS7/ebs7-1 and their binding factors. The anti-EBS7 immunoprecipitates were separated by SDS-PAGE and analyzed by immunoblot with the same anti-GFP antibody (**IP:aEBS7/WB:aGFP**). Despite low levels of GFP-ebs7-1 in both input and IP fractions (lanes 3 & 6), the AtHrd1a-GFP signal was easily detected in the anti-EBS7 immunoprecipitate obtained from tobacco leaf cells coexpressing AtHrd1-GFP and GFP-ebs7-1 (lane 6).

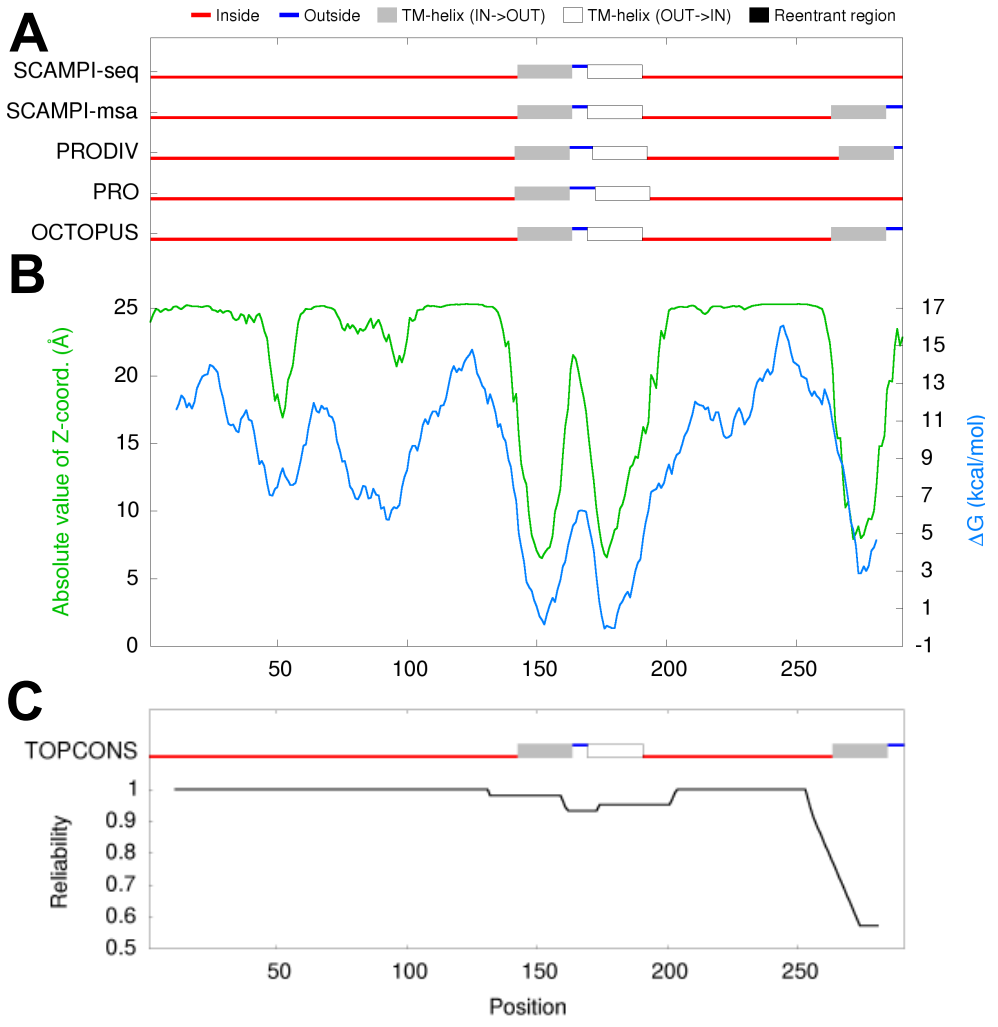

Figure 3.15. The predicted topology of EBS7.
Shown here are the graphic outputs from the TOPCONS web server at http://topcons.cbr.su.se/.
(A) EBS7 topologies predicted by various indicated methods with inside red line being in the cytosol.
(B) Shown here are the Z-coordinates (estimated distance of each amino acid to the membrane center) and DG values (theoretically calculated free-energy contribution of translocon-mediated membrane insertion of a 21-amino acid oligopeptide around each amino acid of EBS7).
(C) The consensus prediction of the EBS7 topology by the TOPCONS algorithm along with the reliability scores, which is based on the level of agreement between individual methods shown in (A).

Table 3.1. A list of primers used in Chapter 3.

Name	Sequence	Usage
G3883	CATCCATCAAACAAACTCC TGTTTCAGAGTAGCCAATTC	SSLP Ws-2 < Col-0
DHS1	CAAGTGACCTGAAGAGTATCG AGAGAGAATGAGAAATGGAGG	dCAPs DdeⅠ cut Col-0
13978	AAGTAAGAGTAACCGAGGCGATC TAGGGAGGAGACAGAATCAGGGAA	dCAPs EcoRⅠ cut Col-0
15000	ACAATACAGAAGTTGCATAACTGCA AAACTATACCATGTGAAATACGGG	dCAPs PstⅠ cut Col-0
16546	CAGATAAAAGAAATAGATCTTCCCACTA TGTTGAAGGCTCTTGGTACACAG	dCAPs SpeⅠcut WS-2
GFPN	TACGAGCTCATGAGTAAAGGAGAAGAACTTTTCA GGGGTACCTTTGTATAGTTCATCCATGCCATGT	Generation of pCHF1-GFPN vector
GFPC	CGGGATCCATGAGTAAAGGAGAAGAAC GACGTCGACTTATTTGTATAGTTCATCCATGC	Generation of pCHF1-GFPC vector
gEBS7	TGCGTCGACGGAGTTGTACCTGACTCGATC TCGGCAGCTTGTTTCTGAACC	Generation of EBS7 genomic transgene
GFPN-EBS7	GAAGATCTATGACGGAAGAACCAGAGAAGGTG CATGTCGACCTACTCTATGTTGTGAAAACCAGGGA	Generation of *GPF-EBS7* fusion transgene
EBS7-GFPC	GCTCTAGAGAAAATGACGGAAGAACCAG GAAGATCTTCTATGTTGTGAAAACCAGGGAG	Generation of *EBS7-GFP* fusion construct
EBS7N-GST	TCGAATTCATGACGGAAGAACCAGAGAAGG TGCGTCGACTCACTGAAATCTCCTTTCCACAACATG	Expression of EBS7-GST fusion protein in E.coli
EBS7-MBP	TCGAATTCATGACGGAAGAACCAGAGAAGG TGCGTCGACTCAAGGTAGCTGCTGCTGCTGACC	Expression of EBS7-MBP fusion protein in E.coli
HERP-GFP	CGGGATCCATGGAGTCCGAGACCGAACCCG CCGCTCGAGTCAGTTTGCGATGGCTGGGG	Generation of hsHERP cDNA-GFP fusion transgene
Hrd1a-GFP	GGGGTACCCATAGAAACACCGTTTCCTCCTC CGGGATCCCTCTGCTGCATCAGCAACCGAC	Generation of AtHrd1a cDNA-GFP fusion transgene

352-Usa1	ATGTCTGAATATCTAGCTCAGACGC GCTCTAGATTAGTCTTCATCAGGAATGTAGAGATG	Expression of yeast Usa1 in yeast
352-EBS7	ATGACGGAAGAACCAGAGAAGGT GCTCTAGACTACTCTATGTTGTGAAAACCAGGGA	Expression of AtEBS7 in yeast

CHAPTER 4
CONCLUSIONS AND FUTURE DIRECTIONS

Conclusion

ER-quality control (ERQC) is an essential cellular process that supervises the protein folding and degradation process to maintain the ER homeostasis. One of the well-studied ERQC machinery that regulates the glycoprotein folding is called CNX/CRT cycle in which CNX/CRT serve as chaperone-like lectins to bind incompletely-folded glycotproteins. Although the biological functions of CNX/CRT have been thoroughly investigated, the corresponding motifs that are responsible for these functions are largely unknown. Previous *in vitro* biochemical assays and crystallographic analysis of recombinant CRT protein suggested the identity of amino acids that play important role in the chaperone function of the lectin (133-135). However, lacking of CRT knockout animal models due to the early embryonic lethality effect makes it difficult to pursue the *in vivo* importance of these amino acids (22). In this study, the use of a vital plant model of a insertional mutant of AtCRT3 *Arabidopsis* line provided the first *in vivo* evidence for the physiological importance of these putative carbohydrate-binding residues. In *Arabidopsis*, CTR3 but not the other CRTs (CRT1/2) plays a crucial role in retaining the misfolded bri1-9 and completing the folding cycle of EFR. In the AtCRT3 insertional mutant named *ebs2-8*, bri1-9 protein is not retained in ER. Combining the site-directed

mutagenesis and *Agrobacterium*-mediated plant transformation experiments, I discovered that five out of six predicted carbohydrate-binding sites are indispensable for CRT3 to retain bri1-9 and mutations in these amino acids resulted in a dysfunctional CRT3 protein that failed to complement the loss-of-function *ebs2-8* mutant. In contrast, a residue corresponding to a mammalian CNX glucose-binding site is dispensable for the folding sensor ability of CRT3, indicating the structural diversity between these two close homologs. In addition, the substrate specificity of CRT3 compared with CRT1/2 was examined. A positively charged tetrapeptide in the C-terminal of CRT3 was identified that is conserved among CRT3 groups in different plant species but is distinct from the CRT1/2 group. Through complementation experiments, it was revealed that this basic tetrapeptide plays an important role in maintaining the chaperone function of CRT3. This functional study of *Arabidopsis* CRT3 was described in Chapter 2.

As part of the ERQC system, the ER-associated degradation (ERAD) machinery handles the terminally-misfolded proteins and eliminates them by ubiquitin-mediated degradation. Comparing with the comprehensive studies of yeast and mammalian ERAD machineries, the plant ERAD system remains elusive. In this thesis, the identification and characterization of a novel plant-specific ERAD component EBS7 was described. EBS7 encodes a plant-specific protein that has homologs in many land plant species. Mutations in EBS7 block the degradation of bri1-5 and bri1-9, two misfolded BRI1 alleles that undergo degradation via ERAD. In addition, the elimination of incomplete/misfolded EFR is abolished in *ebs7* mutant. EBS7 participates in plant response to ER and salt stress as mutations in EBS7 activate UPR and cause plants to become less tolerant to salt stress. EBS7 interacts with AtHrd1, the central E3 ubiquitin ligase in the ERAD

machinery and maintains its stability. Loss of EBS7 in plant cell destabilizes AtHrd1 and leads to the proteasome-mediated degradation of this E3. In the current model, EBS7 is proposed to indirectly affect the degradation of ERAD substrates by regulating the stability of E3 in the ERAD machinery. Collectively, the study of EBS7 has not only illustrated a novel component of the *Arabidopsis* ERAD system, but also shed light on mechanisms of plant-specific ERAD regulation. The characterization of EBS7 was decribed in Chapter 3.

Future Directions

Defining the function of EBS7 in AtHrd1 complex

Chapter 3 has focused on the role of EBS7 in regulating *Arabidopsis* ERAD via its interaction with AtHrd1. Despite this discovery, there are still some open questions about the function of this plant-specific ERAD component. One question is how EBS7 affects the stability of the E3 ligase AtHrd1. Our previous hypothesis is that EBS7 may act as a functional homolog of one of the known ERAD components though it does not have sequence level similarity with other ERAD members. In the yeast Hrd1 degradation complex, factors including Hrd3, Usa1 and Der1 were reported to participate in regulating the E3 ligase activity and/or stability (94, 177). The Hrd3 homolog in *Arabidopsis* was previously reported named EBS5 (73). Usa1 is predicted to have two transmembrane motifs and a N-terminal region containing an ubiquitin-like (Ubl) domain (77). In early studies, it was shown that Usa1 is required for the degradation of both luminal and membrane-anchored substrates (ERAD-L and ERAD-M, respectively) and that this function is not through the Ubl domain (77, 94, 96). On the contrary, Ubl domain

is indispensable the regulation of Hrd1 self-destruction. Usa1 promotes the interactions between different Hrd1 molecules and it is involved in the regulation of the E3 enzymatic activity directly through the Ubl domain (94). Der1 is a four-transmembrane protein. It is recruited to the ERAD complex through Usa1 and it participates in the substrate retrotranslocation from ER to cytosol and Hrd1 stability regulation (98, 99, 177, 178). The mammalian ERAD system contains multiple Der1 homologs but no obvious Usa1 homolog based on sequence homology. A two-transmembrane ER-anchored protein HERP however, partially complements the ERAD defect in *Δusa1* yeast cells, suggesting their functional similarity. Similar to Usa1, HERP mediates the recruitment of other ERAD members to the E3 complex (96, 179). Moreover, it has been shown to involve in ERAD-L degradation through UBL domain but it does not play any role in regulating the stability or oligomerization of HRD1 (179, 180).

EBS7 is predicted to contain two to three transmembrane domains and it localizes on ER membrane (Fig. 3.5G&H). This topological similarity with Usa1/HERP and its interaction with AtHrd1 initially led to the hypothesis that AtEBS7 might function similar to Usa1 or HERP in the ERAD machinery. However, both yeast and plant complementation experiments disagreed with this idea (Fig. 3.13). The E3 complex formation has no significant change in an *ebs7* loss-of-function mutant (data not shown), suggesting EBS7 may not conduct the oligomerization of the plant E3 ligases as well. This observation may not be surprising as EBS7 lacks the important UBL domain that is required for the normal function of both Usa1 and HERP. One possibility is that an EBS7-interacting protein may contain the UBL domain and it works together with EBS7 to fulfill its multiple functions in degradation machinery. A yeast two-hybrid screening

using EBS7 as a target or purification of EBS7-containing protein complex might provide insight into this idea. Additionally, further investigation of the *Arabidopsis* Der1 homologs will reveal whether EBS7 works as a scaffold protein for the ERAD complex and answer the question whether EBS7 has any functional overlap with Usa1/HERP. *Arabidopsis* contains three Der1 homologs named der1, der2.1 and der2.2 (100, 123, 124). Detecting the existence of these derlins in ERAD complex in the absence of EBS7 and generation of knockout mutants of single or multiple derlin genes will reveal whether these derlins participate in the EBS7-mediated ERAD pathway.

If EBS7 is not a homolog of known ERAD components, it may regulate the function E3 ligase in an alternative way. Hrd1 targets the degradation of HMG-CoA reductase thus regulates the lipid synthesis so its stability is strictly controlled to maintain the homeostasis of sterol biosynthesis. It has been shown that multiple Hrd1 proteins form oligomers and self-ubiquitinate each other in an Hrd3-dependent manner (95, 96, 181). This self-ubiquitination and subsequent degradation of Hrd1 is part of the regulation for the amount of folding intermediates and the degradation targets. As loss-of-function mutation in EBS7 results in AtHrd1 degradation in a proteasome-dependent manner, it is possible that EBS7 may promote the AtHrd1 trans-ubiquitination towards substrate or block its self-ubiquitination. Similar regulation model was identified in another E3 ligase gp78, in which the interaction between gp78 and its E2 UBE2G2 significantly increases the gp78 RING finger polyubiquitination activity (167, 182). To test whether EBS7 participates in regulating the ubiquitination activity of AtHrd1, the polyubiquitination status of AtHrd1 in the presence and absence of EBS7 needs to be examined. If EBS7 indeed regulate the switch between different ubiquitination targets of AtHrd1, a further

investigation on their interaction domains might give us more information of how EBS7 changes the conformation of this E3 ligase to affect its activity.

EBS7 is a plant-specific protein and it may have some universal role in different plant species. The *Arabidopsis* EBS7 takes part in salt stress response thus it worth examining whether its homologs in crop plants have similar functions. EBS7 knockdown or knockout lines in other model organisms including rice, maize, tobacco will be generated to assess their tolerance for environment or biotic stress.

Determining the fate of misfolded ER chaperones and ERAD factors

In previous studies on protein turnover in mammalian systems, it was revealed that most ER-resident chaperones have a relative long half-life (183). In contrast, several ERAD components including EDEM1, OS-9 and HERP are rapidly turned over (184). This post-translational regulation of the ERAD factors ensures that the activity of the degradation machinery is precisely adjusted to the physiological need within the cell. This so-called ERAD tuning system includes the fast turnover of ERAD factors by proteasome or autophagy pathways, the constitutive segregation of ERAD components from the ER via vesicle-mediated transport and the direct distribution regulation by the load of misfolded polypeptides (184, 185). In an earlier study in *Arabidopsis* cells, the long-lived ERQC component BiP and PDI were found to be transported to vacuoles for degradation at a steady state and this transportation bypassed the Golgi apparatus as the vacuole-localized PDI contained only high-mannose type but not complex type glycan (186). Compared with a better understand of tuning mechanism for normal ERAD factors, there are rarely studies that illustrate the fate of misfolded ERQC/ERAD components. Our genetic screening for the suppressors of *bri1-9* and *bri1-5* have revealed several ERQC/ERAD

mutants containing missense mutations including AtCRT3/EBS2 (*ebs2-7*), AtOS9/EBS6 (*ebs6-1*) and AtEBS7 (*ebs7-1*) (12). In all three mutant plants, the expression levels of the mutated protein are beyond detection limit while their RNA levels are comparable to WT lines, suggesting that post-transcriptional regulation might take part in altering their protein abundance. Further investigations of these mutants may lead to the discoveries on how misfolded ER chaperones, especially ERAD components are recognized and eliminated. In order to detect whether these misfolded ER-resident proteins undergoes regular ERAD, crosses between the three missense ERQC/ERAD plants and other known *Arabidopsis* ERAD mutants including *ebs5*, *ebs6*, *ebs7*, *ubc32*, *Δhrd1aΔhrd1b*, *Δdoa10aΔdoa10b* will be generated to detect their protein amount in these mutants (72, 73, 84, 85, 92). In addition, drugs that inhibit the proteinases in vacuole or the vesicle-related transport will be used to examine whether the mutated ERQC/ERAD proteins are transported to other organelles for degradation. Furthermore, a genetic screen looking for additional mutations that can rescue the protein abundance of EBS2/EBS6/EBS7 in these missense lines will be performed to further investigate the pathway that controls the fate of the mutated ER-resident proteins.

Investigating the ERAD complex modularity for diverse substrates

Based on the findings in yeast and mammalian, the Hrd1 ERAD complex degrades luminal and membrane-bound substrates. Recent reports have shown that the yeast Hrd1 system can modularly handles different types of substrates through the assistance of specific factors that recognize diverse degradation signals. For example, a core machinery including E2, E3, Hrd3 and Cdc48 sub-complex in yeast cells are required for all degradation and are sufficient for some ERAD-M substrates. Usa1 together with Der1

extends the substrate range to glycan-independent luminal substrates while the addition of Yos9 ensures that glycan signals will be properly recognized (97). The existence of bri1-9/bri1-5 as ERAD substrates provides a convenient genetic tool to study whether plant cells have this kind of E3 functional modularity. Both bri1-9 and bri1-5 are glycoproteins that undergo degradation through the Hrd1 machinery. Generation of non-glycosylated version of these two substrates combined with the use of ERAD mutants identified in previous studies will help us to understand which factor is responsible for the recognition of glycosylated/non-gycosylated substrates. From current yeast model, we hypothesized that AtOS9/EBS6 binds the N-glycan signal on the glycosylated polypeptides while AtSEL1/EBS5 recognizes the exposed hydrophobic amino acids on misfolded proteins (70, 71, 97). To test this hypothesis, we will compare the degradation efficiency of normal bri1-9 and glycan-depleted bri1-9 in *ebs5* and *ebs6* mutants. Moreover, as one substrate may contain both glycan-dependent and glycan-independent signals, the question is raised as to if the two determinants for ERAD work separately or they collaborate with each other to increase the efficiency of degradation. To address this question, we will generate both glycan-maintained/depleted and partial truncated of bri1-9/bri1-5 and measure their degradation rate in known ERAD mutants. Besides, we will co-express glycan-dependent and glycan-independent substrates in plant cell to investigate whether the two classes of misfolded proteins compete for the same degradation machinery or they use separate ERAD system for degradation.

REFERENCES

1. Aebi M (2013) N-linked protein glycosylation in the ER. *Biochim Biophys Acta* 1833(11):2430-2437 .
2. Mohorko E, Glockshuber R, & Aebi M (2011) Oligosaccharyltransferase: the central enzyme of N-linked protein glycosylation. *J Inherit Metab Dis* 34(4):869-878 .
3. Aebi M, Bernasconi R, Clerc S, & Molinari M (2010) N-glycan structures: recognition and processing in the ER. *Trends Biochem Sci* 35(2):74-82 .
4. Caramelo JJ & Parodi AJ (2008) Getting in and out from calnexin/calreticulin cycles. *J Biol Chem* 283(16):10221-10225 .
5. D'Alessio C, Caramelo JJ, & Parodi AJ (2010) UDP-GlC:glycoprotein glucosyltransferase-glucosidase II, the ying-yang of the ER quality control. *Semin Cell Dev Biol* 21(5):491-499 .
6. Hammond C, Braakman I, & Helenius A (1994) Role of N-linked oligosaccharide recognition, glucose trimming, and calnexin in glycoprotein folding and quality control. *Proc Natl Acad Sci U S A* 91(3):913-917 .
7. Meaden P*, et al.* (1990) The yeast KRE5 gene encodes a probable endoplasmic reticulum protein required for (1----6)-beta-D-glucan synthesis and normal cell growth. *Mol Cell Biol* 10(6):3013-3019 .
8. Jin H, Yan Z, Nam KH, & Li J (2007) Allele-specific suppression of a defective brassinosteroid receptor reveals a physiological role of UGGT in ER quality control. *Mol Cell* 26(6):821-830.
9. Li J & Chory J (1997) A putative leucine-rich repeat receptor kinase involved in brassinosteroid signal transduction. *Cell* 90(5):929-938 .
10. Noguchi T*, et al.* (1999) Brassinosteroid-insensitive dwarf mutants of *Arabidopsis* accumulate brassinosteroids. *Plant Physiol* 121(3):743-752 .
11. Hong Z*, et al.* (2009) Mutations of an alpha1,6 mannosyltransferase inhibit endoplasmic reticulum-associated degradation of defective brassinosteroid receptors in *Arabidopsis*. *Plant Cell* 21(12):3792-3802.
12. Jin H, Hong Z, Su W, & Li J (2009) A plant-specific calreticulin is a key retention factor for a defective brassinosteroid receptor in the endoplasmic reticulum. *Proc Natl Acad Sci U S A* 106(32):13612-13617 .
13. Li J*, et al.* (2009) Specific ER quality control components required for biogenesis of the plant innate immune receptor EFR. *Proc Natl Acad Sci U S A* 106(37):15973-15978 .
14. Saijo Y*, et al.* (2009) Receptor quality control in the endoplasmic reticulum for plant innate immunity. *EMBO J* 28(21):3439-3449 .
15. Saijo Y (2010) ER quality control of immune receptors and regulators in plants. *Cell Microbiol* 12(6):716-724 .

16. Zipfel C*, et al.* (2006) Perception of the bacterial PAMP EF-Tu by the receptor EFR restricts Agrobacterium-mediated transformation. *Cell* 125(4):749-760 .
17. Lu X*, et al.* (2009) Uncoupling of sustained MAMP receptor signaling from early outputs in an *Arabidopsis* endoplasmic reticulum glucosidase II allele. *Proc Natl Acad Sci U S A* 106(52):22522-22527 .
18. Haweker H*, et al.* (2010) Pattern recognition receptors require N-glycosylation to mediate plant immunity. *J Biol Chem* 285(7):4629-4636 .
19. von Numers N*, et al.* (2010) Requirement of a homolog of glucosidase II beta-subunit for EFR-mediated defense signaling in *Arabidopsis* thaliana. *Mol Plant* 3(4):740-750 .
20. Michalak M, Groenendyk J, Szabo E, Gold LI, & Opas M (2009) Calreticulin, a multi-process calcium-buffering chaperone of the endoplasmic reticulum. *Biochem J* 417(3):651-666 .
21. Nakamura K*, et al.* (2001) Functional specialization of calreticulin domains. *J Cell Biol* 154(5):961-972 .
22. Mesaeli N*, et al.* (1999) Calreticulin is essential for cardiac development. *J Cell Biol* 144(5):857-868 .
23. Szabo E, Qiu Y, Baksh S, Michalak M, & Opas M (2008) Calreticulin inhibits commitment to adipocyte differentiation. *J Cell Biol* 182(1):103-116 .
24. Dihazi H, Asif AR, Agarwal NK, Doncheva Y, & Muller GA (2005) Proteomic analysis of cellular response to osmotic stress in thick ascending limb of Henle's loop (TALH) cells. *Mol Cell Proteomics* 4(10):1445-1458 .
25. Bibi A*, et al.* (2011) Calreticulin is crucial for calcium homeostasis mediated adaptation and survival of thick ascending limb of Henle's loop cells under osmotic stress. *Int J Biochem Cell Biol* 43(8):1187-1197 .
26. Booth C & Koch GL (1989) Perturbation of cellular calcium induces secretion of luminal ER proteins. *Cell* 59(4):729-737 .
27. Thastrup O, Cullen PJ, Drobak BK, Hanley MR, & Dawson AP (1990) Thapsigargin, a tumor promoter, discharges intracellular Ca2+ stores by specific inhibition of the endoplasmic reticulum Ca2(+)-ATPase. *Proc Natl Acad Sci U S A* 87(7):2466-2470 .
28. Peters LR & Raghavan M (2011) Endoplasmic reticulum calcium depletion impacts chaperone secretion, innate immunity, and phagocytic uptake of cells. *J Immunol* 187(2):919-931 .
29. Gardai SJ*, et al.* (2005) Cell-surface calreticulin initiates clearance of viable or apoptotic cells through trans-activation of LRP on the phagocyte. *Cell* 123(2):321-334 .
30. Chaput N*, et al.* (2007) Molecular determinants of immunogenic cell death: surface exposure of calreticulin makes the difference. *J Mol Med (Berl)* 85(10):1069-1076 .
31. Nanney LB*, et al.* (2008) Calreticulin enhances porcine wound repair by diverse biological effects. *Am J Pathol* 173(3):610-630 .
32. Afshar N, Black BE, & Paschal BM (2005) Retrotranslocation of the chaperone calreticulin from the endoplasmic reticulum lumen to the cytosol. *Mol Cell Biol* 25(20):8844-8853 .

33. Shaffer KL, Sharma A, Snapp EL, & Hegde RS (2005) Regulation of protein compartmentalization expands the diversity of protein function. *Dev Cell* 9(4):545-554 .
34. Christensen A*, et al.* (2008) Functional characterization of *Arabidopsis* calreticulin1a: a key alleviator of endoplasmic reticulum stress. *Plant Cell Physiol* 49(6):912-924 .
35. Chen F, Hayes PM, Mulrooney DM, & Pan A (1994) Identification and characterization of cDNA clones encoding plant calreticulin in barley. *Plant Cell* 6(6):835-843 .
36. Dresselhaus T, Hagel C, Lorz H, & Kranz E (1996) Isolation of a full-length cDNA encoding calreticulin from a PCR library of in vitro zygotes of maize. *Plant Mol Biol* 31(1):23-34 .
37. Nardi MC*, et al.* (2006) Expression and localization of calreticulin in tobacco anthers and pollen tubes. *Planta* 223(6):1263-1271 .
38. Nelson DE, Glaunsinger B, & Bohnert HJ (1997) Abundant accumulation of the calcium-binding molecular chaperone calreticulin in specific floral tissues of *Arabidopsis* thaliana. *Plant Physiol* 114(1):29-37 .
39. Li Z, Onodera H, Ugaki M, Tanaka H, & Komatsu S (2003) Characterization of calreticulin as a phosphoprotein interacting with cold-induced protein kinase in rice. *Biol Pharm Bull* 26(2):256-261 .
40. Kim JH, Nguyen NH, Nguyen NT, Hong SW, & Lee H (2013) Loss of all three calreticulins, CRT1, CRT2 and CRT3, causes enhanced sensitivity to water stress in *Arabidopsis*. *Plant Cell Rep* 32(12):1843-1853 .
41. Chen MH, Tian GW, Gafni Y, & Citovsky V (2005) Effects of calreticulin on viral cell-to-cell movement. *Plant Physiol* 138(4):1866-1876 .
42. Jia XY*, et al.* (2008) Molecular cloning and characterization of wheat calreticulin (CRT) gene involved in drought-stressed responses. *J Exp Bot* 59(4):739-751 .
43. Nomura R, Orii M, & Senda T (2011) Calreticulin-2 is localized in the lumen of the endoplasmic reticulum but is not a Ca2+ -binding protein. *Histochem Cell Biol* 135(6):531-538 .
44. Hayashi E*, et al.* (2007) Identification of a novel cancer-testis antigen CRT2 frequently expressed in various cancers using representational differential analysis. *Clin Cancer Res* 13(21):6267-6274 .
45. Persson S, Rosenquist M, & Sommarin M (2002) Identification of a novel calreticulin isoform (Crt2) in human and mouse. *Gene* 297(1-2):151-158 .
46. Persson S*, et al.* (2003) Phylogenetic analyses and expression studies reveal two distinct groups of calreticulin isoforms in higher plants. *Plant Physiol* 133(3):1385-1396 .
47. Del Bem LE (2011) The evolutionary history of calreticulin and calnexin genes in green plants. *Genetica* 139(2):255-259 .
48. Christensen A*, et al.* (2010) Higher plant calreticulins have acquired specialized functions in *Arabidopsis*. *PLoS One* 5(6):e11342 .
49. Qiu Y, Xi J, Du L, Roje S, & Poovaiah BW (2012) A dual regulatory role of *Arabidopsis* calreticulin-2 in plant innate immunity. *Plant J* 69(3):489-500 .

50. Buck TM, Wright CM, & Brodsky JL (2007) The activities and function of molecular chaperones in the endoplasmic reticulum. *Semin Cell Dev Biol* 18(6):751-761 .
51. Sung DY, Vierling E, & Guy CL (2001) Comprehensive expression profile analysis of the *Arabidopsis* Hsp70 gene family. *Plant Physiol* 126(2):789-800 .
52. Hong Z, Jin H, Tzfira T, & Li J (2008) Multiple mechanism-mediated retention of a defective brassinosteroid receptor in the endoplasmic reticulum of *Arabidopsis*. *Plant Cell* 20(12):3418-3429 .
53. Nekrasov V*, et al.* (2009) Control of the pattern-recognition receptor EFR by an ER protein complex in plant immunity. *EMBO J* 28(21):3428-3438 .
54. Pedrazzini E*, et al.* (1997) Protein quality control along the route to the plant vacuole. *Plant Cell* 9(10):1869-1880 .
55. Nuttall J*, et al.* (2002) ER-resident chaperone interactions with recombinant antibodies in transgenic plants. *Eur J Biochem* 269(24):6042-6051 .
56. Reddy P, Sparvoli A, Fagioli C, Fassina G, & Sitia R (1996) Formation of reversible disulfide bonds with the protein matrix of the endoplasmic reticulum correlates with the retention of unassembled Ig light chains. *EMBO J* 15(9):2077-2085 .
57. Anelli T*, et al.* (2003) Thiol-mediated protein retention in the endoplasmic reticulum: the role of ERp44. *EMBO J* 22(19):5015-5022 .
58. Anelli T*, et al.* (2007) Sequential steps and checkpoints in the early exocytic compartment during secretory IgM biogenesis. *EMBO J* 26(19):4177-4188 .
59. Houston NL*, et al.* (2005) Phylogenetic analyses identify 10 classes of the protein disulfide isomerase family in plants, including single-domain protein disulfide isomerase-related proteins. *Plant Physiol* 137(2):762-778 .
60. Vembar SS & Brodsky JL (2008) One step at a time: endoplasmic reticulum-associated degradation. *Nat Rev Mol Cell Biol* 9(12):944-957 .
61. Quan EM*, et al.* (2008) Defining the glycan destruction signal for endoplasmic reticulum-associated degradation. *Mol Cell* 32(6):870-877 .
62. Clerc S*, et al.* (2009) Htm1 protein generates the N-glycan signal for glycoprotein degradation in the endoplasmic reticulum. *J Cell Biol* 184(1):159-172 .
63. Liebminger E*, et al.* (2009) Class I alpha-mannosidases are required for N-glycan processing and root development in *Arabidopsis* thaliana. *Plant Cell* 21(12):3850-3867 .
64. Hong Z*, et al.* (2012) Evolutionarily conserved glycan signal to degrade aberrant brassinosteroid receptors in *Arabidopsis*. *Proc Natl Acad Sci U S A* 109(28):11437-11442 .
65. Henquet M*, et al.* (2008) Identification of the gene encoding the alpha1,3-mannosyltransferase (ALG3) in *Arabidopsis* and characterization of downstream n-glycan processing. *Plant Cell* 20(6):1652-1664 .
66. Kajiura H, Seki T, & Fujiyama K (2010) *Arabidopsis* thaliana ALG3 mutant synthesizes immature oligosaccharides in the ER and accumulates unique N-glycans. *Glycobiology* 20(6):736-751 .
67. Hosokawa N, Kamiya Y, & Kato K (2010) The role of MRH domain-containing lectins in ERAD. *Glycobiology* 20(6):651-660 .

68. Yoshida Y & Tanaka K (2010) Lectin-like ERAD players in ER and cytosol. *Biochim Biophys Acta* 1800(2):172-180 .
69. Hirsch C, Gauss R, Horn SC, Neuber O, & Sommer T (2009) The ubiquitylation machinery of the endoplasmic reticulum. *Nature* 458(7237):453-460 .
70. Denic V, Quan EM, & Weissman JS (2006) A luminal surveillance complex that selects misfolded glycoproteins for ER-associated degradation. *Cell* 126(2):349-359 .
71. Gauss R, Sommer T, & Jarosch E (2006) The Hrd1p ligase complex forms a linchpin between ER-lumenal substrate selection and Cdc48p recruitment. *EMBO J* 25(9):1827-1835 .
72. Huttner S, Veit C, Schoberer J, Grass J, & Strasser R (2012) Unraveling the function of *Arabidopsis* thaliana OS9 in the endoplasmic reticulum-associated degradation of glycoproteins. *Plant Mol Biol* 79(1-2):21-33 .
73. Su W, Liu Y, Xia Y, Hong Z, & Li J (2011) Conserved endoplasmic reticulum-associated degradation system to eliminate mutated receptor-like kinases in *Arabidopsis*. *Proc Natl Acad Sci U S A* 108(2):870-875 .
74. Su W, Liu Y, Xia Y, Hong Z, & Li J (2012) The *Arabidopsis* homolog of the mammalian OS-9 protein plays a key role in the endoplasmic reticulum-associated degradation of misfolded receptor-like kinases. *Mol Plant* 5(4):929-940 .
75. Liu L*, et al.* (2011) The endoplasmic reticulum-associated degradation is necessary for plant salt tolerance. *Cell Res* 21(6):957-969 .
76. Muller J*, et al.* (2005) Conserved ERAD-like quality control of a plant polytopic membrane protein. *Plant Cell* 17(1):149-163 .
77. Carvalho P, Goder V, & Rapoport TA (2006) Distinct ubiquitin-ligase complexes define convergent pathways for the degradation of ER proteins. *Cell* 126(2):361-373 .
78. Vashist S & Ng DT (2004) Misfolded proteins are sorted by a sequential checkpoint mechanism of ER quality control. *J Cell Biol* 165(1):41-52 .
79. Olzmann JA, Kopito RR, & Christianson JC (2013) The mammalian endoplasmic reticulum-associated degradation system. *Cold Spring Harb Perspect Biol* 5(9) .
80. Younger JM*, et al.* (2006) Sequential quality-control checkpoints triage misfolded cystic fibrosis transmembrane conductance regulator. *Cell* 126(3):571-582 .
81. Matsuda N & Nakano A (1998) RMA1, an *Arabidopsis* thaliana gene whose cDNA suppresses the yeast sec15 mutation, encodes a novel protein with a RING finger motif and a membrane anchor. *Plant Cell Physiol* 39(5):545-554 .
82. Huttner S & Strasser R (2012) Endoplasmic reticulum-associated degradation of glycoproteins in plants. *Front Plant Sci* 3:67 .
83. Son O, Cho SK, Kim EY, & Kim WT (2009) Characterization of three *Arabidopsis* homologs of human RING membrane anchor E3 ubiquitin ligase. *Plant Cell Rep* 28(4):561-569 .
84. Lu S*, et al.* (2012) *Arabidopsis* ECERIFERUM9 involvement in cuticle formation and maintenance of plant water status. *Plant Physiol* 159(3):930-944 .
85. Doblas VG*, et al.* (2013) The SUD1 gene encodes a putative E3 ubiquitin ligase and is a positive regulator of 3-hydroxy-3-methylglutaryl coenzyme a reductase activity in *Arabidopsis*. *Plant Cell* 25(2):728-743 .

86. Lee HK, *et al.* (2009) Drought stress-induced Rma1H1, a RING membrane-anchor E3 ubiquitin ligase homolog, regulates aquaporin levels via ubiquitination in transgenic *Arabidopsis* plants. *Plant Cell* 21(2):622-641 .
87. Pollier J, *et al.* (2013) The protein quality control system manages plant defence compound synthesis. *Nature* 504(7478):148-152 .
88. Pickart CM (2004) Back to the future with ubiquitin. *Cell* 116(2):181-190 .
89. Bagola K, *et al.* (2013) Ubiquitin binding by a CUE domain regulates ubiquitin chain formation by ERAD E3 ligases. *Mol Cell* 50(4):528-539 .
90. Metzger MB, *et al.* (2013) A structurally unique E2-binding domain activates ubiquitination by the ERAD E2, Ubc7p, through multiple mechanisms. *Mol Cell* 50(4):516-527 .
91. Kraft E, *et al.* (2005) Genome analysis and functional characterization of the E2 and RING-type E3 ligase ubiquitination enzymes of *Arabidopsis*. *Plant Physiol* 139(4):1597-1611 .
92. Cui F, *et al.* (2012) *Arabidopsis* ubiquitin conjugase UBC32 is an ERAD component that functions in brassinosteroid-mediated salt stress tolerance. *Plant Cell* 24(1):233-244 .
93. Kostova Z, Tsai YC, & Weissman AM (2007) Ubiquitin ligases, critical mediators of endoplasmic reticulum-associated degradation. *Semin Cell Dev Biol* 18(6):770-779.
94. Carroll SM & Hampton RY (2010) Usa1p is required for optimal function and regulation of the Hrd1p endoplasmic reticulum-associated degradation ubiquitin ligase. *J Biol Chem* 285(8):5146-5156 .
95. Carvalho P, Stanley AM, & Rapoport TA (2010) Retrotranslocation of a misfolded luminal ER protein by the ubiquitin-ligase Hrd1p. *Cell* 143(4):579-591 .
96. Horn SC, *et al.* (2009) Usa1 functions as a scaffold of the HRD-ubiquitin ligase. *Mol Cell* 36(5):782-793 .
97. Kanehara K, Xie W, & Ng DT (2010) Modularity of the Hrd1 ERAD complex underlies its diverse client range. *J Cell Biol* 188(5):707-716 .
98. Lilley BN & Ploegh HL (2004) A membrane protein required for dislocation of misfolded proteins from the ER. *Nature* 429(6994):834-840 .
99. Ye Y, Shibata Y, Yun C, Ron D, & Rapoport TA (2004) A membrane protein complex mediates retro-translocation from the ER lumen into the cytosol. *Nature* 429(6994):841-847 .
100. Kirst ME, Meyer DJ, Gibbon BC, Jung R, & Boston RS (2005) Identification and characterization of endoplasmic reticulum-associated degradation proteins differentially affected by endoplasmic reticulum stress. *Plant Physiol* 138(1):218-231 .
101. Hampton RY & Sommer T (2012) Finding the will and the way of ERAD substrate retrotranslocation. *Curr Opin Cell Biol* 24(4):460-466 .
102. Plemper RK, Bohmler S, Bordallo J, Sommer T, & Wolf DH (1997) Mutant analysis links the translocon and BiP to retrograde protein transport for ER degradation. *Nature* 388(6645):891-895 .

103. Pilon M, Schekman R, & Romisch K (1997) Sec61p mediates export of a misfolded secretory protein from the endoplasmic reticulum to the cytosol for degradation. *EMBO J* 16(15):4540-4548 .
104. Brandizzi F*, et al.* (2003) ER quality control can lead to retrograde transport from the ER lumen to the cytosol and the nucleoplasm in plants. *Plant J* 34(3):269-281 .
105. Di Cola A, Frigerio L, Lord JM, Ceriotti A, & Roberts LM (2001) Ricin A chain without its partner B chain is degraded after retrotranslocation from the endoplasmic reticulum to the cytosol in plant cells. *Proc Natl Acad Sci U S A* 98(25):14726-14731 .
106. Di Cola A, Frigerio L, Lord JM, Roberts LM, & Ceriotti A (2005) Endoplasmic reticulum-associated degradation of ricin A chain has unique and plant-specific features. *Plant Physiol* 137(1):287-296 .
107. Marshall RS*, et al.* (2008) The role of CDC48 in the retro-translocation of non-ubiquitinated toxin substrates in plant cells. *J Biol Chem* 283(23):15869-15877 .
108. Lord JM*, et al.* (2003) Retrograde transport of toxins across the endoplasmic reticulum membrane. *Biochem Soc Trans* 31(Pt 6):1260-1262 .
109. Bagola K, Mehnert M, Jarosch E, & Sommer T (2011) Protein dislocation from the ER. *Biochim Biophys Acta* 1808(3):925-936 .
110. Wolf DH & Stolz A (2012) The Cdc48 machine in endoplasmic reticulum associated protein degradation. *Biochim Biophys Acta* 1823(1):117-124 .
111. Schuberth C & Buchberger A (2005) Membrane-bound Ubx2 recruits Cdc48 to ubiquitin ligases and their substrates to ensure efficient ER-associated protein degradation. *Nat Cell Biol* 7(10):999-1006 .
112. Schuberth C & Buchberger A (2008) UBX domain proteins: major regulators of the AAA ATPase Cdc48/p97. *Cell Mol Life Sci* 65(15):2360-2371 .
113. Neuber O, Jarosch E, Volkwein C, Walter J, & Sommer T (2005) Ubx2 links the Cdc48 complex to ER-associated protein degradation. *Nat Cell Biol* 7(10):993-998 .
114. Raasi S & Wolf DH (2007) Ubiquitin receptors and ERAD: a network of pathways to the proteasome. *Semin Cell Dev Biol* 18(6):780-791 .
115. Rancour DM, Dickey CE, Park S, & Bednarek SY (2002) Characterization of AtCDC48. Evidence for multiple membrane fusion mechanisms at the plane of cell division in plants. *Plant Physiol* 130(3):1241-1253 .
116. Feiler HS*, et al.* (1995) The higher plant *Arabidopsis* thaliana encodes a functional CDC48 homologue which is highly expressed in dividing and expanding cells. *EMBO J* 14(22):5626-5637 .
117. Yamamoto M, Kawanabe M, Hayashi Y, Endo T, & Nishikawa S (2010) A vacuolar carboxypeptidase mutant of *Arabidopsis* thaliana is degraded by the ERAD pathway independently of its N-glycan. *Biochem Biophys Res Commun* 393(3):384-389 .
118. Rancour DM, Park S, Knight SD, & Bednarek SY (2004) Plant UBX domain-containing protein 1, PUX1, regulates the oligomeric structure and activity of *Arabidopsis* CDC48. *J Biol Chem* 279(52):54264-54274 .
119. Park S, Rancour DM, & Bednarek SY (2007) Protein domain-domain interactions and requirements for the negative regulation of *Arabidopsis* CDC48/p97 by the

plant ubiquitin regulatory X (UBX) domain-containing protein, PUX1. *J Biol Chem* 282(8):5217-5224 .

120. Masahara-Negishi Y, Hosomi A, Della Mea M, Serafini-Fracassini D, & Suzuki T (2012) A plant peptide: N-glycanase orthologue facilitates glycoprotein ER-associated degradation in yeast. *Biochim Biophys Acta* 1820(10):1457-1462 .
121. Diepold A, Li G, Lennarz WJ, Nurnberger T, & Brunner F (2007) The *Arabidopsis* AtPNG1 gene encodes a peptide: N-glycanase. *Plant J* 52(1):94-104 .
122. Molinari M, Galli C, Vanoni O, Arnold SM, & Kaufman RJ (2005) Persistent glycoprotein misfolding activates the glucosidase II/UGT1-driven calnexin cycle to delay aggregation and loss of folding competence. *Mol Cell* 20(4):503-512 .
123. Wang Y*, et al.* (2008) Transcriptome analyses show changes in gene expression to accompany pollen germination and tube growth in *Arabidopsis*. *Plant Physiol* 148(3):1201-1211 .
124. Kamauchi S, Nakatani H, Nakano C, & Urade R (2005) Gene expression in response to endoplasmic reticulum stress in *Arabidopsis* thaliana. *FEBS J* 272(13):3461-3476 .
125. Suzuki T, Park H, Till EA, & Lennarz WJ (2001) The PUB domain: a putative protein-protein interaction domain implicated in the ubiquitin-proteasome pathway. *Biochem Biophys Res Commun* 287(5):1083-1087 .
126. Ueda T, Matsuda N, Uchimiya H, & Nakano A (2000) Modes of interaction between the *Arabidopsis* Rab protein, Ara4, and its putative regulator molecules revealed by a yeast expression system. *Plant J* 21(4):341-349 .
127. Galvao RM, Kota U, Soderblom EJ, Goshe MB, & Boss WF (2008) Characterization of a new family of protein kinases from *Arabidopsis* containing phosphoinositide 3/4-kinase and ubiquitin-like domains. *Biochem J* 409(1):117-127 .
128. Bachmair A, Novatchkova M, Potuschak T, & Eisenhaber F (2001) Ubiquitylation in plants: a post-genomic look at a post-translational modification. *Trends Plant Sci* 6(10):463-470 .
129. Farmer LM*, et al.* (2010) The RAD23 family provides an essential connection between the 26S proteasome and ubiquitylated proteins in *Arabidopsis*. *Plant Cell* 22(1):124-142 .
130. Taylor SC, Ferguson AD, Bergeron JJ, & Thomas DY (2004) The ER protein folding sensor UDP-glucose glycoprotein-glucosyltransferase modifies substrates distant to local changes in glycoprotein conformation. *Nat Struct Mol Biol* 11(2):128-134 .
131. Schrag JD*, et al.* (2001) The Structure of calnexin, an ER chaperone involved in quality control of protein folding. *Mol Cell* 8(3):633-644 .
132. Leach MR & Williams DB (2004) Lectin-deficient calnexin is capable of binding class I histocompatibility molecules in vivo and preventing their degradation. *J Biol Chem* 279(10):9072-9079 .
133. Thomson SP & Williams DB (2005) Delineation of the lectin site of the molecular chaperone calreticulin. *Cell Stress Chaperones* 10(3):242-251 .

134. Gopalakrishnapai J*, et al.* (2006) Isothermal titration calorimetric study defines the substrate binding residues of calreticulin. *Biochem Biophys Res Commun* 351(1):14-20 .
135. Kozlov G*, et al.* (2010) Structural basis of carbohydrate recognition by calreticulin. *J Biol Chem* 285(49):38612-38620 .
136. Thelin L, Mutwil M, Sommarin M, & Persson S (2011) Diverging functions among calreticulin isoforms in higher plants. *Plant Signal Behav* 6(6):905-910 .
137. Jia XY, He LH, Jing RL, & Li RZ (2009) Calreticulin: conserved protein and diverse functions in plants. *Physiol Plant* 136(2):127-138 .
138. Kinoshita T*, et al.* (2005) Binding of brassinosteroids to the extracellular domain of plant receptor kinase BRI1. *Nature* 433(7022):167-171 .
139. Kunze G*, et al.* (2004) The N terminus of bacterial elongation factor Tu elicits innate immunity in *Arabidopsis* plants. *Plant Cell* 16(12):3496-3507 .
140. Chouquet A*, et al.* (2011) X-ray structure of the human calreticulin globular domain reveals a peptide-binding area and suggests a multi-molecular mechanism. *PLoS One* 6(3):e17886 .
141. Wijeyesakere SJ, Gafni AA, & Raghavan M (2011) Calreticulin is a thermostable protein with distinct structural responses to different divalent cation environments. *J Biol Chem* 286(11):8771-8785 .
142. Li J, Nam KH, Vafeados D, & Chory J (2001) BIN2, a new brassinosteroid-insensitive locus in *Arabidopsis*. *Plant Physiol* 127(1):14-22 .
143. Bechtold N & Pelletier G (1998) In planta Agrobacterium-mediated transformation of adult *Arabidopsis* thaliana plants by vacuum infiltration. *Methods Mol Biol* 82:259-266 .
144. Mora-Garcia S*, et al.* (2004) Nuclear protein phosphatases with Kelch-repeat domains modulate the response to brassinosteroids in *Arabidopsis*. *Genes Dev* 18(4):448-460 .
145. Ruggiano A, Foresti O, & Carvalho P (2014) Quality control: ER-associated degradation: protein quality control and beyond. *The Journal of cell biology* 204(6):869-879.
146. Hebert DN & Molinari M (2012) Flagging and docking: dual roles for N-glycans in protein quality control and cellular proteostasis. *Trends Biochem Sci* 37(10):404-410 .
147. Gauss R, Jarosch E, Sommer T, & Hirsch C (2006) A complex of Yos9p and the HRD ligase integrates endoplasmic reticulum quality control into the degradation machinery. *Nat Cell Biol* 8(8):849-854 .
148. Xie W & Ng DT (2010) ERAD substrate recognition in budding yeast. *Seminars in cell & developmental biology* 21(5):533-539.
149. Ceriotti A & Roberts LM (2006) Endoplasmic reticulum-associated protein degradation in plant cells. *The Plant Endoplasmic Reticulum*, ed Robinson DG (Springer-Verlag, Berlin Heidelberg), pp 75-98.
150. Jin H, Hong Z, Su W, & Li J (2009) A plant-specific calreticulin is a key retention factor for a defective brassinosteroid receptor in the endoplasmic reticulum. *Proc Natl Acad Sci U S A* 106(32):13612-13617.
151. Hong Z & Li J (2012) *The protein quality control of plant receptor-like kinases in the endoplasmic reticulum* (Springer-Verlag, Berlin Heidelberg).

152. Liu Y & Li J (2014) Endoplasmic reticulum-mediated protein quality control in *Arabidopsis*. *Frontiers in plant science* 5:162.
153. Huttner S, Veit C, Schoberer J, Grass J, & Strasser R (2012) Unraveling the function of *Arabidopsis* thaliana OS9 in the endoplasmic reticulum-associated degradation of glycoproteins. *Plant Mol Biol* .
154. Huttner S*, et al.* (2014) *Arabidopsis* Class I alpha-Mannosidases MNS4 and MNS5 Are Involved in Endoplasmic Reticulum-Associated Degradation of Misfolded Glycoproteins. *The Plant cell* 26(4):1712-1728.
155. Yin Y*, et al.* (2002) BES1 accumulates in the nucleus in response to brassinosteroids to regulate gene expression and promote stem elongation. *Cell* 109(2):181-191.
156. Saijo Y (2010) ER quality control of immune receptors and regulators in plants. *Cell Microbiol* 12(6):716-724.
157. Knop M, Finger A, Braun T, Hellmuth K, & Wolf DH (1996) Der1, a novel protein specifically required for endoplasmic reticulum degradation in yeast. *Embo J* 15(4):753-763 .
158. Obayashi T, Hayashi S, Saeki M, Ohta H, & Kinoshita K (2009) ATTED-II provides coexpressed gene networks for *Arabidopsis*. *Nucleic Acids Res* 37(Database issue):D987-991 .
159. Winter D*, et al.* (2007) An "electronic fluorescent pictograph" browser for exploring and analyzing large-scale biological data sets. *PLoS One* 2(1):e718 .
160. Schwacke R*, et al.* (2003) ARAMEMNON, a novel database for *Arabidopsis* integral membrane proteins. *Plant Physiol* 131(1):16-26.
161. Mitra SK, Walters BT, Clouse SD, & Goshe MB (2009) An efficient organic solvent based extraction method for the proteomic analysis of *Arabidopsis* plasma membranes. *J Proteome Res* 8(6):2752-2767.
162. Benschop JJ*, et al.* (2007) Quantitative phosphoproteomics of early elicitor signaling in *Arabidopsis*. *Mol Cell Proteomics* 6(7):1198-1214.
163. Liu CJ & Dixon RA (2001) Elicitor-induced association of isoflavone O-methyltransferase with endomembranes prevents the formation and 7-O-methylation of daidzein during isoflavonoid phytoalexin biosynthesis. *Plant Cell* 13(12):2643-2658.
164. Elbein AD (1981) The tunicamycins - useful tools for studies on glycoproteins. *Trends Biochem Sci* 6:219-221.
165. Hetz C (2012) The unfolded protein response: controlling cell fate decisions under ER stress and beyond. *Nat Rev Mol Cell Biol* 13(2):89-102.
166. Howell SH (2013) Endoplasmic reticulum stress responses in plants. *Annu Rev Plant Biol* 64:477-499 .
167. Weissman AM, Shabek N, & Ciechanover A (2011) The predator becomes the prey: regulating the ubiquitin system by ubiquitylation and degradation. *Nature reviews. Molecular cell biology* 12(9):605-620.
168. Kim I, Li Y, Muniz P, & Rao H (2009) Usa1 protein facilitates substrate ubiquitylation through two separate domains. *PLoS One* 4(10):e7604 .
169. Leitman J*, et al.* (2014) Herp coordinates compartmentalization and recruitment of HRD1 and misfolded proteins for ERAD. *Molecular biology of the cell* 25(7):1050-1060.

170. Bernsel A, Viklund H, Hennerdal A, & Elofsson A (2009) TOPCONS: consensus prediction of membrane protein topology. *Nucleic Acids Res* 37(Web Server issue):W465-468.
171. Clouse SD, Langford M, & McMorris TC (1996) A brassinosteroid-insensitive mutant in *Arabidopsis* thaliana exhibits multiple defects in growth and development. *Plant Physiol* 111(3):671-678.
172. Friedrichsen DM, Joazeiro CA, Li J, Hunter T, & Chory J (2000) Brassinosteroid-insensitive-1 is a ubiquitously expressed leucine-rich repeat receptor serine/threonine kinase. *Plant Physiol* 123(4):1247-1256.
173. Fankhauser C*, et al.* (1999) PKS1, a substrate phosphorylated by phytochrome that modulates light signaling in *Arabidopsis*. *Science* 284(5419):1539-1541.
174. Voinnet O, Rivas S, Mestre P, & Baulcombe D (2003) An enhanced transient expression system in plants based on suppression of gene silencing by the p19 protein of tomato bushy stunt virus. *Plant J* 33(5):949-956 .
175. Wang ZY, Seto H, Fujioka S, Yoshida S, & Chory J (2001) BRI1 is a critical component of a plasma-membrane receptor for plant steroids. *Nature* 410(6826):380-383.
176. Gietz RD & Woods RA (2002) Transformation of yeast by lithium acetate/single-stranded carrier DNA/polyethylene glycol method. *Methods Enzymol* 350:87-96.
177. Plemper RK, Deak PM, Otto RT, & Wolf DH (1999) Re-entering the translocon from the lumenal side of the endoplasmic reticulum. Studies on mutated carboxypeptidase yscY species. *FEBS Lett* 443(3):241-245 .
178. Hitt R & Wolf DH (2004) Der1p, a protein required for degradation of malfolded soluble proteins of the endoplasmic reticulum: topology and Der1-like proteins. *FEMS Yeast Res* 4(7):721-729 .
179. Huang CH, Chu YR, Ye Y, & Chen X (2014) Role of HERP and a HERP-related protein in HRD1-dependent protein degradation at the endoplasmic reticulum. *J Biol Chem* 289(7):4444-4454 .
180. Kny M, Standera S, Hartmann-Petersen R, Kloetzel PM, & Seeger M (2011) Herp regulates Hrd1-mediated ubiquitylation in a ubiquitin-like domain-dependent manner. *J Biol Chem* 286(7):5151-5156 .
181. Gardner RG*, et al.* (2000) Endoplasmic reticulum degradation requires lumen to cytosol signaling. Transmembrane control of Hrd1p by Hrd3p. *J Cell Biol* 151(1):69-82 .
182. Das R*, et al.* (2009) Allosteric activation of E2-RING finger-mediated ubiquitylation by a structurally defined specific E2-binding region of gp78. *Mol Cell* 34(6):674-685 .
183. Bernasconi R, Galli C, Kokame K, & Molinari M (2013) Autoadaptive ER-associated degradation defines a preemptive unfolded protein response pathway. *Mol Cell* 52(6):783-793 .
184. Merulla J, Fasana E, Solda T, & Molinari M (2013) Specificity and regulation of the endoplasmic reticulum-associated degradation machinery. *Traffic* 14(7):767-777 .
185. Bernasconi R*, et al.* (2012) Role of the SEL1L:LC3-I complex as an ERAD tuning receptor in the mammalian ER. *Mol Cell* 46(6):809-819 .

186. Tamura K, Yamada K, Shimada T, & Hara-Nishimura I (2004) Endoplasmic reticulum-resident proteins are constitutively transported to vacuoles for degradation. *Plant J* 39(3):393-402 .